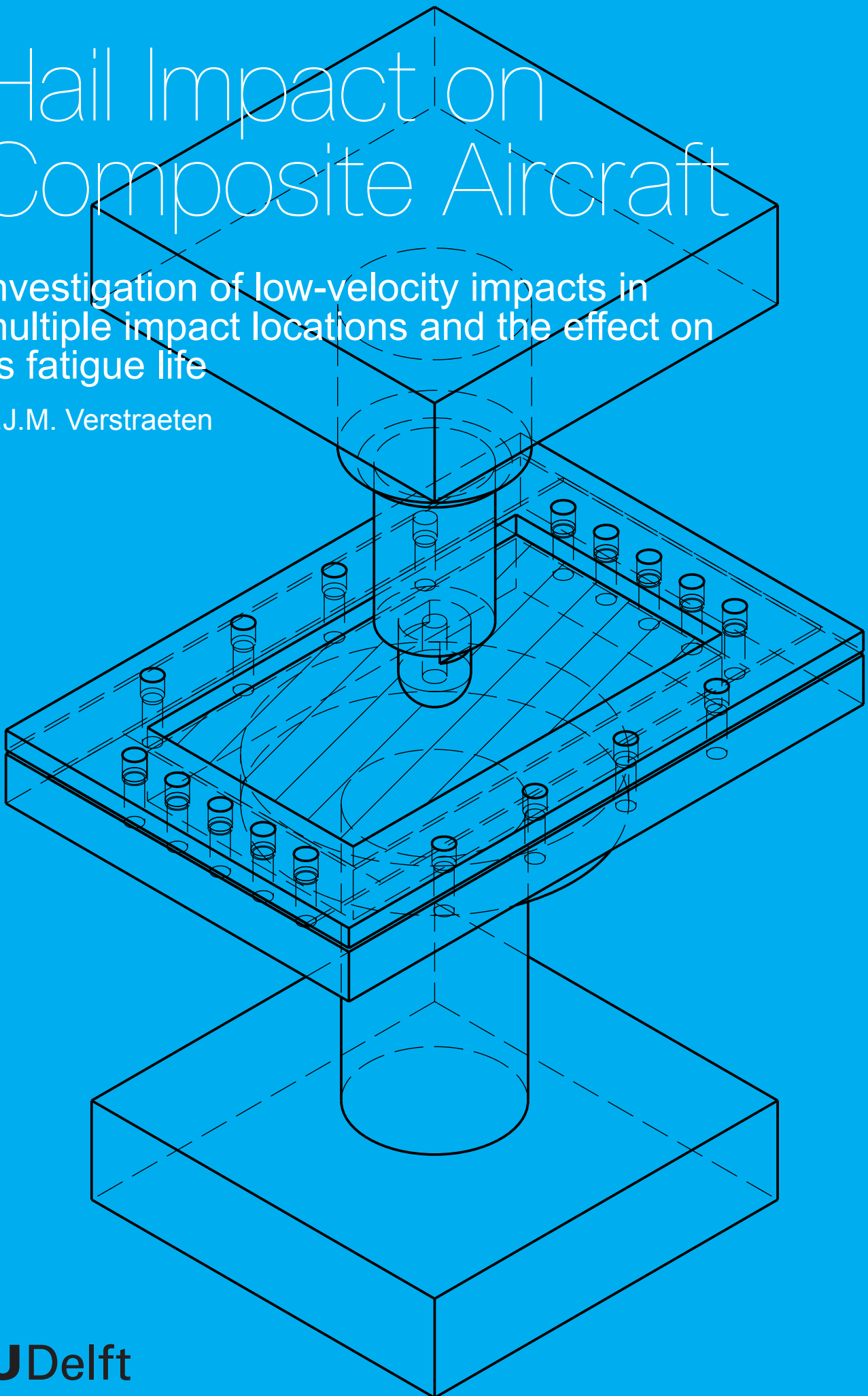


Hail Impact on Composite Aircraft

Investigation of low-velocity impacts in multiple impact locations and the effect on its fatigue life

A.J.M. Verstraeten



Hail Impact on Composite Aircraft

Investigation of low-velocity impacts in multiple impact locations and the effect on its fatigue life

by

A.J.M. Verstraeten

to obtain the degree of Master of Science

at the Delft University of Technology,

to be defended publicly on Wednesday June 19, 2019 at 09:30 AM.

Student number: 4355768
Project duration: November 19, 2018 – June 19, 2019
Thesis supervisor: Dr. ir. René Alderliesten

Delft University of Technology
Faculty of Aerospace Engineering
Department of Aerospace Structures and Materials

GRADUATION COMMITTEE

Graduation Date: June 19, 2019

Chair of the Committee:

Dr.ir. R.C. Alderliesten

Additional Member:

Dr.ir. O.K. Bergsma

External Member:

Dr.ir. C. Kassapoglou

Acknowledgements

I would like to express my deepest gratitude towards my supervisor, René Alderliesten. Throughout the last 10 months I have received an enormous amount of support, knowledge and guidance from him. A few elements really stood out to me in terms of his excellent supervision. Firstly, meetings every week where I could debate my findings to come to a better understanding of the subject matter. Secondly, his feedback and critical questions have allowed me to dissect my findings and conclusions to what they are now. Finally, his assistance and knowledge of all the tenuous administrative aspects of the thesis has also been of much help during this whole process. It has been a great pleasure working with you.

Furthermore, I would like to thank all the technicians from the Delft Aerospace Structures and Materials Laboratory (DASML). You have put an enormous amount of time and effort into me and my experiments. Furthermore, you have helped me in not only operating all the machines but also in explaining how the software works so I would be able to operate the machines without your guidance. You know who you are, but thank you Berthil Grashof, Misja Huizinga, Gertjan Mulder, Johan Boender, Victor Horbowiec, Fred Bosch, Cees Paalvast, Frans Oostrum, Durga Mainali, Ed Roessen, Peter den Dulk, and Rob van der List. I needed each and every one of you at one point and your expertise and help was always needed but especially greatly appreciated. I couldn't have done it without you!

Finally, a big thanks to the members of the committee for taking the time to review my work and for your interest in my research. Thank you René Alderliesten, Christos Kassapoglou and Otto Bergsma.

Abstract

The aerospace industry has made the transition from aluminium to carbon fibre composites on the newest, most advanced aircraft. One of the main disadvantages of composites is its high susceptibility to impacts, such as tool drops which occurs on a single point of impact. As such, these types of impact have been thoroughly studied. Nevertheless, a much less studied phenomenon but with possible catastrophic consequences is the effect of impacts covering a large area, such as hail. This research, therefore, investigates the differences between a single point of impact and multiple points of impact through a purely experimental analysis.

Upon investigating the difference, the research focused on three crucial hail event parameters which are impact separation, impact energy and the number of repeated impacts per impact location. The main results revealed that even though the damage response is worse for multiple location impacts, the overall damage response for hail events can be approximated with the available research on single point impacts. This observation remains unacceptable because the complete top surface of the aircraft is damaged and can have serious implications for the structural strength and can cause unexpected and unknown reductions in aircraft fatigue life.

There are two essential topics for future research which prevail. The first is due to the crushing effect of hail upon impact and is the the investigation of the difference in damage response of steel and hail impactors. The second is the investigation of 4-point bending fatigue on a plate impacted in multiple locations to investigate the damage growth and flexural stiffness. By understanding these additional matters it will become possible to determine if the new state of the art composite aircraft is susceptible to hail and if it will have a vulnerable fatigue life. Regardless of the outcome, it remains of utmost importance to possess this knowledge for the safety of air travel.

Contents

Acknowledgements	iii
Abstract	iv
1 Introduction	1
I Literature Review	3
2 Literature Review	4
2.1 Damage in UD composites.	4
2.2 Hail Properties	8
2.3 Research outside Delft University of Technology	11
2.4 Research at Delft University of Technology	14
3 Research Questions	16
II Methodology, Results and Discussion	17
4 Methodology.	18
4.1 Chapter Structure.	18
4.2 Key Definitions	19
4.3 Experimental Setup	19
4.4 E-series: Effect of Impact Energy	22
4.5 R-series: Effect of Impact Fatigue	23
4.6 S-series: Effect of Impact Spacing	24
4.7 L-series: Required Spacing for Link-Up (S-series Cont'd)	24
4.8 O-series: Effect of Impact Orientation (S-series Cont'd)	26
4.9 F-series: Effect of Mechanical Fatigue	26
5 Results	28
5.1 Results Structure	28
5.2 Reading C-scans and Microscopy images	28
5.3 Effect of Impact Energy	29
5.4 Effect of Repeated Impacts	31
5.5 Effect of Impact Spacing	34
5.6 Effect of Mechanical Fatigue.	39
6 Discussion.	42
6.1 Effect of impact Energy.	42
6.2 Effect of Repeated Impacts	44
6.3 Effect of Spacing	44
6.4 Effect of Mechanical Fatigue.	45
6.5 Impactor Material - Ice versus Steel	46
6.6 Effect of Residual strength.	46
III Conclusion and Recommendations	47
7 Conclusion and Recommendations	48
7.1 Conclusion	48
7.2 Recommendations	49

IV Appendix	50
A Damage Thresholds	51
A.1 Methodology	51
A.2 Results	54
A.3 Lessons Learned	54
B Laminate Manufacturing	57
B.1 General Concerns	57
B.2 Laminate Manufacturing Process	57
C Additional Results	60
C.1 E-Series	60
C.2 Optical Microscopy Specimen Cutting Plan	61
C.3 Hemispherical Impactor	63
C.4 MATLAB Method for Delaminations	63
C.5 S-series	64
Bibliography	68

Chapter 1

Introduction

Aviation was thought to be impossible until the two American aviation pioneers known as the Wright Brothers proved the world wrong in 1903 with their first successful powered flight. Unfortunately, to arrive at that point they had to learn from the crashes they experienced. Aviation crashes are inevitable but sometimes happen. However, every disaster or accident contributes to the body of knowledge so that the same mistake can be prevented in future events.

A prime example of a crash which contributed to the body of knowledge and changed the structural design of commercial aircraft forever is that of the De Havilland Comet in 1954. It was the first pressurised commercial jet airliner but resulted in two fatal crashes only months apart because of metal fatigue which was recognised but clearly not fully understood. Fatigue cracking was found to start at a square shaped window and escape hatch. Such sharp corners provide favourable conditions for the growth of fatigue crack due to high stress concentrations. The unfavourable stress concentration together with the type of rivets which were used caused the structure to fail at a much earlier stage than anticipated. As a consequence, the windows were changed into an oval design and the general design philosophy was changed from safe-life (designed not to fail, not safe if failed) to a fail-safe (failure allowed to occur but still safe) [1]. The introduction of the De Havilland Comet could only have taken place if there was confidence in the safety of the product, however it did not turn out well. Now, with the quest of searching for light but strong materials, the aerospace industry has made a big leap forward to implementing carbon fibre composite material for aircraft primary structures (e.g. fuselage and wings) instead of traditional aluminium but skepticism remains concerning its safety.

However, a known drawback of composite material is its susceptibility to impacts which cause up to 80% of damage [26]. For example, during maintenance inspection of an aircraft it could be possible that impacts occur on top of a fuselage due to a technician accidentally dropping a tool. Such an impact is called an 'out-of-plane' impact and such impacts generally cause debonding of layers in composites, known as a 'delamination'. Delaminations are undesirable because it is damage and according to the US Department of Defence, delaminations are responsible for 60% of failures in structures [6]. Another possible scenario is that aircraft standing on the ground suffer through a harsh hailstorm event. This means that there are out-of-plane impacts along the entire fuselage and wings as opposed to an impact in one location. Single location impacts such as tool drops are extensively covered in literature but the damage response is obviously not the same as for multiple impacts in multiple locations and deems it unsatisfactory. Based on this knowledge gap, this paper launches an investigation into the problem of hail impact and furthermore, what a hail impacted structure may imply for its remaining fatigue life. Currently a 'no-growth' design philosophy is endorsed for composite damage but perhaps as with the Comet aircraft this philosophy may have to change because the design of the Boeing 787 and Airbus A350 may have overlooked or oversimplified some critical scenarios.

Since hail has a stochastic impact nature, it must be simplified. To do that, this research applies a purely experimental approach to investigate and answer three important questions with regard to: the effect of impact spacing, impact energy, number of repetitions in each location. Furthermore, the research investigates what the effect of multiple impact locations implies for the structure's fatigue life. All the experimental work is based on the top of aircraft fuselages standing stationary on the ground which classifies hail impacts as low-velocity impacts. By answering the above issues, the research goal is to present the differences between multiple impact locations compared to single impact locations.

The report is split up into 4 parts. The first part of this report is a literature review which provides an understanding of damage in composites, hailstorms and hailstones, and finally an overview of relevant research performed both inside and outside of Delft University of Technology to present where this research fits in. Part II explains the methods and choices made for all experiments (methodology), the results of these experiments (results) and is finalised with a discussion of the results (discussion). Part III contains the conclusion of the research and the author's personal recommendations for future research. Finally, Part IV supplies any supplementary material given in the form of an appendix which will be referred to in the text where appropriate.

Part I

Literature Review

Chapter 2

Literature Review

2.1. Damage in UD composites

This research will focus and perform out of plane impacts on composite specimens at a later stage. However, before reaching that stage a basic understanding of the type of damage that can be expected and what causes this damage must be present to be able to reason why certain damage is seen at the later stage of this research. This chapter provides a broad overview of the damage mechanisms which are commonly seen in low-velocity impacts.

2.1.1. Low & High Velocity Definition

The transition between a low and high velocity impact is vague. Each researcher will have a slightly different definition of a low velocity impact [29, 30]. This section strives to clarify the difference.

There are four ranges of velocity: low-, high-, ballistic- and hyper-velocity. Ballistic and hyper velocity concerns military and space applications so these will not be discussed any further. Some define low-velocity impacts as an impact where a 'stress wave' propagation plays a role. A high-velocity impact would then be an impact where the structure does not have the time to respond to stress wave propagation [29]. In other words, a low-velocity impact causes a dynamical response of the structure whereas high-velocity impacts do not.

Some define low velocity impacts to be within the velocity range of 1 to 10's of m s^{-1} . Moreover, a low velocity impact is sometimes also defined as any impact under 100 m s^{-1} [29]. A suggestion is to judge if an impact is low or high velocity on the basis of the damage on it caused the structure. That means a high velocity impacts would penetrate the structure while low velocity impacts cause delamination and matrix cracking [29].

Later in section 2.2.2 it is seen that when the aircraft is on the ground, the terminal velocity of hail is below 50 m s^{-1} . Based on the above paragraphs it is seen that 10's of m s^{-1} is considered a low-velocity impact. Therefore, judging by hail's terminal velocity and the damage it causes a structure on the ground (non-penetrative), it is considered a low-velocity impact for the remainder of this research.

2.1.2. Damage formation for LVI

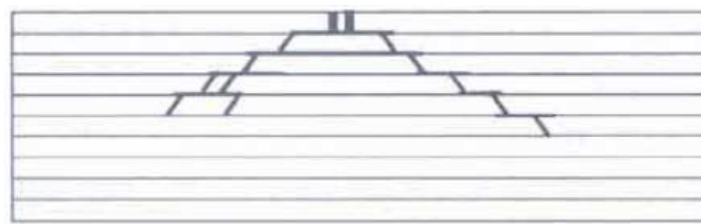
Some of the many parameters that affect the damage response upon impact are discussed in this section. Each combination of parameters will form a certain damage response, hence it is important to understand each parameter individually as is provided here. The entire discussion is based on low-velocity impacts.

Damage Initiation Site and Propagation

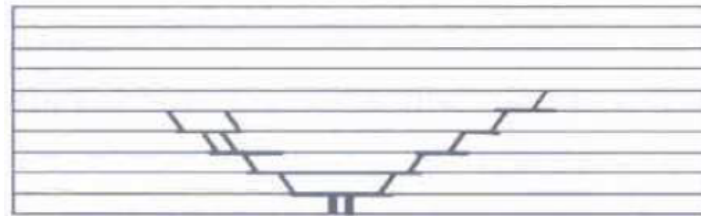
The thickness of the laminate can determine the location of damage initiation. Thick laminates experience damage initiation near the vicinity of the impact location, the front side. Damage grows from the top towards the bottom in a pyramid formation. Thin laminates experience damage initiation near the tensile side of the laminate, on the back side. For thin laminates, damage grows from the back side towards the front side in an inverse pyramid formation [11, 14, 29]. The damage growth morphology is presented in fig. 2.1.

Matrix Cracking

A matrix crack is the first damage to be created under LVI. These cracks run through the thickness and parallel to the reinforcement of layers. These cracks occur due to material properties mismatch but



(a) Thick laminate: pine tree damage pattern.



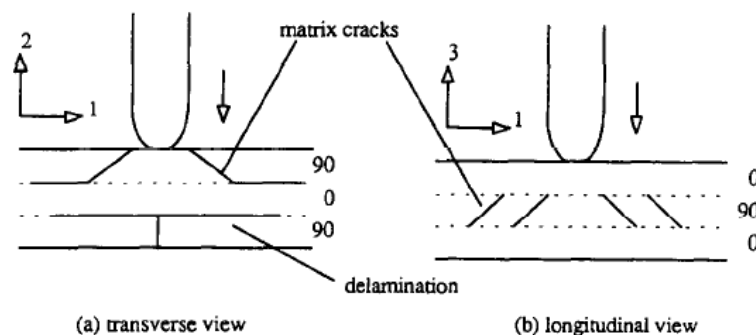
(b) Thin laminate: reversed pine tree damage pattern.

Figure 2.1: Damage propagation in thick and thin laminates [11].

also because of exceedingly high tension and shear stresses (explained below). Fortunately, matrix cracks are confined within the thickness of layers of the same orientation because adjacent layers of different orientation arrest crack propagation [29, 30, 32].

There are in general two types of matrix cracks [29] (see fig. 2.2):

1. Shear cracks: Formed by very high transverse shear stresses by the out-of-plane impactor. These cracks are formed at an angle of approximately 45° .
2. Tensile cracks: Formed by high tensile forces on the non-impacted side. This is caused by bending of the plate upon impact. See fig. 2.2a where the tensile crack is the vertical crack on the bottom layer.

Figure 2.2: Shear and tensile matrix cracks. 90° layer has the reinforcement pointing out of the page.

Delamination

Delaminations are simply stated the continuation of matrix cracks and propagate predominantly between layers of different orientation, through the so called 'resin-rich' areas [29]. The picture in fig. 2.2 has indicated delaminations as horizontal lines between layers.

Two essential factors contributing to the onset of delamination are [29, 32]:

- Bending stiffness mismatch between adjacent layers due to different fibre orientations. Larger orientation mismatch will cause a higher stiffness mismatch
- Bending induced interlaminar stresses.

Furthermore, delaminations are usually formed in the shape of a peanut. The longer axis of the peanut is aligned with the fibre direction of the lower layer. When more layers are considered, delaminations can occur in segments of 45° (in the case layups are stacked in steps of 45°). Each segment (as before) has its longer axis in the direction of the lower layer. When stacked on top of each other, it creates a spiral effect [14]. These delamination shapes are presented in fig. 2.3.

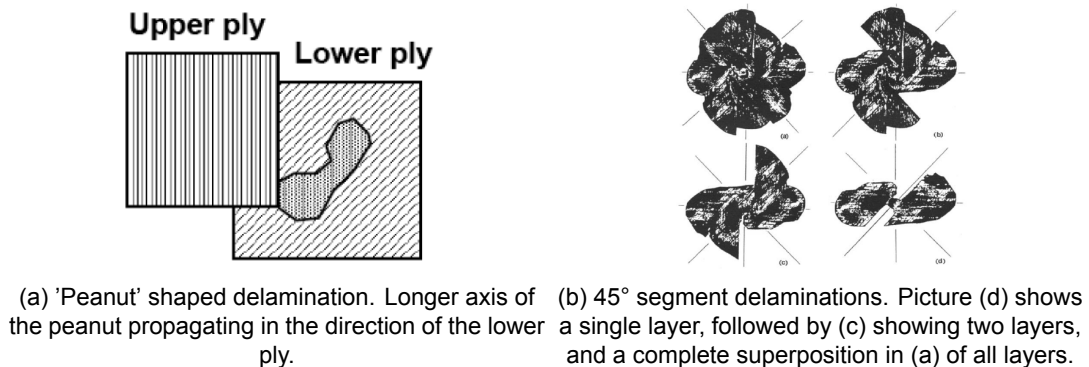


Figure 2.3: Delamination shapes seen from impact damage [14].

Fibre Fracture

Fibre fracture can be considered not to happen under LVI. If it does occur, it is either due to a too high impact energy (on the verge to a high-velocity impact) or at a much later stage which would be after a very large number of impacts [29]. This damage mechanism may be on the front side (due to fibre crushing or buckling) and/or the back side (due to exceedingly high tension stress due to bending) [14, 29].

2.1.3. Damage Variables

The damage response of composite material is extremely sensitive to changes in impact conditions [36]. The moment one variable changes, the damage response may prove to be completely different. In fact, according to ASTM standards [8]:

"The response of a laminated plate specimen to an out-of-plane force is dependent upon many factors, such as laminate thickness, ply thickness, stacking sequence, environment, geometry, indenter tip geometry, and boundary conditions."

Furthermore, the following literature [19, 29, 36, 37] provides additional information on some of the variables listed above by the ASTM standard and other variables which may affect the damage response:

- Impactor geometry may change the damage response. E.g. a large impact object with 5 J will give an overall response, while a small impact object with the same energy of 5 J will give a localised response.
- Specimen geometry. The geometry may affect energy absorption for low-velocity impacts. Larger specimens are not guaranteed to be better than smaller specimens.
- Laminate stacking sequence. Fibre orientation steps should be small. Large changes are unfavourable and cause greater stiffness mismatch. Woven fabrics are more resistant to damage.
- Fibre stress/strain curve with regard to fibre fracture. A large area under the stress/strain curve results in better energy absorption.
- Specimen thickness. Thicker specimens are able to absorb more energy, hence withstand more impacts.

It is important to be aware what typical effects are of changing certain parameters. If this is understood, it will be understood which parameters will need to be varied or controlled in the design of future experiments.

2.1.4. Quasi-static indentation

Quasi-static indentation is an alternative to drop-weight impact testing for out-of-plane tests. The difference is that QSI slowly presses a hemispherical head into the surface of the laminate rather than dropping a weight [8]. The biggest advantage of this test for this research is that the impact energy can be much better controlled and that the sequence of damage can also be recorded. The test setup can be seen in fig. 2.4.

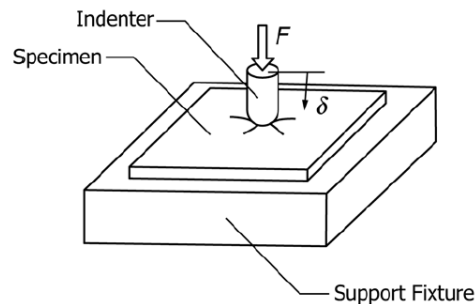


Figure 2.4: Quasi-static indentation test setup [8].

The ASTM standards [8] say the following:

"...this test method (quasi-static indentation) does not address wave propagation and vibrations in the specimen, time-dependent material behaviour, or inertia-dominated impact events."

However, even though the difference in wave propagation and vibrations between the two methods, both the ASTM standards for QSI and drop-weight [7, 8] say it is acceptable to use quasi-static indentation as an alternative to drop-weight tests.

2.1.5. C-scan

More advanced techniques must be used because visual inspection cannot see through the thickness to detect delaminations. The C-scan is a common inspection method to investigate damage below the surface. It uses piezoelectric transducers to transmit ultrasonic waves into the part to be inspected. C-scans make a 2D scan of the inspection area and show where the delamination is located and how big it is [35].

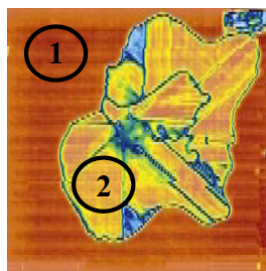


Figure 2.5: C-scan of a simulated hail impacted area [35].

2.2. Hail Properties

This research is to execute impact experiments based on real life hail characteristics in order to determine if hail causes a threat to composite structural integrity. The required hailstorm knowledge for the experiments in the later stage of this research are hail impact energy and hail impact surface morphology. Both topics are explored in more detail below.

2.2.1. Density

Hailstone density is not always comparable to solid ice (917 kg m^{-3}), its density varies significantly from hailstorm to hailstorm for all dimensions of hailstones. An EASA hail report has summarised hailstone densities according to hailstone dimension. Hailstone densities were found to vary between 310 kg m^{-3} to 915 kg m^{-3} for sizes between 8 mm to 39 mm [19]. The results are presented in fig. 2.6

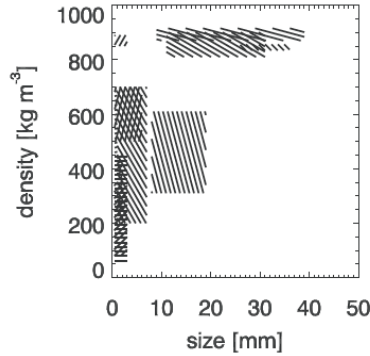


Figure 2.6: Hail density according to hailstone size [19].

The reason for this variation is due the conditions at which it is formed but this is outside the scope of the research. However, according to [15] the density of larger hailstones are usually close to the density of solid ice which may be relevant because it is probably only the larger hailstones which will cause impact damage.

2.2.2. Terminal Velocity

The velocity at which hailstones impact the ground is called the terminal velocity. First of all, the research is based on aircraft standing stationary on the ground because in-flight impacts have velocities in excess of 100 m s^{-1} which is not low-velocity according to section 2.1.1. Furthermore, it is assumed hailstones impact the ground vertically because the angle is negligible [19].

For perfectly spherical hailstones, the equation used to determine the terminal velocity of a hailstone is [19]:

$$V_{\text{terminal}} = \sqrt{\frac{2m_{\text{hail}}g}{\rho_{\text{air}}A_{\text{hail}}C_D}} \quad (2.1)$$

where ρ_{hail} and ρ_{air} are the density of hail and air, respectively. g is the acceleration due to gravity. C_d is the drag coefficient. D is the diameter of the hailstone. V is the terminal velocity, the parameter of interest.

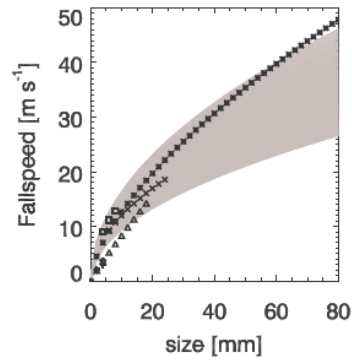


Figure 2.7: Terminal velocity in function of hailstone size. Gray zone is based on eq. (2.1), a density of 917 kg m^{-3} and drag coefficient ranging between 0.5 to 1.5 [19].

Using eq. (2.1) to calculate the terminal velocity with drag coefficients between 0.5 to 1.5, a range of terminal velocities is calculated for hailstone sizes between 0 mm to 80 mm which is indicated by the grey zone in fig. 2.7. Furthermore, empirical observations are indicated in the same figure by the individual data points. It is seen that the theoretical calculations are a very good approximation of the terminal velocity.

2.2.3. Hailstone Kinetic Energy

Kinetic energy is a parameter required for any further impact testing in this research. It is a function of mass and velocity, the ranges of values of these parameters can be extracted from the sections above. In this section, the kinetic energy is calculated for hailstones with diameters between 0 cm to 10 cm, based on a drag coefficient $C_D = 0.5$, hailstone density $\rho = 900 \text{ kg m}^{-2}$, using the eq. (2.1). The theoretical hailstone impact energy is presented in fig. 2.8.

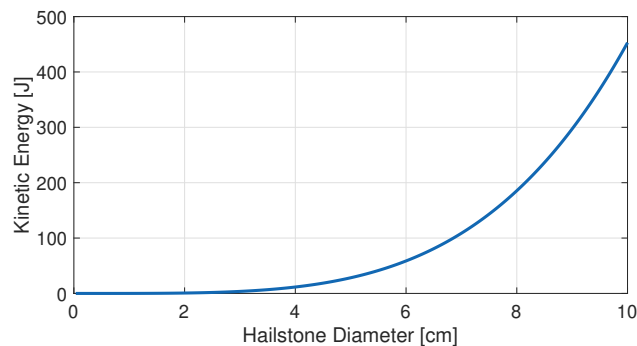


Figure 2.8: Kinetic energy as a function of hailstone size.

The values for kinetic energy are relatively low for hailstones $\lesssim 4 \text{ cm}$, however have a strong increase as its diameter increases.

2.2.4. Hailpads

Hailpads are commonly used in hail climatology studies and are made of styrofoam (typically of dimensions $300 \text{ mm} \times 300 \text{ mm}$) which records valuable information for this research. Hailpads reveal hailstorm information such as which size hailstones have impacted the surface, how far hailstones were separated from each other and the total number of hailstones which have impacted the hailpad. Three examples of real hailpad surfaces are presented in figs. 2.9a to 2.9c on the next page.

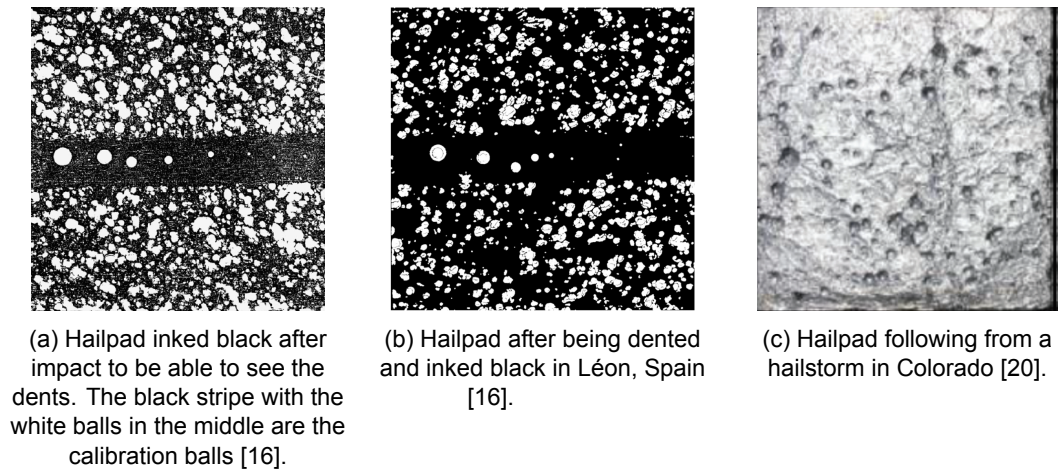


Figure 2.9: Real impact surfaces.

From the three hailpads above, hail is clearly a stochastic phenomenon which severely complicates the problem. Moreover, hailstone impacts are of different size, energy and impact separation density. Thus, simplifying a hailstorm to impacts of constant size, energy and separation is not possible. In summary, the more variables present themselves the more complicated the experiments are to design.

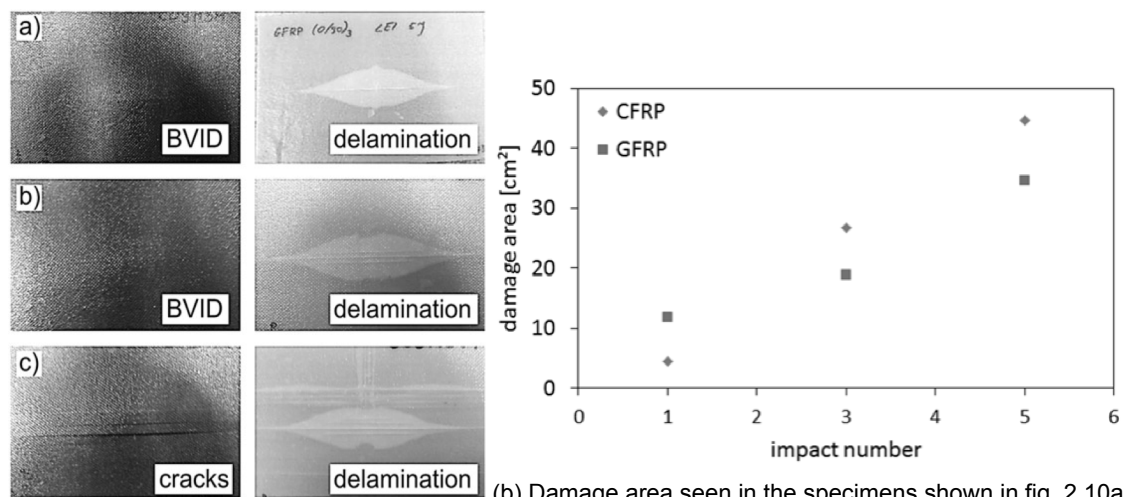
2.3. Research outside Delft University of Technology

There has been a vast amount of research performed on out-of-plane impacts. This section has included some research that identifies which areas of research have generally been looked at and which are relevant to this study on hail.

2.3.1. Influence of Repeated Impacts on Delamination Area Growth

The research performed by three researchers at Lublin University of Technology [22] aimed to show the delamination growth as a function of number of impacts for different materials. For that, glass and carbon fibre reinforced polymer laminates were compared. Each laminate had dimensions of 150 mm × 100 mm and a thickness of 1.5 mm but with different layups, i.e. the CFRP and GFRP had a $(0_6/90_6)$ and $(0_3/90_3)$ layup, respectively. A total of 5 impacts were performed on each laminate, each impact at 5 J and with a hemispherical impactor diameter 38.1 mm [22].

CFRP showed no visible damage until the specimen was impacted five times at which a crack towards the surface became visible. GFRP on the other hand showed a delamination after only one impact. Even though CFRP does not show damage under the surface, delaminations were caused in both materials after the first impact and propagated with repeated impacts in what seems an almost linear fashion for this limited dataset, see fig. 2.10.



(a) Images of the impact sites. CFRP (L) and GFRP (R). a) 1 impact, b) 3 impacts, c) 5 impacts [22].

(b) Damage area seen in the specimens shown in fig. 2.10a [22].

Figure 2.10: Images of carbon fibre and glass fibre specimens after repeated impacts on the left and the damaged area graph on the right.

2.3.2. Delamination Growth for Different Thickness Laminates

One of the research goals of the work of Atas, Icten and Küçük [37] aimed at investigating the damage growth of delaminations upon repeated impacts for laminates of different thicknesses. The research used quasi-static indentation instead of the traditional drop-tower and its advantages are illustrated in this section.

All laminates were manufactured from woven glass fabric with thicknesses of 2.70 mm, 3.35 mm, 4.05 mm, 5.05 mm and 5.75 mm i.e. 8, 10, 12, 16 and 18 layers, respectively. A high fibre volume fraction similar to that of the aerospace industry was obtained, that is $V_f \approx 0.58$ [37]. Furthermore, each laminate was impacted with 20 J (≈ 46 mm sized hailstones) until perforation occurred.

As described in section 2.1.4, force-deflection curves reveal the sequence of damage. For example, upon the first impact, two peaks are seen in the force-deflection curve on the ascending part. The first peak refers to the dent created on the surface and the second peak is the maximum contact force [37]. Furthermore, the slope of the ascending part also reveals the bending stiffness. In other words, if the slope decreases then so does the bending stiffness. The first impact is illustrated for the

laminates of 16 layers in fig. 2.11a. Upon impacting this laminate until perforation, it is seen that the bending stiffness remained fairly constant until the 60th impact and decreased immensely towards the last 133rd indentation when perforation occurred, see fig. 2.11b.

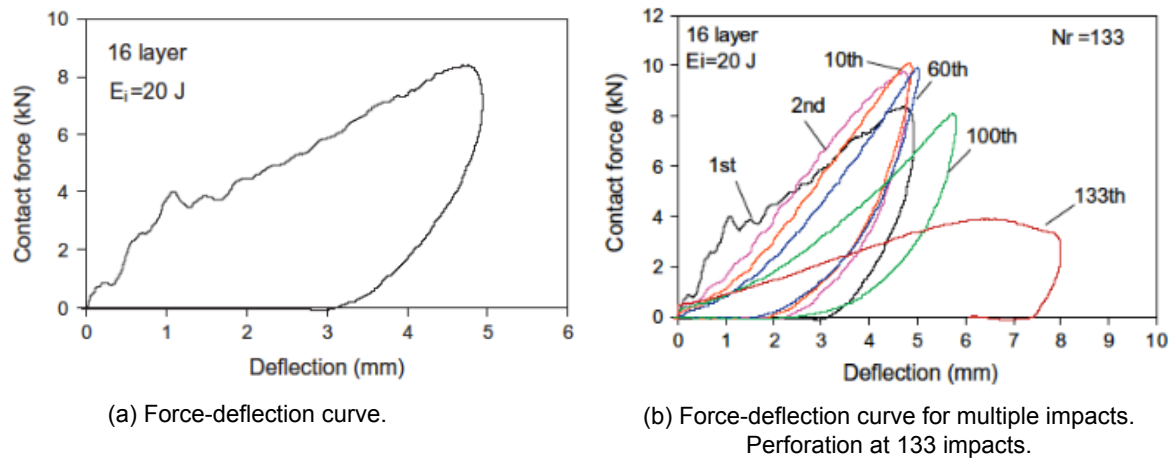


Figure 2.11: Force-deflection curves for 16 layer laminates impacted with an impact energy of 20 J [37].

Different thickness laminates were tested and their delamination area was recorded as well. The delamination area growth shows that thicker laminates were able to withstand more impacts until perforation. The trend also indicates that delamination area growth decreases with increasing number of impacts. The delamination area progression is shown in fig. 2.12 for the different thickness laminates. The delamination growth shown in fig. 2.12 shows that the delamination growth rate is not unique to a certain laminate but is in general a slow phenomenon.

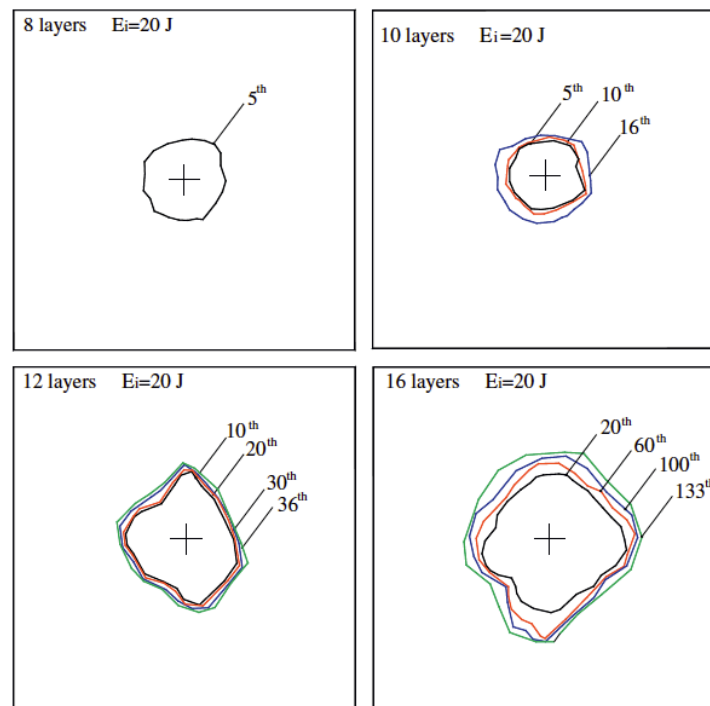


Figure 2.12: Damage progression for composite plates with different thicknesses and layups [37].

2.3.3. Effect of Impactor Material

The study performed by the North Dakota State University [27] investigated the difference between impactor materials ice and aluminium. The impacted specimens were then put under constant amplitude tension fatigue tests.

The material used for these specimens was CFRP with a layup of $[45, 0, -45, 90]_{2s}$ and dimensions of 254 mm \times 76.2 mm. Ice impactors had diameters equal to 25.4 mm and 38.1 mm, impacted at 7.1 J and 27.4 J, respectively. Aluminium impactors had a smaller diameter equal to 12.7 mm, impacted with the same impact energies as those for ice. The specimens were impacted only once [27]. Only the aluminium impact of 27.4 J caused delamination damage.

To investigate post-impact fatigue life, the specimens (including a non-impacted virgin specimen as a reference point) were cyclically loaded. It was found that all specimens provided the same fatigue life as the virgin specimen, except for the 12.7 mm 27.4 J aluminium impactor as shown in fig. 2.13 [27].

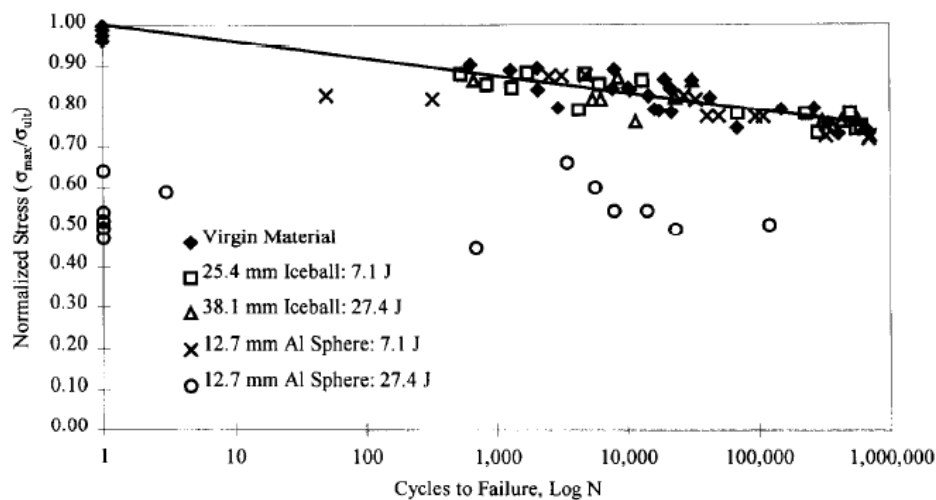


Figure 2.13: Post-impact S-N curves according to impactor material [27].

The results are not what would be expected. It was expected that even the 7.1 J impacts would cause damage. Other research have shown damage with lower levels of impact energy and a similar sized impactor diameter. Remember that the size of the impactor plays an important role in the damage it creates, see section 2.1.3.

This research is important to future research as it makes aware that impactor material/size may play a crucial role in the damage response of a laminate. This research also showed that if damage is inflicted, the fatigue life suffers.

2.4. Research at Delft University of Technology

Research outside Delft University of technology is predominantly limited to single location impacts. Due to this limitation, the research performed at the department of Aerospace Engineering at Delft University of Technology has shifted its focus towards multiple impact locations. This section presents a summary of the most relevant results.

2.4.1. Through-thickness Damage Response

Huber [21] performed repeated impacts on two locations and investigated the damage response through the thickness of the laminate. The two locations were separated with a distance of either 15 mm or 20 mm which is indicated in fig. 2.14 by the two black dots on the centre line. The report unfortunately did not come up with concrete conclusions on what the effect of impact location separation has on the damage response. Nevertheless, the analysis of the results proved interesting because of through the thickness microscopic images.

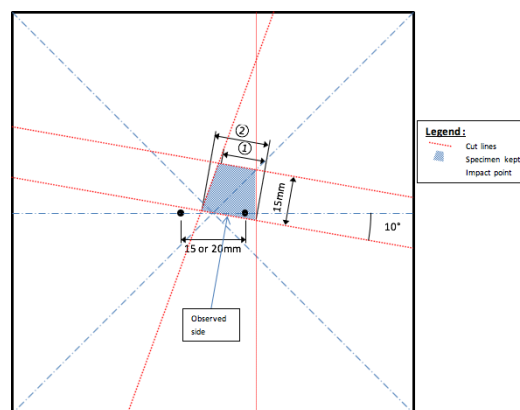


Figure 2.14: Impact map to determine the interaction between impact location distance and impact fatigue. The two black dots indicate the impact location, these may be either 15 mm or 20 mm [21].

The laminates were made of carbon fibre reinforced polymer, had dimensions of 123 mm × 123 mm and a layup of $[45,-45,0,90,45,-45,0,90]_s$ with a thickness of 1.5 mm. The specimens were impacted with 4 J to 6 J using a drop-tower. According to fig. 2.8 in the previous chapter, a 4 J impact is equivalent to a hailstone with a diameter of 30 mm.

By optical microscopy it was observed that delaminations occurred rather fast. After only two 4 J impacts, a delamination occurred in the topmost interface of the laminate. After 4 impacts, a much larger portion of the thickness was delaminated. Finally after 8 and 12 impacts, delamination jumps between layers were seen and the delaminated interfaces worsened. The optical microscopy images are presented in figs. 2.15a to 2.15d.

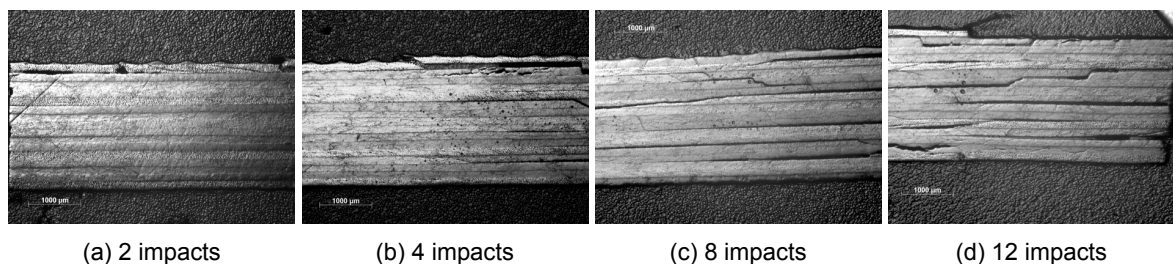


Figure 2.15: The effect of repeated impacts on a CFRP. Impact locations at 15 mm and at 4 J each [21].

2.4.2. Impact Damage Link-up

In contrast to the work of Huber which looked at damage growth microscopically, this research performed repeated impacts in 7 locations, investigated delamination area growth (2D) and link-up. Link-up refers to the joining of delaminations from two separated impacts (explained in more detail below). The experiment impact map is illustrated in fig. 2.16.

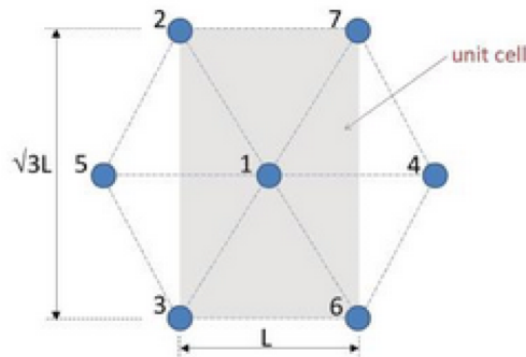


Figure 2.16: Impact surface map used by Laurencon to investigate the effect of multiple impacts in multiple locations [28]. Blue dots indicate the impact locations.

The CFRP specimen plates had dimensions of 430 mm \times 430 mm and a laminate layup of $[0,90,45,-45]_s$ with a plate thickness of ≈ 1.2 mm. The impact energy was varied in the range of 2 J to 8 J, that corresponds to hailstones with a diameter of 26 mm to 36 mm. Delamination damage was recorded through c-scans which offer the ability to track damage growth without the need to cut open the specimens as with those of Huber.

The c-scans revealed that delaminations were caused already after one impact. After the first jump in delamination area, there was little damage growth. The affected area then suddenly increased dramatically after about 14 impacts in all locations, see fig. 2.17. The dramatic increase in delamination area is what is referred to as 'link-up'.

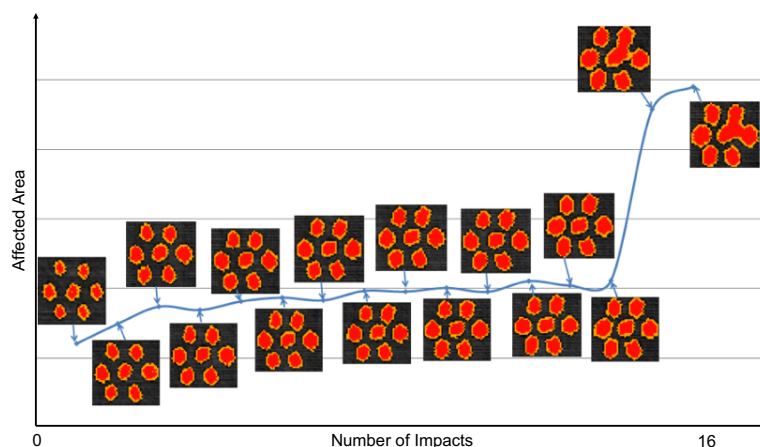


Figure 2.17: 2D images of the results obtained from repeated low energy impacts in a hexagon shape. The results obtained by the C-scan show that delaminations at impact location link up to delaminations at other impact locations [28].

The link-up phenomenon is important to consider for hail impact experiments. A hail impacted surface contains closely spaced impacts which might result in 'link-up' which could delaminate large portions of a composite plate. This may have negative consequences on fatigue life and residual strength.

Chapter 3

Research Questions

The literature review has made clear that past research focused predominantly on single and repeated impacts in a single location. However, hail is a problem of single/repeated impacts in *multiple* locations. Hence, the research questions presented here shift the focus towards multiple locations.

Furthermore, hailpads show a stochastic impact distribution which complicates the attempt at understanding the effect of impacts in multiple locations. There is too few available data on hailstorms and hailpads to base this research on, so the problem must be broken down into a deterministic approach which produces knowledge that can be applied to any impacted surface.

Even though hailpad surfaces show a stochastic hailstone distribution, three observations which are inherent to all hailpads are:

- Impacts are spaced at random distances from each other
- Every hailpad reveals a different number of impacts depending on the hailstorm
- Hailstones impact the surface with different impact energies

The hope is that if the above three relations are understood deterministically then it will be easy to apply this knowledge to an entirely impacted fuselage to produce an indication of the damage that was done.

Based on the above, the **first three research questions** are:

1. What is the effect of impact spacing on the damage response of the laminate?
2. What is the effect of repeating impacts on the damage response of the laminate?
3. What is the effect of impact energy on the damage response of the laminate?

Understanding the damage response created by the three hailstorm parameters is one aspect. However, taking it one step further brings the research to investigating its remaining fatigue life. Hence, one **additional research questions** is posed:

4. Does impact damage propagate by mechanical fatigue loading the specimen?

The above 4 research questions should give insight on what is important and should be considered in further research as well as if a hailstorm can reduce the service life of a composite aircraft.

Part II

Methodology, Results and Discussion

Chapter 4

Methodology

This research is based on a purely experimental approach and this chapter introduces all the experiments performed which are designed to answer the research questions in the previous chapter. More specifically, the choices for the test setup and experiment design for the impact and fatigue tests are described below.

4.1. Chapter Structure

The experiments were divided into 6 'series' with each series based on one of the research questions described in chapter 3. For example, there is the 'E-series' where the E stands for **E**nergy hence this looks into the effect of impact energy on the damage response. The series abbreviations are explained below:

- **S-series**: **S**pacing-series or, effect of impact spacing on the damage response.
- **L-series**: **L**ink up-series or, the investigation of when link-up occurs. Continuation of S-series.
- **O-series**: **O**rientation-series or, effect of impact location orientation on the damage response. Second continuation of S-series.
- **R-series**: **R**epeated-series or, effect of repeated impacts on the damage response.
- **E-series**: **E**nergy-series or, effect of impact energy on the damage response.
- **F-series**: **F**atigue-series or, effect of mechanical fatigue on the damage response.

Furthermore, each series is explained by three parts which are the 'impact surface', 'impact energy' and 'number of impacts per location'. The impact surface refers to where on the specimen impacts are located, as shown in fig. 4.1. Furthermore, each series impacts the specimens with a specific impact energy which is referred to as 'impact energy'. Finally, each impact location shown in the impact pattern is impacted a specific number of times which is explained by the 'number of impacts'.

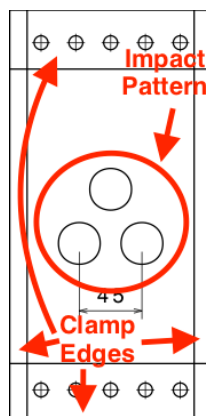


Figure 4.1: Test specimen configuration example. Triangular impact pattern, black circles indicate the impact locations which are for example, each impacted 5 times with an impact energy of 6 J. The 'clamp edges' are the parts of the specimen which are clamped by the test clamp which is explained later in section 4.3. Finally, the black circles have a diameter of 3 cm which is the diameter of the impactor.

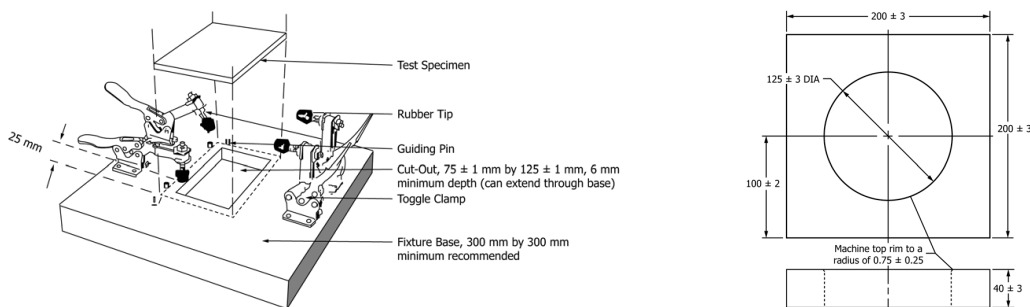
4.2. Key Definitions

As there are many new terms in this research area, the remainder of the report uses phrases and terms which may not always be self-explanatory. To avoid any confusion, the most important terms are explained below.

- **'Delamination area'** - The 2D delamination area as seen from the top of the specimen.
- **'Delamination long axis'** - Delaminations usually present themselves in an oval/peanut shape. The long axis is the longer dimension of this oval.
- **'Delamination short axis'** - Same as the previous but now this is the shorter side of such an oval.
- **'Link-up'** - to understand this best, please refer to fig. 2.17. When referring to the figure, a small initial jump in delamination area is seen that corresponds to the 1st to 3rd impacts. Upon the 15th impact there is a second, larger jump. This big jump is what is referred to as 'link-up', the sudden growth of delaminations towards each other.
- **'One impact in a one location'** - A 'location' is the point of impact. Hence, one impact in one location means that this point of impact is impacted only once.
- **'Repeated impacts in a one location'** - The same as the previous definition, however this single point of impact is impacted multiple times in the exact same location.
- **'One impact in multiple locations'** - This means that there is more than one point of impact. Each point of impact is impacted only one time.
- **'Repeated impacts in a multiple locations'** - The same definition as above, but every point of impacted is impacted multiple times.

4.3. Experimental Setup

ASTM clamps (as shown in fig. 4.2) are often used for low-velocity impacts, however these do not satisfy the purpose for multiple location impacts due to the cutout area and inconsistent/unreliable clamping conditions (read appendix A for more information on the ASTM clamps). Hence, a redesigned clamp which satisfies the needs for this research was designed.



(a) ASTM support fixture for drop-weight experiments. (b) ASTM support fixture for quasi-static experiments.

Figure 4.2: ASTM support fixtures [7, 9].

The redesigned, improved clamp was based on a fuselage bay which is the area between two stringers and two frames, as shown in fig. 4.3. The centre of the hatched area indicates the area of interest for this research which was chosen to avoid impact conditions such as impacts next to a stringer and had dimensions of 150 mm × 300 mm. The width of the specimen was set at 150 mm because this was the maximum width to fit in the fatigue bench for further fatigue testing.

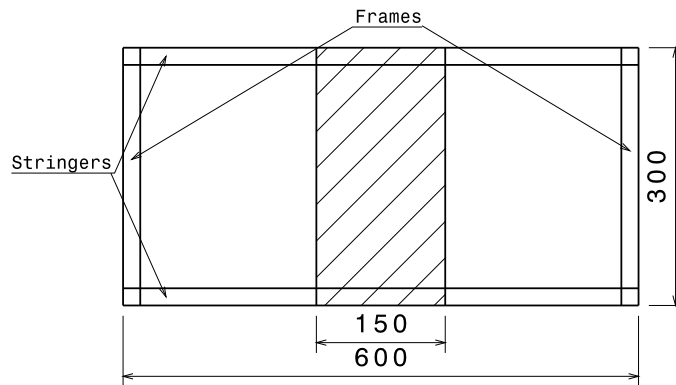


Figure 4.3: Estimate dimensions of a fuselage bay. Hatched area indicates the research space/specimen dimensions.

Furthermore, the stringer edges were assumed to be clamped edges (with bolts) while the other two edges were clamped only by friction to recreate a bi-axial stress state while also allowing movement. The final test specimen and test clamp configurations are shown in fig. 4.4 where the hatched areas indicate the hatched area from the fuselage bay in the previous figure, fig. 4.3.

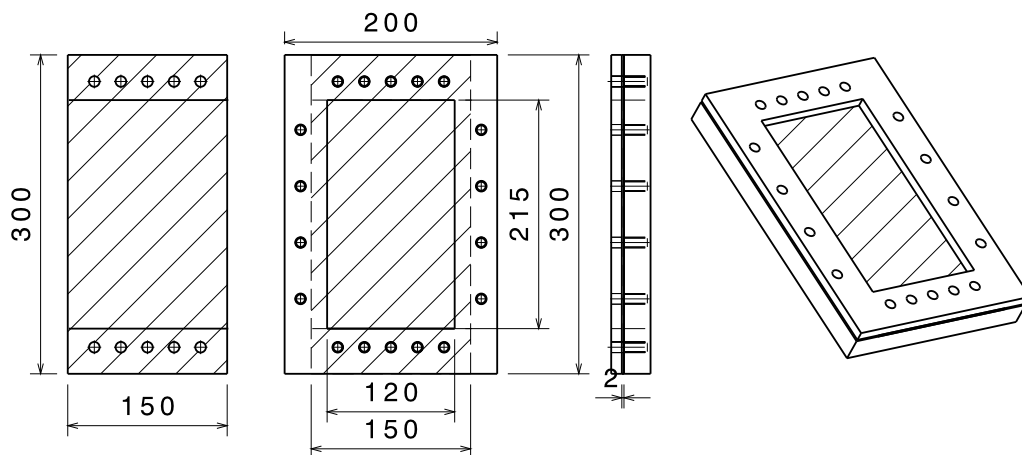


Figure 4.4: Test specimen (far left) and the test clamp containing the test specimen. Test specimen clamped by bolts on the top and bottom, not on the vertical sides.

Assuming the bolts are all torqued to the same amount, this test clamp is able to satisfy consistent boundary conditions for all tests. Furthermore, the clamp offers enough space to examine the effect of multiple impact locations.

Furthermore considering the specimen material, composites are available in many configurations such as uni-directional/woven layers or the type of fibre/matrix material, etc. Unfortunately, the exact material and the fuselage layup for composite aircraft such as the Boeing 787 were unknown to base the material choices on. The research must therefore assume similarities of the Boeing 787 to aircraft with similar fuselage dimensions such as the Boeing 777.

Fortunately, it was known that the Boeing 787 is made from uni-direction carbon fibre polymer layers. However, the correct matrix material, carbon fibre material or layup remained unknown. Hence, the material choice reduced to the material available at Delft University of Technology. This material is called 'Delta-Tech 120' which is UD carbon fibre prepreg with material specifications shown in table 4.1.

Furthermore as mentioned above, the layup used on the Boeing 787 was unknown but is assumed similar to the skin thickness of the Boeing 777 which is in the range of 2.0 mm to 2.3 mm [38]. Given that a DT120 cured layer has a thickness of 0.156 mm, the choice was made to use a 16 layer laminate with a total thickness of 2.5 mm which is comparable to that of the Boeing 777.

Table 4.1: Delta-Tech 120 UD material properties based on average properties [18].

Mechanical Tests	Room Temp.
Tensile Strength (0°) [MPa]	3010
Tensile Modulus (0°) [GPa]	145
Tensile Strength (90°) [MPa]	39
Tensile Modulus (90°) [GPa]	6.4
Compression Strength (0°) [MPa]	1020
Compression Modulus (0°) [GPa]	133
Compression Strength (90°) [MPa]	138
Compression Modulus (90°) [GPa]	8.1
In-Plane Shear Strength [MPa]	95.6
In-Plane Shear Modulus [GPa]	3.4

Furthermore, the layup was chosen as quasi-isotropic, symmetric and balanced based on the complex and large number of load-cases that the fuselage must be able to endure. The 16 layer stacking sequence provided in the ASTM standards is also used for this research, which is equal to $[45, 0, -45, 90, 45, 0, -45, 90]_S$ with laminate properties listed in table 4.2 and the layup fibre directions shown in fig. 4.5 [9].

Table 4.2: Laminate properties based on average properties presented in table 4.1.

Mechanical Tests	Room Temp.
Tensile Modulus (0°) [GPa]	59.1
Tensile Modulus (90°) [GPa]	59.1
In-Plane Shear Modulus [GPa]	2.03
Ply Thickness [mm]	0.156
Laminate Thickness [mm]	2.5

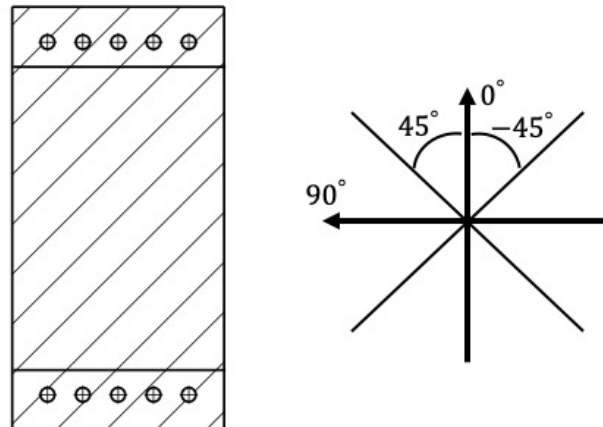


Figure 4.5: Test specimen on the left and the fibre directions shown on the right.

4.4. E-series: Effect of Impact Energy

Moving on to the impact experiments, the primary goal of the E-series was to determine the relation between impact energy and delamination area. The E-series was introduced on the basis of the following research question:

- What is the effect of impact energy on the damage response of the laminate?

To determine the relation of interest, an impact surface with a single impact location in the centre of the specimen would be sufficient. However, more information and tests can be performed from the large available surface area of the specimen. Therefore, the E-series was assigned a secondary goal, i.e. to investigate at which impact spacing link-up appears.

To satisfy both the E-series' goals there were in total 5 impact locations spaced on a line in the middle of the specimen with impact spacings equal to 3.75 mm, 7.5 mm, 15 mm and 30 mm as illustrated in fig. 4.6. However, if link-up would occur between the impact locations it would not be possible to record the delamination size of a single impact which is required for the primary goal of the series. To avoid this problem two c-scans must be made, one c-scan after the 1st impact in order to record a single delamination and a second c-scan after the 5th impact in other to record any link-up.

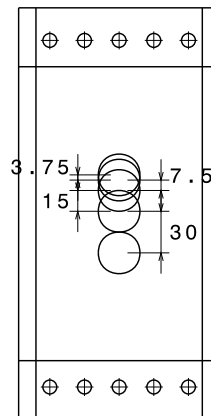


Figure 4.6: Impact surface for E-series experiments.

With the goal of obtaining a relation between delamination area and impact energy, a range of impact energies was required. There were in total 7 different impact energies tested, i.e. 3 J, 6 J, 9 J, 12 J, 15 J, 25 J and 35 J. Furthermore, a 'one impact per location' philosophy must be used because otherwise it is not possible to extract the delamination size corresponding to the specific impact energy.

In summary, there were in total 7 experiments with two variables, i.e. the impact energy and impact spacing/separation. These tests are summarized in the test matrix which is presented in table 4.3.

Table 4.3: E-series test matrix. Test variables are: impact energy and impact spacing/separation.

Test No.	Spacing [mm]	Energy [J]	No. locations [-]	No. Impacts / Location [-]
E.1	3.75, 7.5, 15, 30	3	5	1
E.2	3.75, 7.5, 15, 30	6	5	1
E.3	3.75, 7.5, 15, 30	9	5	1
E.4	3.75, 7.5, 15, 30	12	5	1
E.5	3.75, 7.5, 15, 30	15	5	1
E.6	3.75, 7.5, 15, 30	25	5	1
E.7	3.75, 7.5, 15, 30	35	5	1

4.5. R-series: Effect of Impact Fatigue

Hailpads reveal that hailstones occasionally overlap each other. The overlapping of hailstones is referred to as the repetition of impacts (also known as 'impact fatigue') which led to the R-series experiments where the following research question was considered:

- What is the effect of impact fatigue loading on the damage response of the laminate?

There were in total two experiments in the R-series, i.e. R.1 and R.2. R.1 investigated the damage response of a laminate upon impacting the specimen an extensive number of times and R.2 investigated the difference in damage response by an impact pattern which was impacted 5 times per location (performed in the S-series) opposed to the same impact pattern impacted once in every location.

Starting with experiment R.1, a 'repeated impacts in one location' philosophy was maintained. Hence, a single impact location in the middle of the specimen was used for its impact pattern as shown in fig. 4.7a. Using this configuration, the damage growth due to repeated impacts is able to be recorded by c-scanning the specimen a number of times. Furthermore, the number of impacts was limited to the feasibility of operating the machine manually since it was not possible to do it automatically. A total of 225 impacts were performed with all impacts performed at 6 J.

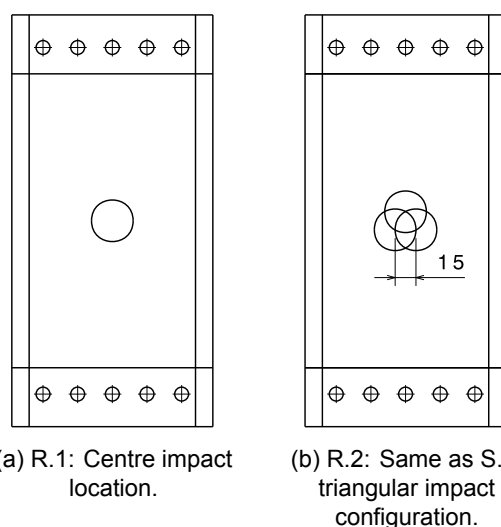


Figure 4.7: Impact surfaces for the R-series experiments.

Moreover, the second experiment (R.2) had the same impact pattern as the test in the S-series with the smallest impact spacing (S.4) in order to explore the difference between the damage response of such a pattern between repeated and single impacts. As mentioned above, this test adopted a 'one impact per location' philosophy. The impacts performed were with the same impact energy as in S.4 and R.1, which was 6 J per impact.

In total, two experiments were performed in this R-series with two test variables, i.e. the number of locations and the number of impacts. The tests are presented in the test matrix shown in table 4.4.

Table 4.4: Impact fatigue loading test matrix with test variables: impact spacing and number of impacts.

Test No.	Spacing [mm]	Impact Energy [J]	No. locations [-]	No. Impacts [-]
R.1	N/A	6	1	225
R.2	15	6	3	1

4.6. S-series: Effect of Impact Spacing

The impact surface due to hail has a stochastic nature i.e. some impacts are spread further apart than others. This series' goal was to explore the effect of impact spacing (an effect such as 'link-up'), based on the following research question:

- What is the effect of impact spacing on the damage response of the laminate?

The stochastic impact surface nature causes complexity in designing the S-series experiments because it is unfortunately not possible to test a stochastic impact pattern with the available technology at Delft University of Technology. Furthermore, testing such an impact pattern may hinder understanding the damage mechanisms and damage responses observed.

Instead, an equilateral triangle was chosen as illustrated in fig. 4.8. There were in total four equilateral triangle impact surfaces with different dimensions, i.e. 30 mm, 45 mm, 60 mm and 15 mm. It is not by coincidence that the fourth impact pattern had a lower spacing value than the previous three which came as a result of the observations originating from the first three which is explained later in the results section (section 5.5).

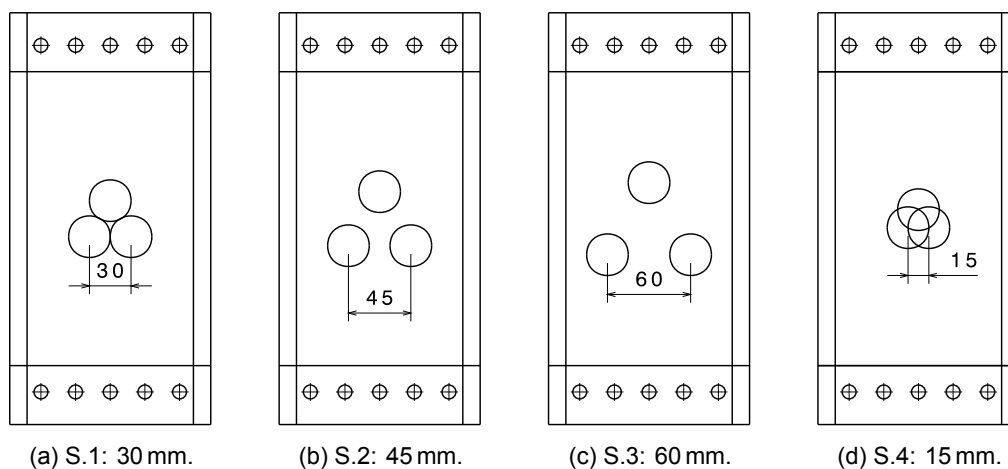


Figure 4.8: Equilateral triangle impact surfaces for the S-series experiments.

Furthermore, the lower impact energy threshold to cause damage was recorded at 5.8 J during the primary test which is explained in more detail in appendix A. Continuing with this threshold, the S-series proceeded its experiments with a rounded value of 6 J. Moreover, an arbitrary number of impacts per location was set at 5 due to insufficient knowledge on the repetition of impacts at the time.

Hence, there were a total of 4 experiments in the S-series. The only variable in the S-series was impact spacing. The details of each experiment are summarised in table 4.5.

Table 4.5: S-series, impact spacing test matrix. Test variable: impact spacing.

Test No.	Spacing [mm]	Impact Energy [J]	No. locations [-]	No. Impacts / Location [-]
S.1	30	6	3	5
S.2	45	6	3	5
S.3	60	6	3	5
S.4	15	6	3	5

4.7. L-series: Required Spacing for Link-Up (S-series Cont'd)

The L-series served as a continuation in the investigation of impact spacing. More particularly, this series looked into the minimum spacing required for delamination link-up without the repetition of impacts.

The impact pattern consisted of 3 impact locations positioned on a straight line as presented by the drawings in fig. 4.9. The total of the 6 experiments adopted the same impact energies as the E-series, i.e. 6 J, 9 J, 12 J, 15 J, 25 J and 35 J with the exception that 3 J was excluded because it does not cause damage. Furthermore as mentioned in the previous paragraph, all impact locations were impacted only once.

The E-series provided delamination sizes for the above mentioned impact energies. Hence, the impact locations were spaced at a distance of the long-axis of the delamination. The reason for spacing impacts at a distance of the long-axis was because delaminations have seen to link-up when the distance between the impact locations is equal to the long-axis of one delamination (in the case both delaminations are created by the same impact energy). Moreover, to determine if the long-axis is the true upper spacing threshold, a third impact is positioned at 110% of the long axis.

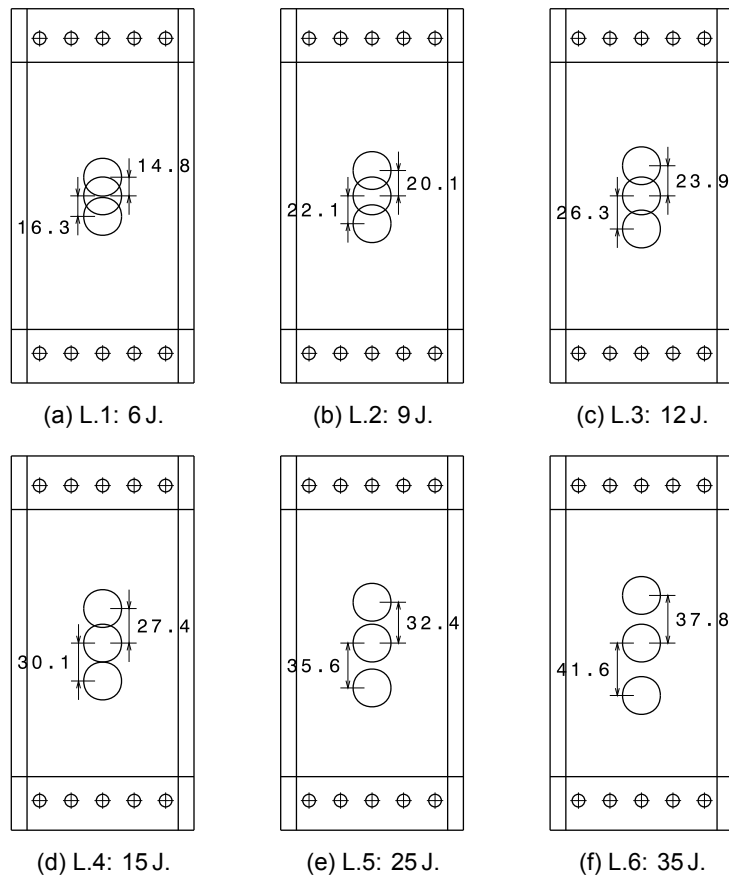


Figure 4.9: Impact surfaces for the L-series experiments.

In this L-series the only two test variables were the distance between impacts and the impact energy. The specifics of each experiment is presented in table 4.6.

Table 4.6: L-series test matrix. Test variables were impact spacing and impact energy.

Test No.	Spacing (L.A., 1.1·L.A.)	Energy	No. locations	No. Impacts / Location
	[mm]	[J]	[-]	[-]
L.1	14.8, 16.3	6	3	1
L.2	20.1, 22.1	9	3	1
L.3	23.9, 26.3	12	3	1
L.4	27.4, 30.1	15	3	1
L.5	32.4, 35.6	25	3	1
L.6	37.8, 41.6	35	3	1

4.8. O-series: Effect of Impact Orientation (S-series Cont'd)

The final series on impacts was the O-series which was also a continuation of the S-series. The L-series exposed a hint of delamination directionality which triggered the onset of the O-series which investigated the effect of positioning/orienting impact locations at an angle.

Delaminations expose a long-axis bias in the -45° direction. Hence, the straight impact pattern in the previous L-series now has its long axis positioned along the -45° line and its short axis positioned along the 45° line. Furthermore, two impact energies were tested, i.e. 15 J and 35 J. Finally as for the previous L-series, each test had 3 impact locations each impacted only once. The impact surfaces are shown in fig. 4.10.

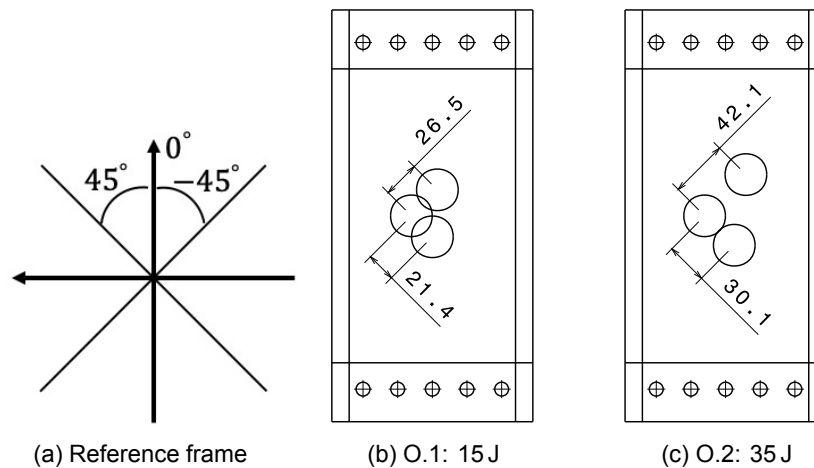


Figure 4.10: Impact surfaces for the O-series experiments.

The experiment choices and variables for the O-series are summarised in the test matrix presented in table 4.7. There were in total two experiments and two variables which were impact spacing and energy.

Table 4.7: O-series test matrix. Test variables were impact spacing and impact energy.

Test No.	Spacing [mm]	Impact Energy [J]	No. locations [-]	No. Impacts / Location [-]
O.1	21.4, 26.5	15	3	1
O.2	30.1, 42.1	35	3	1

4.9. F-series: Effect of Mechanical Fatigue

There were two impacted specimens mechanically fatigued in tension to investigate delamination growth. This series is based on the following research question:

- Does impact damage propagate by mechanical fatigue loading the specimen?

The first experiment design choice considered the number of fatigue cycles which was once again based on the application of the Boeing 787. The Boeing 787 is designed to be able to sustain 66 000 flights (cycles), hence the experiments will adopt this number of cycles [12].

Furthermore, the cabin pressure must be known to calculate the load in the fuselage skin. Each flight must be able to withstand a peak cabin pressure at cruise altitude of 12 000 m with the cabin doors of a Boeing 787 closing at 1830 m [4]. The cabin pressure at this altitude is equal to (using the static atmospheric model, ISA):

$$\left. \begin{array}{l} P_{1830m} = 81.2\text{kPa} \\ P_{12000m} = 19.3\text{kPa} \end{array} \right\} P_{\text{cabin}} = 81.2 - 19.3 = 61.9\text{kPa} \quad (4.1)$$

Furthermore, a simplistic model is assumed where the fuselage stringers hold the longitudinal loads, the frames maintain the shape of the fuselage and the skin holds the cabin pressure and shear loads [3]. Hence, it is assumed here that the skin is loaded only in tension due to the cabin pressure.

Moreover, to calculate the maximum cabin stress, the fuselage radius and skin thickness is required. The Boeing 787 has a diameter of $D = 5.74$ m [4] and the fuselage skin thickness was assumed equal to the thickness which was previously agreed on, = 2.5 mm. Lastly, assuming the fuselage to be a pressure vessel the hoop stress is used since it is twice as large as the longitudinal stress and hence considers the worst case scenario.

$$\sigma_{\max(\text{hoop})} = \frac{P_{\text{cabin}} R}{t} = \frac{61.9 \text{ kPa} \cdot 2.87 \text{ m}}{0.0025 \text{ m}} \Rightarrow \sigma_{\max(\text{hoop})} = 71 \text{ MPa} \quad (4.2)$$

There were in total 2 specimens tested. The first specimen was fatigued at 71 MPa which was c-scanned both at 66 000 and 132 000 cycles. The additional 66 000 cycles were introduced to investigate the damage progression with more cycles. The second specimen was fatigued at 142 MPa but only up to 66 000 cycles to investigate the damage progression at a higher fatigue load. The tests are summarised in table 4.8.

Table 4.8: Mechanical fatigue test matrix. Cyclic loading done at 10 Hz.

Test No.	Stress Ratio, R [-]	Max. Stress, σ_{\max} [MPa]	No. Cycles [-]
F-S.3	0.0	71	132 000
F-S.1	0.0	142	66 000

Important to mention is that composites under fatigue loading tend to suffer from loading frequencies higher than 20 Hz [2]. The reason for this is because heat is built up which may soften the matrix material and can more easily trigger the onset of damage. For this reason the frequency of the fatigue tests was reduced to a conservative value of 10 Hz.

Chapter 5

Results

5.1. Results Structure

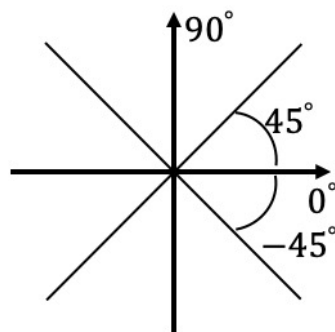
There were in total 6 series of experiments (S, E, R, L, O and F), each having their own research focus. However, some series were used to investigate two topics, each topic belonging to another research question. The results have been organised by research question with the results of each series divided under the appropriate research focus.

For example, the E-series have contributed to both the effect of impact energy and the effect of spacing. Hence, E-series results will be discussed in both the effect of impact energy section and the effect of spacing section (see sections 5.3 and 5.5).

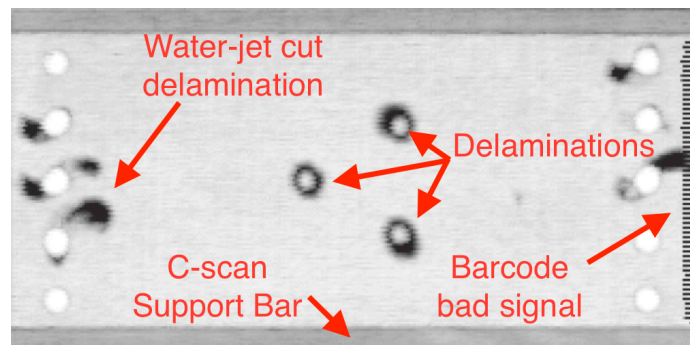
Furthermore, each section first analyses the c-scans made of the specimens which show any delaminations followed by the processed data based on those c-scans. Where applicable, also some microscopy images are presented at the end of each section.

5.2. Reading C-scans and Microscopy images

C-scans are fairly simple to understand, however a drawing is made to clarify. Furthermore, all c-scans provided in this report were made of the entire specimen. The points of attention are indicated in fig. 5.1b. Additionally, to better understand the results later, the fibre directions are shown in fig. 5.1a.



(a) Fibre directions



(b) C-scan example

Furthermore, the original specimens as in fig. 5.1b were cut open for optical microscopy observations. To understand what part of the specimen is cut open, refer to the cutting plans of the specimens in fig. C.2. Furthermore, the picture in fig. 5.2 shows where the impact site, delaminations and delamination layer jumps are to be found.



Figure 5.2: Microscopic image example

5.3. Effect of Impact Energy

The effect of impact energy concern is based on the E-series experiments. This section provides the results for the third research question which was formulated as:

- What is the effect of impact energy on the damage response of the laminate?

5.3.1. C-scans

Upon comparison of the 7 c-scans, a clear increase in delamination area is shown as impact energy increases. Starting with the lowest impact energy, the 3 J test revealed merely small dents. Moving towards higher impact energies there is a gradual increase in delamination area. Noticeable on the c-scans is, the larger the delamination the more pronounced the directionality of a delamination. Based on location 1, the preferred delamination directions are -45° and 90° which is seen on the c-scans in fig. 5.3.

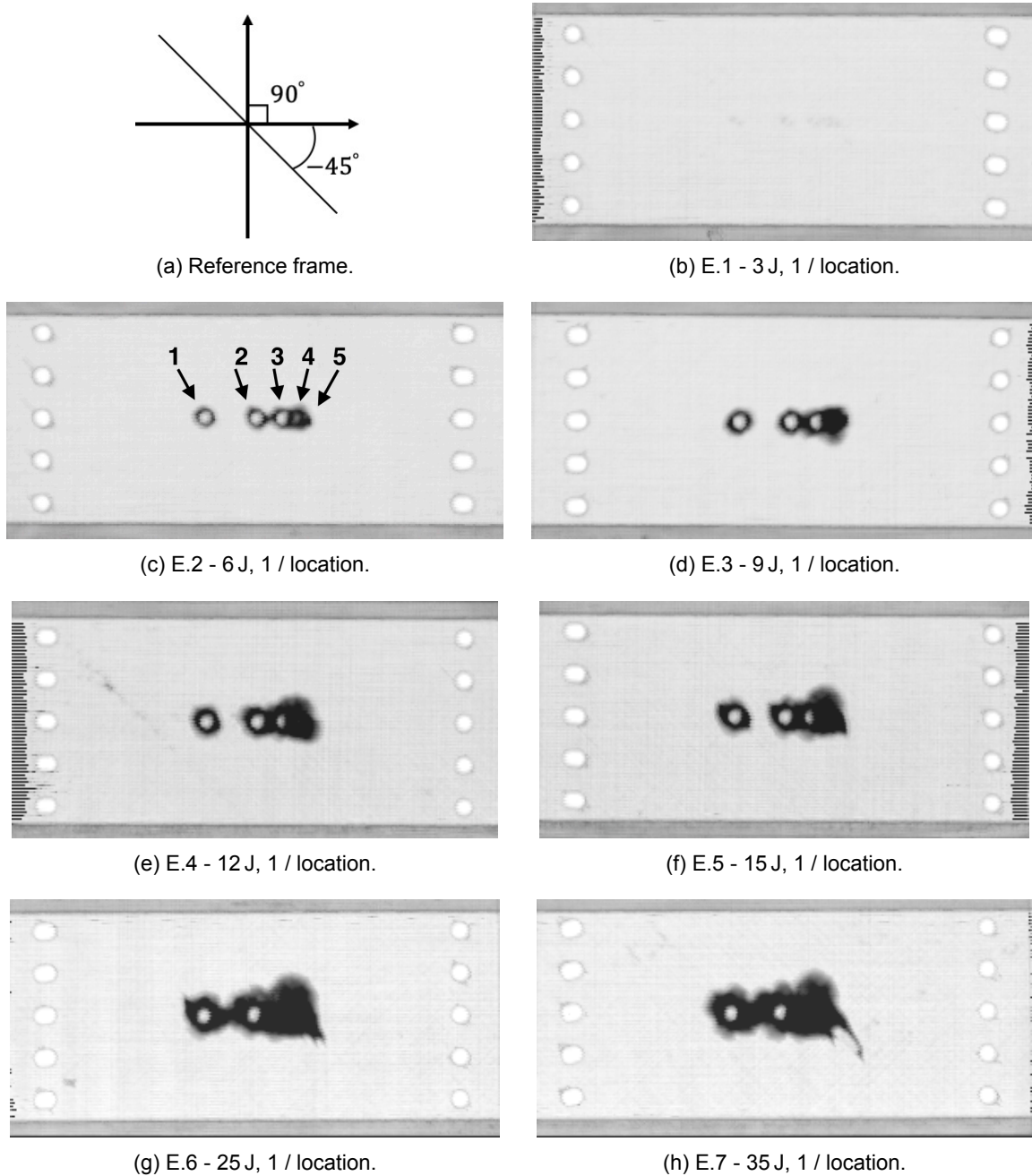


Figure 5.3: E-series c-scans for E.1-7.

The remaining impacts (impacts 2 to 5) on the right hand side are analysed later in the section on spacing (presented in section 5.5).

5.3.2. Processed data

As mentioned before, the specimens were c-scanned twice, the first c-scans were made after impact '1' was performed and the second c-scans (which are displayed in fig. 5.3) were made after the other impacts 2 to 5 were also performed. By quantifying the qualitative c-scan delaminations with a short- and long-axis and a delamination area it is possible to compare them to each other and identify trends. The characteristics are calculated based on the first c-scans to avoid other impacts possibly affecting the first impact.

These characteristics were calculated using MATLAB written software to ensure consistency in measurements (the MATLAB software is explained in appendix C.4). The characteristics are presented in table 5.1 and the delamination area trend is plotted in fig. 5.4. The figure illustrates that delamination area approximately follows a square root equation. The graphs for the short- and -long axes and the ratio are presented in appendix C.1.

Table 5.1: Delamination characteristics for E-Series.

Impact Energy [J]	3	6	9	12	15	25	35
Area [mm²]	0.0	154.0	259.0	378.4	462.4	667.2	909.0
Short Axis [mm]	0.0	13.2	16.4	20.1	21.4	26.2	30.6
Long Axis [mm]	0.0	14.8	20.1	23.9	27.5	32.5	37.9
Short/Long [-]	-	0.89	0.81	0.84	0.78	0.80	0.80

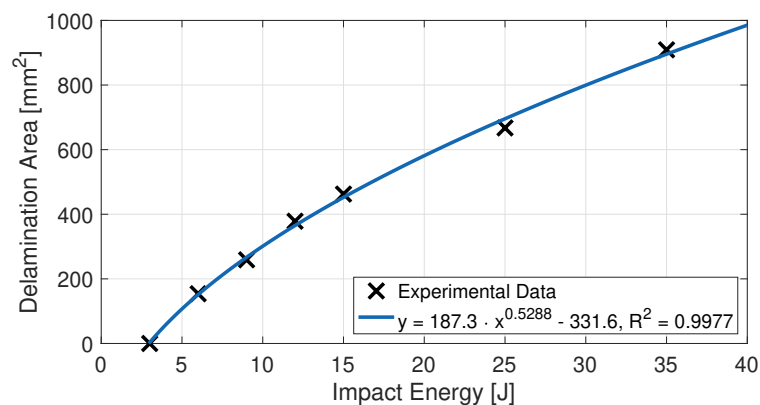


Figure 5.4: Delamination area relation as a function of impact energy. Both the experimental data points and best fit trend are presented.

5.3.3. Optical Microscopy

The 7 specimens have also been cut into smaller specimens to analyse the damage through the thickness of the laminates. All specimens are looked at from the same perspective (the specimen cutting plans for E.1-7 are shown in appendix C.2, figs. C.2a to C.2g). Figure 5.5 presents the 6 microscopy images. The optical microscopy image of E.1 is treated in section 5.4.3 because it considers impact fatigue instead.

The largest delaminations occur predominantly on the interface between the -45° and 90° layers. This is called the preferred interface because delaminations are seen to grow towards it and once there, they continue to propagate further on the same interface. This observation becomes more apparent the higher the impact energy.

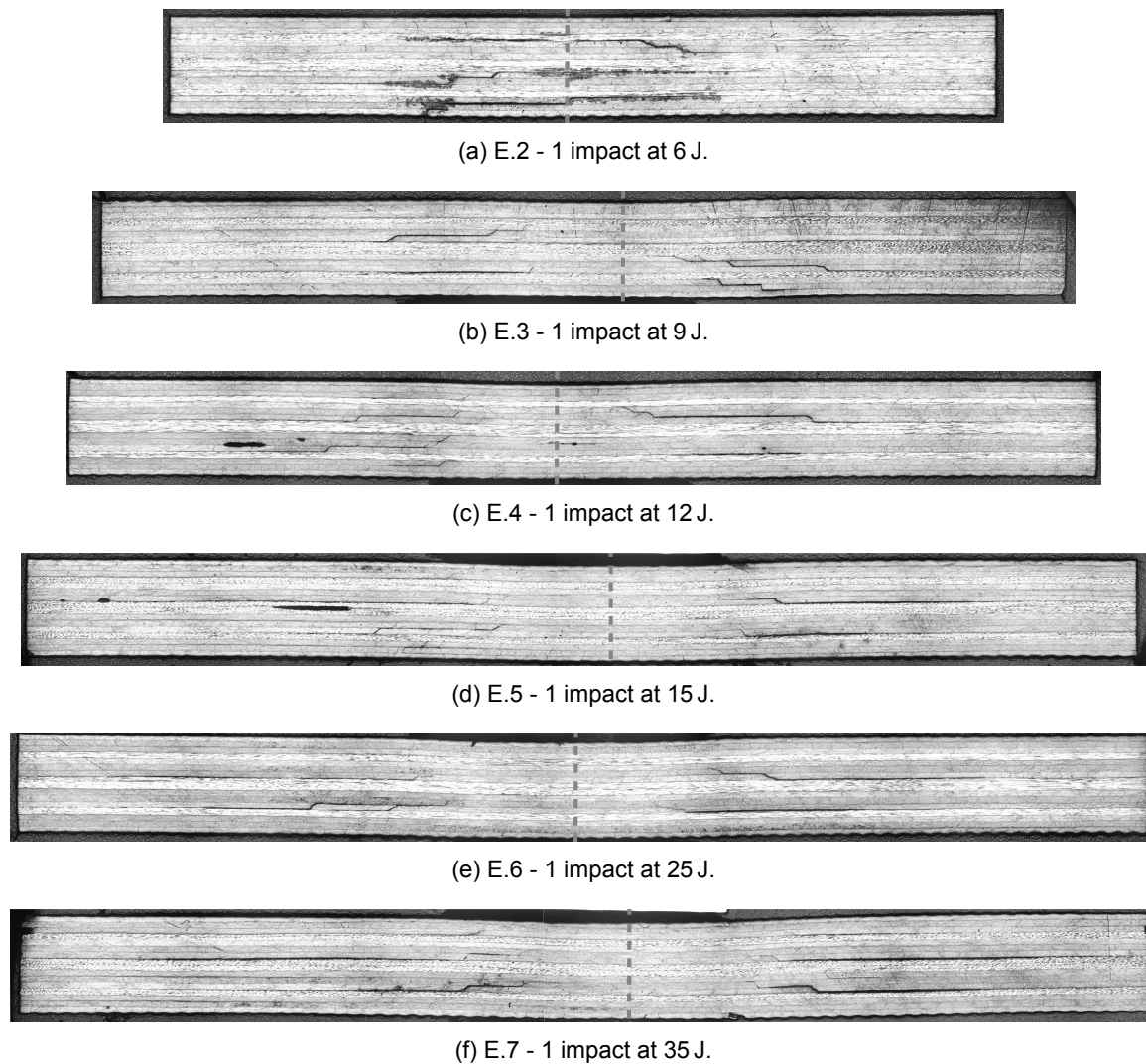


Figure 5.5: Microscopy images to illustrate effect of impact energy. Pictures to scale.

5.4. Effect of Repeated Impacts

The results presented in this section arise from both the R- and E-series experiments and show the effect of repeated impacts on the damage response. The following research question holds for this section:

- What is the effect of repeating impacts on the damage response of the laminate?

5.4.1. C-scans

Optimally for the R.1 experiment that repeated impacts up to 225 times, a c-scan would have been taken every few indentations to record delamination growth. However, due to the labour intensive process of creating one c-scan this was not possible. Instead, c-scans were taken after the 150th and 225th impact and were combined with c-scans of other series, i.e. a c-scan of 1 impact at 6 J (E.2, presented previously in fig. 5.3c) and a c-scan of 5 impacts at 6 J (S.2, presented later in fig. 5.12b).

The c-scans presented in fig. 5.6 shows that delamination area increases with repeated impacts in a stable manner, i.e. no abrupt delamination growth is observed. Furthermore it is seen that the impacts in figs. 5.6a and 5.6b are not positioned in the centre. Arguably, these experience different impact conditions compared to R.1 where the impact is positioned centrally. Comparing the delamination areas calculated later (see table 5.4) shows negligible differences which do not affect any of the conclusions

or observations.

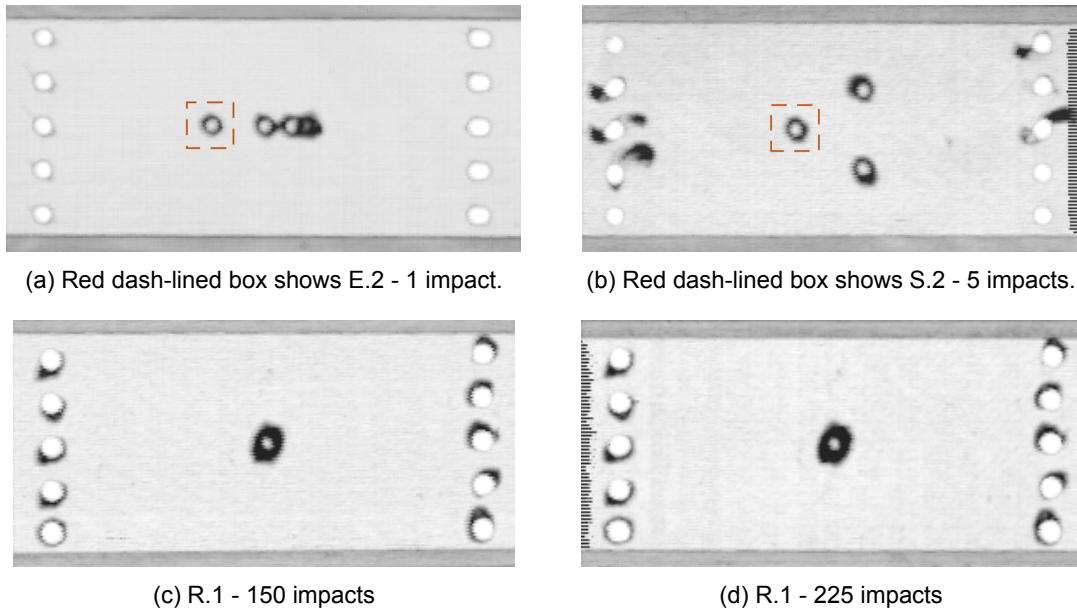


Figure 5.6: C-scans of impacted spacing tests.

5.4.2. Processed Data

The delaminations shown in fig. 5.6 are quantified for all four c-scans using the same MATLAB software as in the previous section. The quantified data reveals delamination area growth in the form of a power equation. Moreover, the delamination area growth rate decreases with an increase in number of impacts. This means that from the 1st to the 2nd impact, there is a larger increment in area compared to that of the 2nd to the 3rd impact. The data is graphed in fig. 5.7 and some data points are also presented in table 5.2 for clarity.

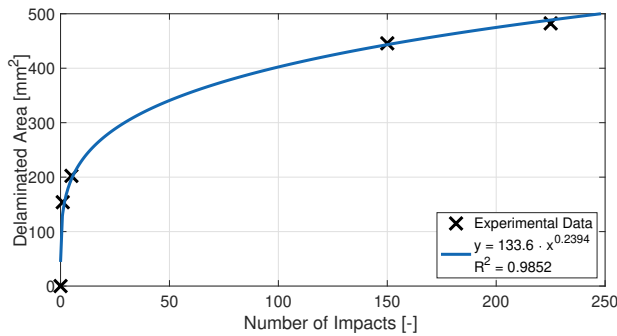


Table 5.2: Delamination area for R.1

Impact Number [-]	Area [mm ²]
0	0.0
1	154.0
5	202.4
150	445.7
225	482.3

Figure 5.7: Delamination area versus the number of impacts including best-fit trend. $R^2 = 0.9852$.

In contrast to the limited amount of c-scans for area growth data, there is plenty of data for absorbed energy. The absorbed energy graph (presented in fig. 5.8) shows a rapid drop to a constant value after about 5 impacts. Although the absorbed energy graph shows consistent values, something unexpected occurred at the 121st and 151st impacts. These two impacts show two peaks in absorbed energy, however the reason for only one of them is known. A c-scan was made at the 150th impact and the repositioning caused an initial jump in absorbed energy due to the material repositioning and the point of impact being slightly different than before. The reason for the 121st impact remains unknown but is most likely also due to a small movement in the test setup.

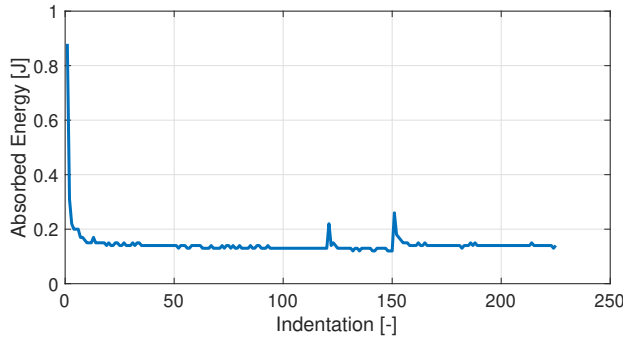


Table 5.3: Absorbed energy for R.1

Indentation [-]	Absorbed Energy [J]
1	0.88
5	0.20
150	0.12
225	0.14

Figure 5.8: Effect of number of impacts on the absorbed energy per impact.

Comparing the graph for absorbed energy with the graph of delamination area (figs. 5.7 and 5.8), it is apparent that the biggest jump in delamination area occurs in sync with the biggest jump in absorbed energy. Plotting the absorbed energy against the increment in delamination area (Δ Area) provides a quasi-linear trend towards the origin with an increase in impacts shown in fig. 5.9. A coherent relation is present between the absorbed energy and increment in delamination area. These results show that there is a clear relation between the amount of damage done and the absorbed energy. This observation can be a powerful tool in revealing if any damage is done during impact experiments without the use of c-scans.

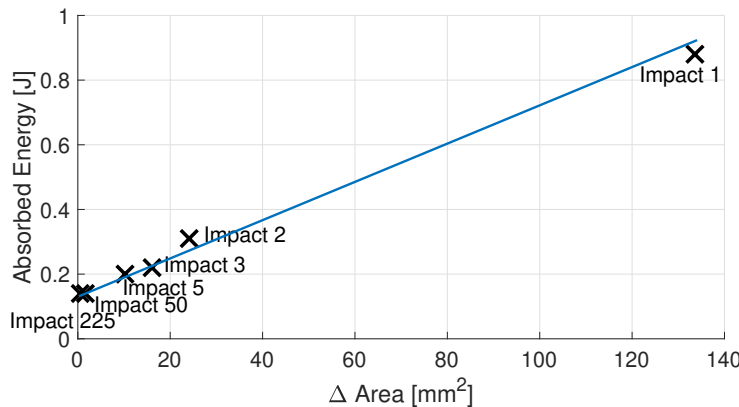


Figure 5.9: Absorbed energy required per Δ Area.

5.4.3. Optical Microscopy R-series

To investigate the effect of repeating impacts on the through thickness damage, three specimens with a different number of impacts (but all impacted with the same impact energy) have been cut open for optical microscopy. The first specimen (E.2) was impacted once, the second specimen (S.2) was impacted 5 times and the third specimen (R.1) was impacted 225 times. The microscopy images of these specimens are shown in fig. 5.10.

Strangely, while comparing the microscopy images for 1 and 5 impacts shows that there are less delaminated layers for the image of 5 impacts. This result may be counter-intuitive, however, cutting the specimens was manual work and the cut for the specimen of 5 impacts was made too far from the impact zone which unfortunately cut away some valuable information for a good comparison.

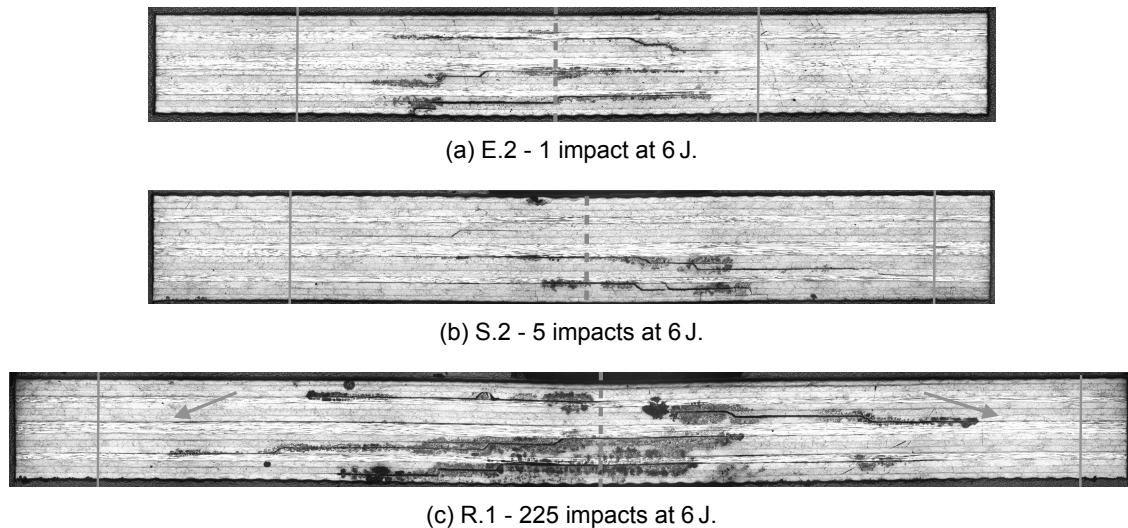


Figure 5.10: Microscopic pictures to illustrate effect of repeated impacts. Delamination width indicated by the solid vertical lines. Preferred interfaces indicated by arrows. Pictures to scale.

Essentially, the images reveal that delamination width increases due to repeated impacts. The delamination width grows from 1 to 5 impacts and grows even further outwards from 5 to 225 impacts. Additionally, as delaminations grow outward due to the number of impacts, the delaminations also jump between layers to propagate towards the preferred layers where it continues to grow outwards. The preferred layers are the widest delaminations seen in fig. 5.10 which occur predominantly on the $-45^{\circ}/90^{\circ}$ interfaces.

E-series

Furthermore, there was one specimen in the E-series which did not show delamination due to its too low impact energy. Hence, the question had arisen i.e. what would happen if repeated impacts at low impact energy would occur. Perhaps very small delaminations could have been created due to impact fatigue. The cutting plan for this specimen is shown in fig. C.2a.

The microscopy image of this specimen is shown in fig. 5.11 but shows no hint of damage. However, remember that the impact zone was at most a few mm wide and cutting the specimen at exactly the right location was extremely difficult to do manually, hence the complete impact zone might not actually be shown in this image.



Figure 5.11: E.1 - 1 impact at 3 J.

5.5. Effect of Impact Spacing

Many experiment series contribute to the first research question. The contributing series are the S-, R-, E-, L- and O-series. The research question regarding the effect of spacing is:

- What is the effect of impact spacing on the damage response of the laminate?

5.5.1. C-scans

S-series

From the total of four S-series tests, only one test showed an effect due to impact spacing. This was the test with impacts spaced at the closest spacing (15 mm, 5 impacts per location at 6 J per impact).

Even though the other tests show no interaction due to spacing, there was interaction with the clamp edge, called the 'edge effect' (seen in both S.2 and S.3). The 'edge' refers to the clamping point of the specimen (see fig. 4.4). In other words, the c-scans reveal that the edge can cause abrupt and unstable advances in damage. These observations are shown in fig. 5.12. Furthermore, the location numbers which will be used for referring to later in the processed data section are indicated in fig. 5.12a.

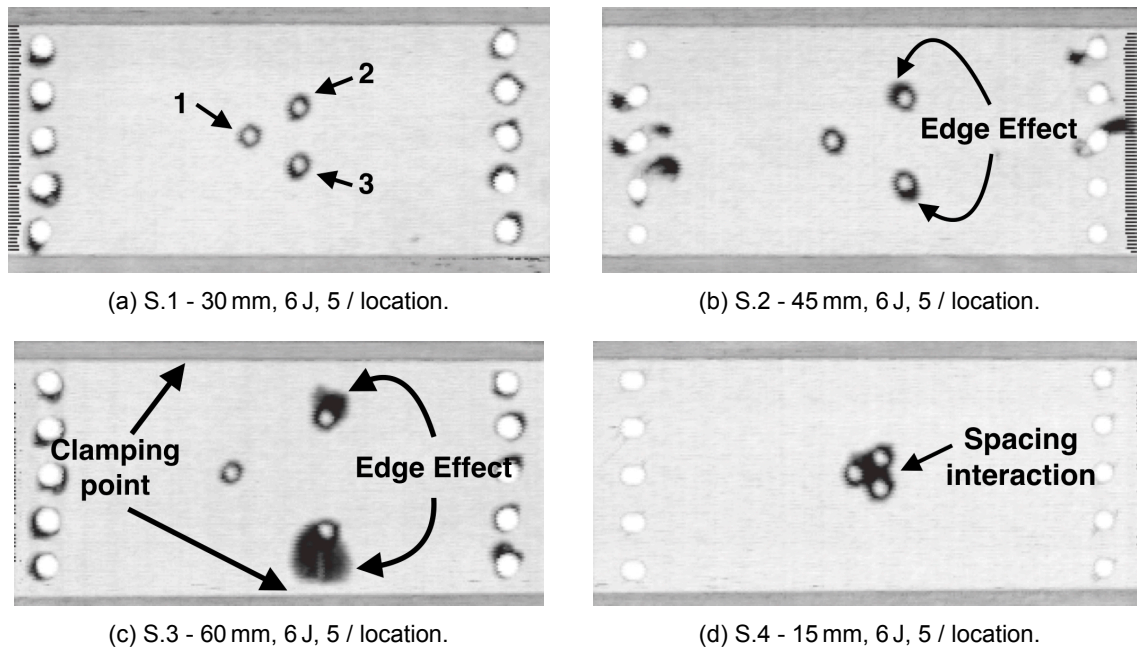


Figure 5.12: S-series c-scans for S.1-4.

R-series

Previously, it was revealed that the first impact causes the largest increment in delamination area. The second R-series test (R.2) with the same impact surface as S.4 (illustrated in fig. 5.12d) was tested to investigate if a '1 impact per location' triggers the link-up as that in S.4.

The answer is not clearly visible at first glance because three points of roughly the same size as that of E.2 are seen. However when carefully investigated, the two vertical impacts just barely show a hint of link-up. This is indeed joining of delaminations as confirmed by the microscopy images discussed later in section 5.5.3. However, the final damage response is not comparable to that of S.4.

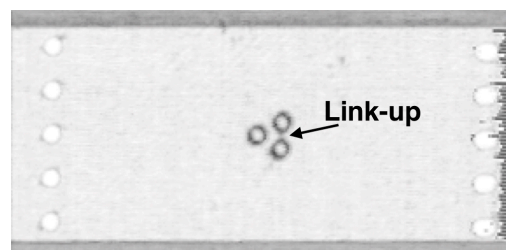


Figure 5.13: R.2 - 15 mm, 6 J, 1 / location.

L-series

From the 6 L-series tests in total, only the 9 J test (L.2) showed link-up. Even the 6 J test (L.1) surprisingly did not show link-up even though it was spaced at 14.8 mm which is a closer separation than in previous tests (S.4, R.2 and E.2) which showed link-up. As for the other four tests (L.3-L.6), merely three independent delaminations were detected. Furthermore, as explained in the E-series it is seen that the higher the impact energy the clearer the preference for delamination directionality becomes. The c-scans are presented in fig. 5.14.

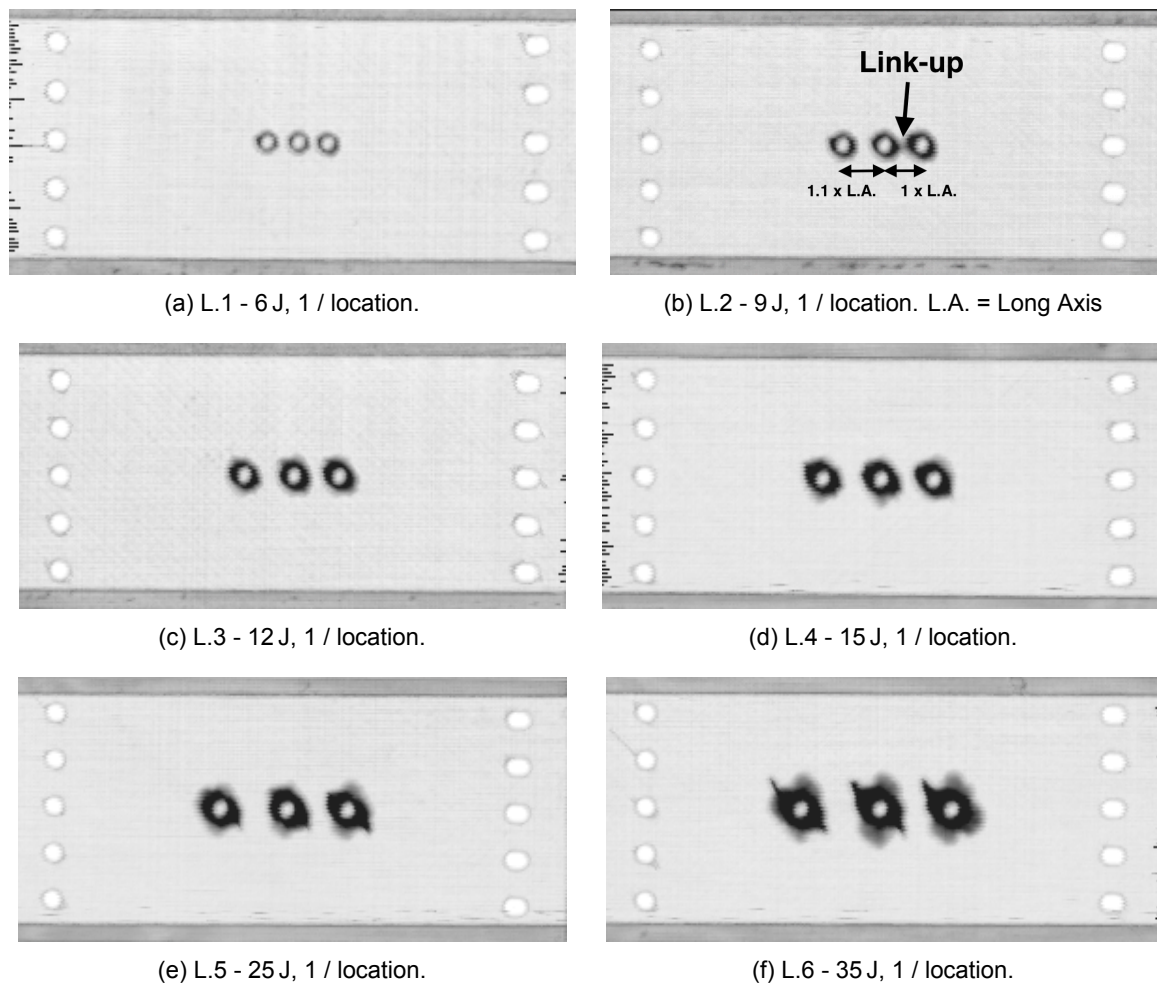


Figure 5.14: L-series C-scans.

The question that remains is why the prediction of link-up spacing is wrong. An intuitive answer considering delamination directionality could be that the orientation of impacts (positioning impact locations at an angle) was neglected and that this is important. However, R.2 and E.2 both showed link-up while neglecting orientation and scatter in delamination size could be the cause.

O-series

The O-series investigated the orientation effect as described above. There were two c-scans one for each test, however only the first c-scan (O.1) proves useful because because the second c-scan for test O.2 is affected due to impacting too close to the edge. Hence, it is difficult to draw comment on it due to the inability to see the order of events.

Nevertheless, the c-scan for the first test (O.1) shows useful results and some things are learned. Link-up is seen along the -45° , long axis line but not perpendicular to that. Positioning impacts at -45° allows delaminations to touch and link-up more easily since delaminations occur in the fibre direction. However, fibres act as a delamination blocker when positioned perpendicular to the fibre direction. The c-scans are presented in fig. 5.15. By now, all logical combinations of impact locations have been attempted to trigger link-up, but no combination is fully successful.

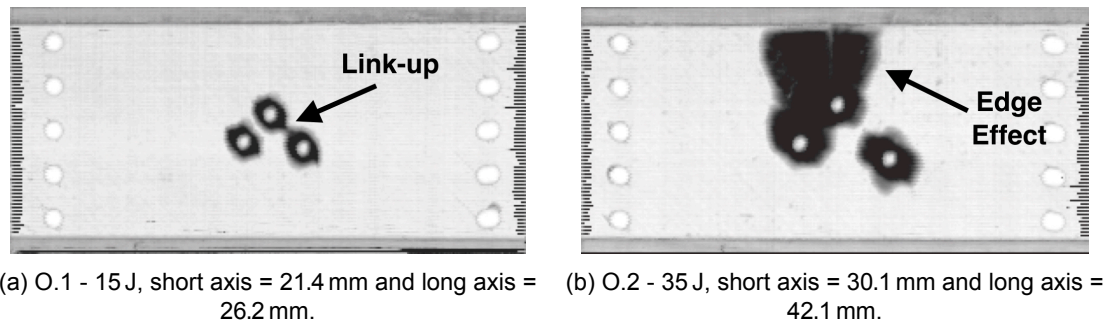


Figure 5.15: C-scans for impacted orientation tests.

5.5.2. Processed Data

S-series

A common method to present quasi-static indentation data is with force-displacement and energy-time curves. These curves have the ability to reveal a lot of information as is illustrated in this section. As long as the data is recorded, a force-displacement and energy-time curve can be calculated for any indentation. It would be unnecessary to present all those graphs here due to their great similarity. To see all the graphs, a full documentation of the results is presented in appendix C.

To illustrate the potential of these graphs, the results for the specimen with the largest delamination (in location 3, see fig. 5.12c) due to the edge effect (S.3) is used because the damage sequence can be easily seen from the graphs. A force-displacement curve shows a loading (top of the curve) and unloading part (bottom of the curve). Energy-time curves reveal the absorbed energy (which is equal to the height of the curve at the endpoint) which is also shown in the legend of the graph. The graphs are shown in fig. 5.16.

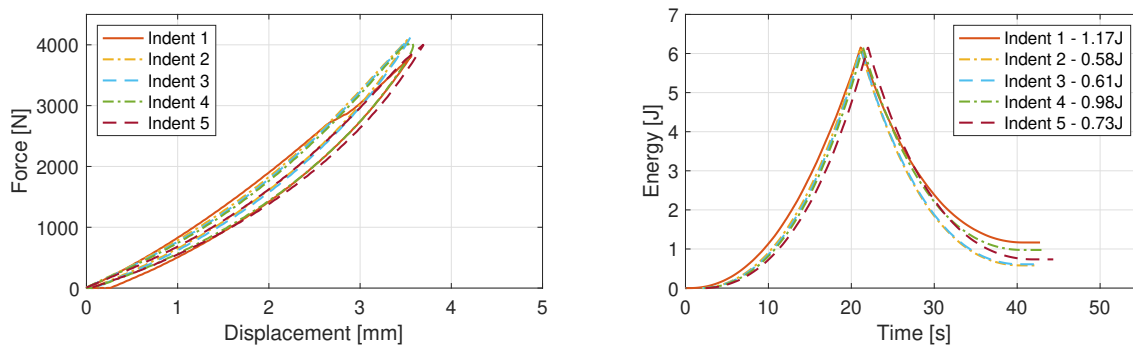


Figure 5.16: Example force-displacement and energy-time graphs for S.3, location 3.

These curves do not reveal their full potential. More information can be extracted if the data is restructured so that the relative maximum force and relative absorbed energy is presented instead. This way it can be seen if these values increase, decrease or remain stable and the same. Continuing with the delamination in location 3, the rearranged graphs are presented in fig. 5.17.

In the case that impacts occur free from the edge (which is not the case for S.3), typical curves show an increase in maximum force and a decrease in absorbed energy as impacts are repeated. A typical example of this looks like the curve for 'location 1' in fig. 5.17. However, it is clearly not the case that all three lines follow that trend. The curve for 'location 2' (top delamination in fig. 5.12) follows the general trend, but is larger in magnitude compared to location 1 due to the cutout edge. The curve for 'location 3' shows an irregular jump in absorbed energy upon the 4th indentation. This increase will now be discussed with more detail.

Upon comparing all force-impact number and absorbed energy-impact number (as in fig. 5.17) graphs obtained for the S-series, the graphs for S.3 clearly show a difference. The maximum indentation force for location 3 drops and the absorbed energy rises upon the 4th impact. Furthermore, significantly

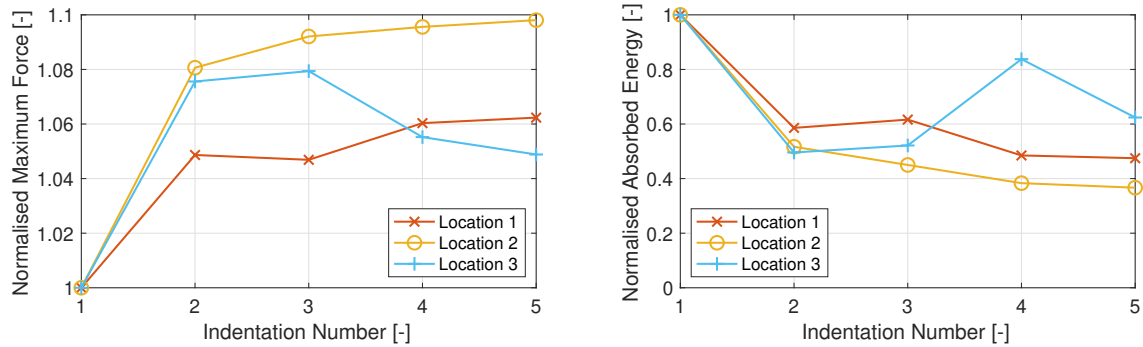


Figure 5.17: Restructured data. Relative maximum force and absorbed energy for S.3.

more cracking was heard upon the 4th and 5th impact. Combining all these observations, the greatest amount of the damage in this location proves to be created during the 4th and 5th indentation. In other words, the relation between absorbed energy and created damage discussed earlier is seen to hold in this case as well.

L-series

The delaminations recorded in the L-series c-scans have been quantified using the same MATLAB code. The quantified results reveal that there is scatter in delamination characteristic values. In other words, each delamination has slightly different dimensions. The characteristics for the left/middle/right delaminations are calculated and presented in table 5.4.

Table 5.4: Delamination characteristics for each delamination seen in L-series experiments.

		Left	Middle	Right	Average
L.1 - 6J	Short Axis	12.7	12.9	13.1	12.9
	Long Axis	13.4	13.3	13.9	13.6
	Area	133.4	134.6	143.2	137.1
L.2 - 9J	Short Axis	16.8	17.1	17.8	17.2
	Long Axis	18.4	19.5	20.6	19.5
	Area	241.6	261.5	288.0	263.7
L.3 - 12J	Short Axis	18.4	18.6	19.0	18.7
	Long Axis	24.6	25.0	25.2	24.9
	Area	355.2	365.3	376.7	365.7
L.4 - 15J	Short Axis	21.1	21.4	21.8	21.4
	Long Axis	25.7	27.0	25.8	26.2
	Area	426.3	455.3	441.4	441.0
L.5 - 25J	Short Axis	24.6	23.8	25.8	24.7
	Long Axis	31.4	32.8	33.6	32.6
	Area	605.4	614.8	680.2	633.5
L.6 - 35J	Short Axis	29.7	29.3	30.9	30.0
	Long Axis	42.1	44.6	43.9	43.5
	Area	980.8	1025.5	1067.2	1024.5

The scatter in the short and long axis values are in the order of magnitude from -1 to 0 in mm. The scatter may make the difference between just causing link-up (as shown by experiment L.2 in fig. 5.14b) or not. Furthermore, as in other experiments delamination orientation preference becomes evident from 12J impacts and higher with a preference again goes to the -45° and 90° layers.

E-series

Moving on to the spacing tests in the E-series (considering all impacts 1 to 5), the absorbed energy is calculated for each impact because this reveals the amount of damage created as spacing varies. As the specimen is impacted from location 1 to location 5, there is a general trend that shows a decrease

in absorbed energy with a decrease in impact spacing. In other words, the further apart impacts occur the more damage is inflicted. This trend can be seen in fig. 5.18 where 'Indentation 1' is the leftmost impact and 'Indentation 5' is the rightmost impact.

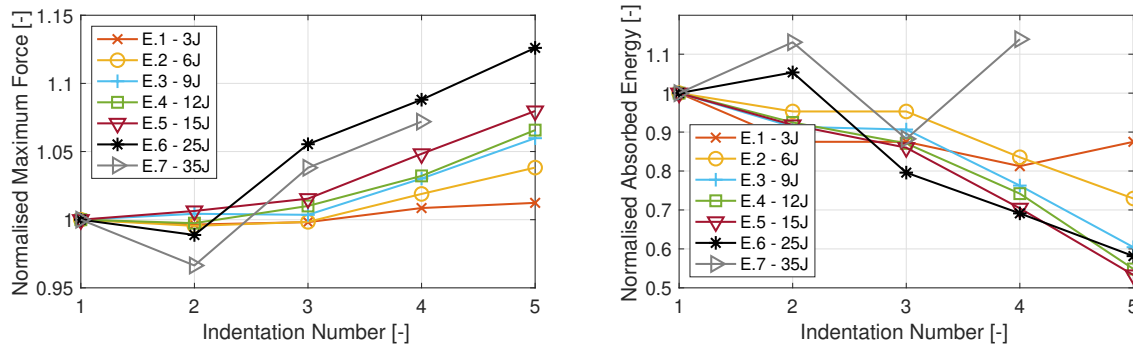


Figure 5.18: Normalised trends for maximum force and absorbed energy for the E-series.

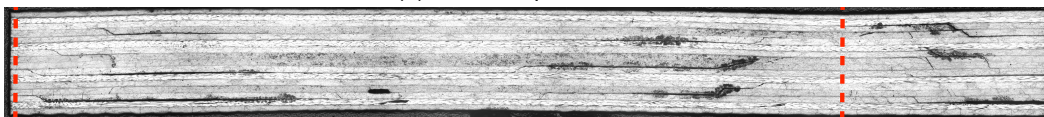
There is the exception of E.7 which is an outlier in the absorbed energy plot. It was observed (by sound) that E.7 caused unfamiliar damage formation upon the 4th because of loud snapping noises rather than having a controlled 'cracking' noise which was observed for all the other tests. The impact energy was too high and the specimen could not sustain many impacts at this impact energy. Hence, it cannot be compared to the other experiments.

5.5.3. Microscopy Link-up Investigation

The phenomenon of joining of delaminations which was previously referred to as 'link-up' did not always show the same extent of uniting delaminations. Repeated impacts tests such as in S.4 and single impacts tests such as L.2 show differences in damage (see both figs. 5.12d and 5.14b) but both show joining of delaminations. The S.4 c-scan showed a 'densely' delaminated area whereas the L.2 c-scans did not show link-up to the same extent. The microscopy images in fig. 5.19 reveal the differences.



(a) S.4 - 5 impacts at 6 J.



(b) L.2 - 1 impact at 6 J.

Figure 5.19: Microscopic pictures to illustrate effect of link-up. Pictures to scale.

The image for S.4 shows a convincingly delaminated laminate containing delaminations on multiple layers. On the other hand there is L.2 which shows a very thin delamination which connects both impact sites (6 interfaces from the bottom).

5.6. Effect of Mechanical Fatigue

Mechanical fatigue in this research refers to cyclic mechanical tension fatigue. The cyclic properties are based on real life conditions of the Boeing 787. The results presented in this section aim to provide answers to the following research question:

- Does impact damage propagate by mechanical fatigue loading the specimen?

5.6.1. C-scans

C-scans were made at different stages of fatigue loading. For F-S.3 two c-scans were made, one at 66 000 cycles and another at 132 000 cycles, fatigued at ≈ 70 MPa. For F-S.1 only one c-scan was made after 66 000 cycles, fatigued at ≈ 140 MPa. The c-scans are shown in fig. 5.20.

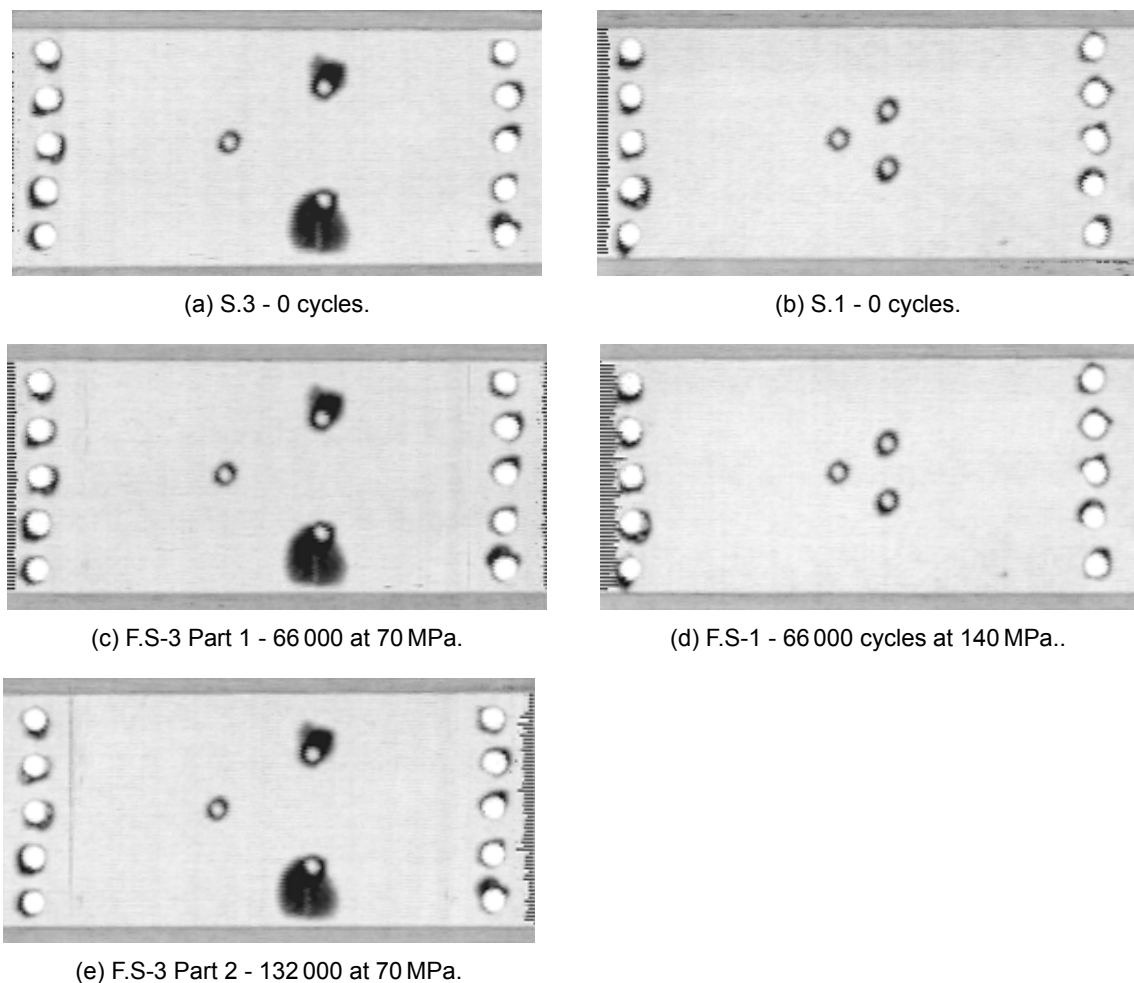


Figure 5.20: F-series C-scans

Neither the c-scans for F-S.1 or F-S.3 show delamination growth. The c-scans look identical by eye. However to be sure, the delaminations are also quantified in the next section, see section 5.6.2.

5.6.2. Processed data

The delamination area presented in table 5.5 was recorded using the MATLAB written software which revealed no more than negligible fluctuations in area with an order of magnitude of no more than 1. This variation came as a result of small differences in c-scans.

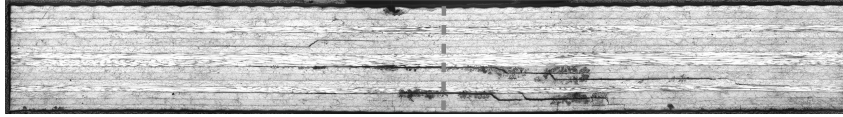
Table 5.5: Delaminated Area for F-Series.

Number of Cycles [-]	Delamination Area [mm ²]		
	0	66 000	132 000
F-S.3	1736	1740	1741
F-S.1	538	516	-

In other words, fatigue tension loading will not propagate delaminations under these conditions (66 000 to 132 000 cycles and 70 MPa to 140 MPa) in this material. However, predictably if the load is high enough damage should initiate/propagate.

5.6.3. Optical Microscopy

Furthermore, the question remains if there is no propagation of damage through the thickness. To investigate this, a specimen which was impacted 5 times per location but remained unfatigued (S.2) and another specimen which was also impacted 5 times per location but fatigued for 132 000 cycles at 70 MPa (S.3) are compared. The microscopy images are shown in fig. 5.21.



(a) S.2 - 5 impacts at 6 J. Not mechanically fatigued.



(b) S.3 - 5 impacts at 6 J. Mechanically fatigued to 132 000 cycles \approx 70 MPa.

Figure 5.21: Microscopic pictures to illustrate effect of mechanical fatigue. Pictures to scale.

From the microscopic pictures it is seen that no extra damage has been created. Remember that the reason for the limited amount of damage in specimen S.2 is due to cutting too far from the impact zone and hence missing the area of interest. The number of affected layers looks consistent between both microscopic pictures. Hence, it is finally concluded that mechanical fatigue in these loading conditions do not affect delamination growth.

Chapter 6

Discussion

6.1. Effect of impact Energy

6.1.1. Delamination Area - Impact Energy Relationship

The primary interest during the investigation of the effect of impact energy was the relation between delamination area and impact energy which has been identified as approximately a square root function. The trend is based on 7 data points, so the result is based on limited confidence. However, the trend obtained in this research is similar to trends for different layups observed by Minot, Aboissi re, Ostr , Bouvet [10], as shown in the side by side comparison in fig. 6.1.

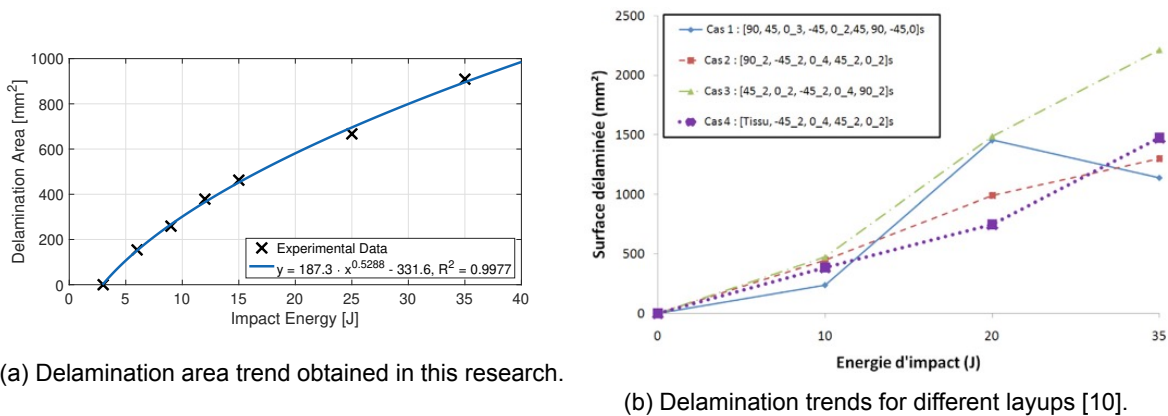


Figure 6.1: Side by side comparison of the delamination trend obtained in this research to the trends for different layups.

The delamination area trend can be a powerful tool considering maintenance and inspection. In the case that a hailstorm event crosses an airport, the top of the fuselage and wings should have to be analysed to identify the damage state. During inspection, the points of impact can be identified (e.g. by locating dents) to produce a drawing indicating the size of each delamination for a small inspection area. Then, the small area can be extrapolated to indicate the damage of the entire fuselage as illustrated in fig. 6.2.

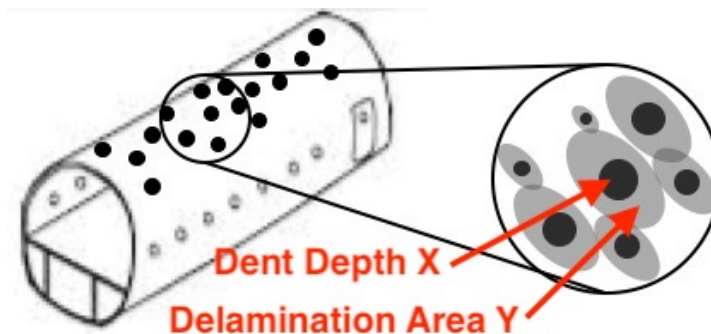


Figure 6.2: Illustration of how the delamination area trend can be used to identify the damage state of a fuselage. The black dots indicate impact dents and the grey zone around it indicates the delamination according to that dent depth and impact energy combination. Fuselage drawing obtained from [17].

However, to make this method work, one additional relation must be known i.e. the relation between dent depth and impact energy. However, this method only works if dents are present which might not be the case for hail impacts due to the crushing effect upon impact. If this would be the case, an alternative would be to use a scanning technique (similar to a c-scan as used in this research) to analyse a small area. The disadvantage is that this technique requires more advanced technology, hence it is more expensive and difficult than measuring a few dents.

Furthermore, very important to note is that even though quasi-static indentation and drop-weight experiments result in a similar damage response, literature has reported that the dents caused by QSI are larger than for drop-weights [13]. Hence, a careful trade-off must be made for which technique is considered more appropriate.

6.1.2. Preferred Delamination Layers

Except for the delamination area trend, delaminations are recorded to propagate along the -45° and 90° fibre directions. In fact, judging by the darker shading of the c-scan, the -45° direction is more preferred than the 90° direction. However, according to [31, 34] delaminations should grow in the direction of the fibres of the lower ply of the delamination interface. Nevertheless, microscopy observations show that the lower ply is in the 90° direction which is not in agreement with the c-scan observations, as can be seen in fig. 6.3. The observations here do not agree with what literature claims and the explanations in the following paragraphs form a hypothesis for why this behaviour is seen.

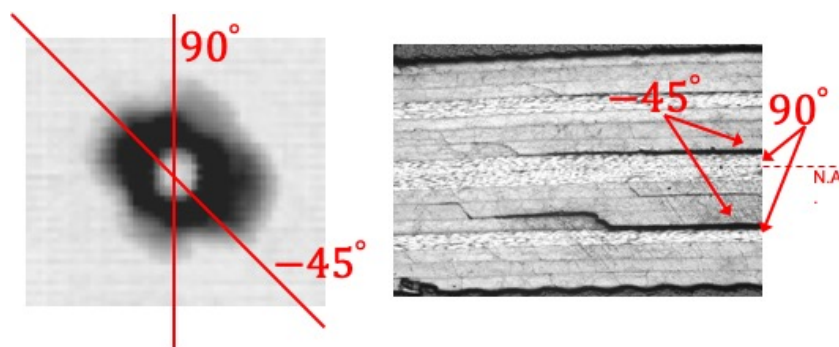


Figure 6.3: Preferred delamination layers in the C-scan and the microscopy image for a specimen impacted once at 35 J (E.7).

There are multiple possible reasons for the inconsistent observation. The first reason considers the stress variation along the thickness of the laminate. The biggest shear stress jump occurs between the $-45^\circ/90^\circ$ interface (a high load carrying layer + semi-high load carrying) as opposed to a $-45^\circ/0^\circ$ interface (semi-high load carrying + minimal load carrying layer). Delaminations are indeed expected on the interfaces containing the highest shear stress. However, this does not explain why one of the two delaminations shown in fig. 6.3 propagates in the -45° direction.

Furthermore considering layer stiffness, the 90° layer is stiffer in compression than the (top) -45° layer because the 90° layer has fibres in the direction of the bending (remember that there is bi-axial bending). Since everything above the neutral axis is compressed, it may be possible that the -45° fibres cannot hold the compressive loads and is forced into a local buckle/kink which requires the least energy perpendicular to the fibres. It is for this reason that there is one delamination travelling along the -45° direction.

These observation were far from obvious upon discovery but has important implications for the future where care must be taken before concluding on which interface delaminations are to be found. It is now clear that what literature says, is generally true but by no means a rule that can be applied to 100% of the cases.

6.2. Effect of Repeated Impacts

6.2.1. Damage Growth Rate

Delamination area was shown to increase approximately as a square root function, hence the delamination area growth rate decreases with an increasing number of impacts. In fact, the largest increment in delamination area is caused by the first impact. This means that 2 impacts in 2 separate locations would cause more damage (300 mm^2) whereas 5 impacts in 1 location cause less damage (200 mm^2 , as illustrated in table 5.2). Moreover, having 5 impacts in one location is questionable and since 4 additional impacts only cause an increase in 50 mm^2 , the need for testing repeated impacts is also questionable (explained further below) because neglecting repeated impacts would significantly reduce the complexity of hail experiments.

Besides the above, only one laminate was tested in this research for impact fatigue. This gives no information on the damage response in other laminates and for other impact energies. However, de Morais, Monteiro and Almeida [37] have looked at damage progression for woven composites with different laminate thicknesses and repeated 20 J impacts which clearly reveals that the first impact causes the largest increment in delamination area, followed by ever decreasing increments in delamination area just as observed in this research [37]. This means that the observation of the largest delamination area increase upon the first impact is applicable to more than one type of laminate.

6.2.2. Hail Experiment Model Simplification

Furthermore, Giaiotti, Stel, Fraile, Palencia and Castro [16] reveal that hailstones overlap approximately 20% of the time, but the larger the hailstones the less the overlap. The minimum hailstone required in this research (ignoring the crushing effect) to cause damage has a 3.39 cm diameter (6 J impact) which is by no means a rare sized hailstone [19, 20, 24, 33]. Moreover, hailstones of these dimensions rarely overlap. Hence, together with the above discussion on damage growth upon repeated impacts, hail impact models can be reduced from multiple impacts in multiple locations to single impacts in multiple locations. This would significantly simplify the complexity of hail experiments while being based on more realistic observations.

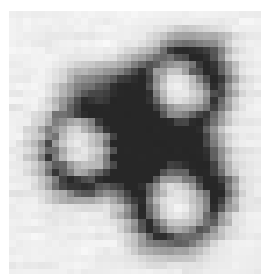
6.3. Effect of Spacing

6.3.1. Delamination Link-up

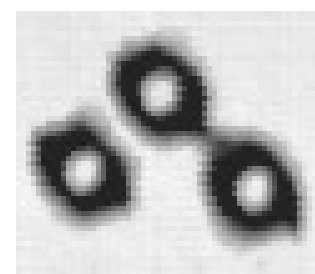
Since hail impact experiments can be approximated by single impacts in multiple locations, the effect of spacing research scope changed to investigating the minimum required impact spacing for link-up (as presented in fig. 6.4a) delaminations for single impacts rather than repeated impacts. This research varied some parameters to trigger the same phenomenon, as discussed below.



(a) Link-up observed by Laurencon [28].



(b) Link-up in S.4 due to repeated impacts.



(c) Delamination touching in O.1 due to single impacts.

Figure 6.4: Comparison between link-up and delamination touching.

The first variable tested for delamination link-up was the distance between two impacts. The upper bound for spacing proved to be the sum of the radii of delaminations. In other words, the two delaminations must just touch. If this spacing is reduced, then delaminations simply 'overlap'. The second variable was the orientation of the delaminations, which was set along the preferred -45° fibre direction. This indeed facilitated delaminations to touch. However, whichever the combination of parameters, the delamination touching by single impacts shown in fig. 6.4c is visibly not the same or even similar to

link-up by repeated impacts as shown in figs. 6.4a and 6.4b.

Since link-up has only been observed for experiments with repeated impacts but not by the more realistic experiments involving single impacts in multiple locations. Hence, the definition of link-up must be reconsidered and extended from,

Link-up is the uniting of delaminations by a sudden increase in delamination area.

to

*Link-up is **an impact fatigue phenomenon** uniting delaminations by a sudden increase in delamination area **due to the repetition of impacts**.*

6.3.2. Impact Interaction

In addition to the discussion on repeated impacts in one location (i.e. the more impacts the lower the damage growth rate, see section 6.2.1), a similar relation is seen in impact separation. Impact separation refers to the distance between two impacts. Upon investigating the increase in delamination area for each impact in the E-series it revealed that the closer the impacts are together, the lower the increment in delamination damage. Going back to the discussion of hailstone overlap, larger hailstones (e.g. hailstones ≥ 30 mm) do not overlap, therefore they cause the maximum amount of damage according to this observation.

6.4. Effect of Mechanical Fatigue

The simple and short answer to research question on mechanical tension fatigue is that there is no reduction of fatigue life for impacted material in the conditions it has been tested in here. The first reason may be that the tension load was simply not high enough. Assuming that these specimens are able to strain a maximum of 2% before fracture and given that this layup provides a stiffness of 59 GPa, this material has an ultimate strength of 1180 MPa ($\sigma = E\epsilon$). This means that the fatigue tests are performed at a normalised stress ($\sigma_{\text{applied}}/\sigma_{\text{ult}}$) of 0.06 and 0.12 which is low. However, the fatigue tests performed by Mahinfalah and Skordahl [27] had normalised stress values in the range of 0.5 to 0.9 which is much higher and showed a difference in fatigue life between impacted and non-impacted material. Even though there is mode III shear stress in tension, the combination of tension which closes the delamination (as illustrated in fig. 6.5) halts the mode III fracture growth.

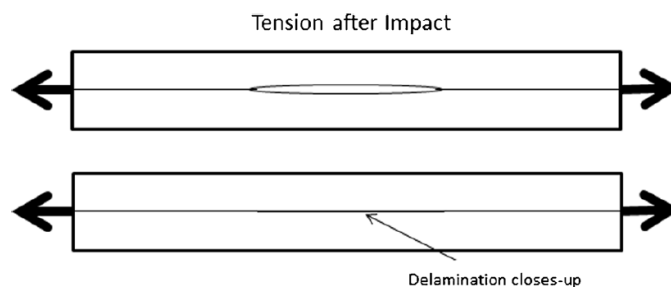


Figure 6.5: Delamination closure during tension fatigue [5].

Another reason can be related to the number of cycles performed. According to the research by Mahinfalah and Skordahl [27], the specimens were able to last up to 1 million cycles in some cases. This hints that the number of cycles tested in the F-series may have been too few. Especially when combining the number of cycles together with the normalised stress it becomes obvious that this research found itself to be in a completely different part in the fatigue graph seen in fig. 2.13.

Nevertheless, the story of fatigue is far from finished. Every flight causes the cabin to be pressurised, forcing the fuselage skin into a combined tension and bending state. According to [25] even loads well below the static failure strength may degrade the material. Degradation due to low loads was not the case for tension fatigue, however, bending can cause pure mode II fractures and may be sufficient for delamination growth. In other words, bending fatigue of specimens impacted in multiple locations should be the next step in the investigation.

6.5. Impactor Material - Ice versus Steel

Most likely the biggest limitation of this work is the unknown relationship between ice and metal impactors on the damage response. The big difference between these two materials is that ice crushes into pieces whereas steel stays intact. The complication here is that a portion of the impact energy goes into crushing of the ice rather than deforming the specimen. Hence, the damage response of a 20 J steel impact will not be the same as a 20 J hailstone impact.

6.6. Effect of Residual strength

Unfortunately due to the limited timespan of the research it was not possible to investigate the effect of delaminations on residual strength. However, some speculations are presented here of what could cause a problem. The discussion will focus on tension after impact (TAI), compression after impact (CAI) and bending after impact (BAI). Furthermore, what makes this discussion particularly important is that literature has covered residual strength on a single location impacted specimens but this may not be representative for hail in all cases.

Starting with TAI, literature has reported a small reduction in tensile strength. The research performed by Malhotra and Guild [5] reports approximately a 5% reduction in tensile strength for impacts in the centre of the plate impacted at 2 J to 4 J. This is very worrying for two reasons, i.e. the first reason is that the specimen was impacted only once which means the tensile strength is most likely even lower for a specimen impacted in multiple locations. The second reason is that 2 J to 4 J is very low considering the impact energies hail can reach up to (up to 35 J was tested in this research).

Furthermore the same paper ([5]) has reported a reduction in compression strength for CAI. The reduction it reports for an impact at 4 J in the centre is approximately 20%. More research performed by Järneteg [23] confirms this magnitude of reduction for very similar impact conditions. Again, this is for a single impact in a single location at a relatively low impact energy. Must this have been tested for various locations at a higher impact energy, it would arguably be much worse and more representative for hail.

The final concern discussed here is BAI performed by 4-point bending tests. The research by Järneteg [23] has revealed that damage created by impacts in the range of 5 J to 10 J results in delaminations in the range of 90 mm² to 150 mm² (which is in the same range as this research for this range of impact energy) reduces the bending strength by a factor of two. Furthermore, damage of size 450 mm² reduces the bending strength to approximately 40% of the original strength. This research was performed for single location impacts which is again probably not representative for hail. Hence, must this have been applied to multiple impact locations, the bending strength would probably be reduced even more.

Part III

Conclusion and Recommendations

Chapter 7

Conclusion and Recommendations

7.1. Conclusion

Composites are susceptible to out-of-plane impacts which is why there is such a vast amount of previous research on impacts in a single point of impact. However in the case of hail (when the aircraft is stationary on the ground), the impact scenario shifts to a case of impacts in multiple locations which might not be accurately represented by the findings of single location research. To investigate the difference in damage response between the two cases, this thesis work adopted a purely experimental approach to investigate four relationships which were impact energy, impact spacing, impact repetitions and finally, mechanical fatigue.

This research has shown that the effect of repeatedly impacting the same location causes delamination growth, but the total delamination area from two repeated hailstone impacts in the same location is much lower than that of two hailstone impacts in two independent locations. Although hailstones may impact the same location more than once, this is only a problem for small hailstones which do not contain sufficient impact energy to harm the material. In other words, big hailstones which contain enough impact energy do not overlap hence hail impact is regarded as a problem of 'one impact per location' rather than 'repeated impacts per location'. As a consequence, hail experiments will show a larger, more realistic delaminated area than in the previous case.

Hence, simplifying hail to a 'one impact per location' philosophy has important implications for the damage response of the material. Previously, the abrupt increase in delamination area (which is called link-up) was thought to be a problem for hail impact, however, this proves not to be the case. Upon attempting to trigger link-up with a one impact per location philosophy, many parameters were tested but no combination of parameters led to an abrupt increase in delamination area, merely a summation of delamination area of the individual impacts. This led to the conclusion that link-up is an impact fatigue phenomenon and does not have to be taken into account in future hail impact discussions. Moreover, hail can be represented as single impacts in multiple locations. In fact, due to the non-interaction between delaminations for single impacts, damage response results (such as delamination area) from single location impact experiments are also applicable to hail impact.

Furthermore, the mechanical tension fatigue tests showed no damage growth for the conditions specimens were tested. Whether tension fatigue is harmful or not for impacted material remains open for discussion, however it seems that it did not cause damage growth in this research due to the very low fatigue loads and few cycles which were applied. Nevertheless, the analysis on fatigue is far from accomplished as there are other critical fatigue tests to be performed in the future, as discussed in the recommendations.

Unfortunately, the biggest limitation of this research is the use of a steel impactor. The damage response of a laminate impacted by a hailstone or steel ball of equal energy will cause a different level of damage because energy is required by the crushing of the hailstone upon impact. In order to cause the same damage response, hailstones must contain more energy than the equivalent steel ball in order to damage the structure the same amount. However, in contrast to what literature may have reported, it is highly doubtful that hailstones cannot cause delaminations due to the crushing effect.

Considering the very limited amount of available data on hailstorms and hail impacts and its very complicated nature, this research has made a tremendous contribution to the body of knowledge by showing how hail can be approximated and what is and what is not important to consider. Moving forward from here, future experiments must now focus on questioning the fatigue life of hail impacted structures to determine if composite aircraft such as the Airbus A350 and the Boeing 787 are prone to a reduced fatigue life like with the De Havilland Comet without being aware of it.

7.2. Recommendations

There are in total two primary recommendations which should be carried out in future research, i.e. the effect of bending fatigue for specimens with impacts in multiple locations and the relation between metal and ice impactors. Both these recommendations are discussed below, as well as some additional, secondary recommendations which did not receive the required time to fully explore in this research but remain important to investigate.

7.2.1. Primary Recommendations

From the previous discussion on residual strength, it was clear that bending after impact (BAI) showed the biggest reduction (by a factor of two). However, this was only for specimens impacted one time in the middle of the specimen at a low impact energy. The questions which now remain to be answered are, what the effect is of bending fatigue and the reduction in fatigue life for specimens impacted in multiple locations at a slightly higher impact energy. Given the large reduction for 1 impact, it looks unfavourable for multiple impacts. It is furthermore recommended to use a 4-point bending setup to avoid contact with the inflicted impact damage. It is predicted that BAI will severely propagate the damage of delaminated structures because the laminate layers are loaded in shear, which is the most unfavourable fracture mechanics for delaminations. Furthermore, this recommendation is of utmost relevance because upon pressurising the fuselage, the skin is loaded in bending (as well as tension).

Moreover, it is obvious that steel and ice impactors will cause different damage responses in a laminate. This research has identified the relation between impact energy and delamination area for a steel impactor. However, hailstones have a crushing effect upon impact which takes away energy from going into the deformation of the material which is not the case for steel impactors. Hence, it is vital to know what the equivalent impact energy of hail is to steel impactors. It must also not be forgotten while making the comparison to take into account that the impactor diameter must be the same, otherwise a different damage response can be expected.

7.2.2. Secondary Recommendations

Last but not least, it was assumed in this research if the first impact does not cause damage then no consecutive impacts with the same impact energy will cause damage. However, (in Europe) hailstorms mostly consist of small hailstones. Hence, the question is if damage can be initiated by many small hailstorms impacting the fuselage (hence repeated impacts in multiple locations). Furthermore, perhaps when a delamination has been created by a hailstone, smaller hailstones which are otherwise deemed harmless may propagate the already present delamination if impacted right next to it.

Part IV

Appendix

Chapter A

Damage Thresholds

A.1. Methodology

As explained in the literature review summary (see section 2.1.3), the damage response of a laminate is dependent on many variables. This test aims to reduce these variables as it is impossible to account for all the mentioned variables in such a short period of time.

Impact energy is such a variable. The experiments following this shall be performed with impact energies between the lower and upper limit. With this test, the aim is to find the:

1. Lower limit: the impact energy below which no damage is created.
2. Upper limit: The impact energy at which a physically visible dent is visible by common inspection intervals.

The reason for introducing the lower limit was based on past research [27]; if there is no initial damage created the fatigue life remains unaffected as well. The reason for having an upper limit was because this research focused on BVID and having visible damage should be covered by regular inspection intervals. Hence anything outside the boundaries of this limit is per definition outside the scope of this research.

As impact energy changed, so does the impactor size when hail is considered. This test will account for that. Based on research in the USA and other research on hail climatology [19, 20, 33], hailstone diameters range from less than 1 cm up to about 10 cm. In theory, larger impactors should cause less damage than smaller impactors with the same impact energy.

Table A.1: Hailstone properties [19, 20, 33]. Velocities are calculated with a hailstone drag coefficient $C_D = 1$.

Diameter [cm]	Mass [kg]	Terminal Velocity [m s^{-1}]	Kinetic Energy [J]
1.0	0.00047	9.8	0.02
2.0	0.00377	13.9	0.4
3.0	0.01272	17.0	1.8
4.0	0.03016	19.6	5.8
5.0	0.05890	21.9	14.1
6.0	0.10179	24.0	29.3
7.0	0.16163	25.9	54.4
8.0	0.24127	27.7	92.7
9.0	0.34353	29.4	149
10.0	0.47124	31.0	226

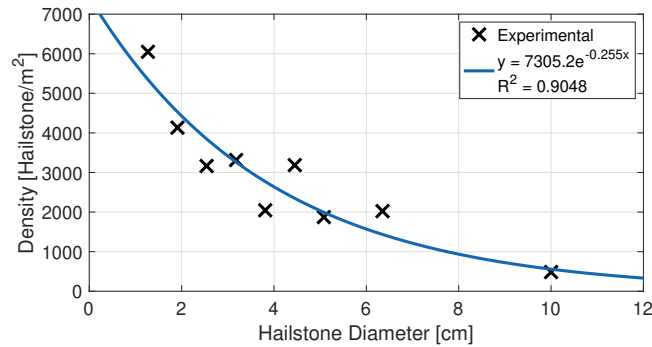
Considering the number of impacts, some things can be said as well. Hailstorms vary in intensity; less severe hailstorms cause more dense impact surfaces (more impacts) with lower energy hailstones; more severe hailstorms cause a less dense impact surfaces with high energy hailstones, see table A.2.

To transform the scattered data in table A.2 to useful data which can be worked with, some adjustments were made. The following adjustments were made:

Table A.2: Maximum hailstone diameter per hailpad recording versus the impact concentration of that hailpad [20].

Maximum hailstone diameter [cm]	Concentration [m ⁻²]
< 1.27	6049
1.27–1.91	4133
1.91–2.54	3165
2.54–3.18	3315
3.18–3.81	2045
3.81–4.45	3186
4.45–5.08	1873
5.08–6.35	2024
> 6.35	484

1. The upper limit of the maximum hailstone diameter column in table A.2 is used to obtain the general trend line in fig. A.1. This assumes a worst case scenario; more impacts per area than when taking the average maximum hailstone diameter.

Figure A.1: Number of hailstones m⁻² versus hailstone size.

The data is coarse and includes inconsistencies as explained in [20]. Hence, looking at fig. A.1 which is the plotted data in table A.2, the equation of the trend line is the following, with a goodness-of-fit of $R^2 = 0.9048$:

$$y = 7305.2e^{-0.255x} \quad (\text{A.1})$$

2. While observing table A.2 some choices must be made regarding the hailstone diameters to be tested. These choices are limited to manufacturing and total number of tests concerns.

Practical diameters are in steps of 1 cm. Again looking at the data in table A.2, a minimum diameter could be 1 cm, while a maximum diameter could be 6 cm. This is because there are measurement errors in the severe hailstorm records [20]. Hence the following hailstone diameters would have an impact energy of:

Table A.3: Kinetic energy per tested hailstone diameter.

Impactor diameter [cm]	1	2	3	4	5	6
Kinetic Energy [J]	0.02	0.36	1.83	5.8	14.15	29.34

1 cm hailstone impact the ground with 0.02 J. This is very low energy. From literature, an assumption is made that this size hailstone will not cause damage. Hence 1 cm are omitted from further discussions.

3. It is impossible to test 6049 impacts in the laboratory, this number must be scaled down to a feasible number of impacts. It must also be reduced to the correct number of impacts to be carried out in a single location.

From hailpad observations it is known that the most severe hailstorms have sparsely distributed hail impacts. This implies that the largest hailstones impact a single location only once, this is used as the reference 'point'. So, less severe hailstorms hence impact the specimen in that single location more than once.

Hence this becomes a scaling issue, using the best-fit equation eq. (A.1):

- Hailstone diameter = 6 cm causes 1582 impacts/m².
- Hailstone diameter = 1 cm causes 5661 impacts/m².

Thus for every impact with a diameter of 6 cm, $5661/1582 \approx 4$ times as many hailstones of 1 cm impact the ground.

Using this logic, the following table is generated:

Table A.4: Number of impacts per tested hailstone diameter.

Impactor diameter [cm]	2	3	4	5	6
Number of impacts [-]	3	2	2	1	1

However, it is not useful to impact 3 cm and 4 cm the same number of times because the outcome is already known: if damage is caused, the 4 cm would cause more damage. The same goes for impactors of 5 cm and 6 cm. Hence the following adjusted table was proposed:

Table A.5: Adjusted number of impacts per tested hailstone diameter.

Impactor diameter [cm]	2	3	4	5	6
Number of impacts [-]	5	4	3	2	1

Adjusting the number of impacts this way may be considered incorrect at first glance. However, considering the large scatter in hail data, this is considered acceptable.

A.1.1. Test Setup

The test machine used was quasi-static indentation (see section 2.1.4 for more details on QSI). This choice was made for two reasons:

1. The drop tower was unable to obtain energies lower than ≈ 3 J.
2. QSI offers much higher consistency in impact energy.

The specimens used were pre-made specimens from a previous intern. The specimens had dimensions of 12.3 cm \times 12.3 cm and a thickness of 2 mm. The plates had a stacking sequence of [0, 90, 45, -45, 0, 90, 45, -45]_S.

A.1.2. Test Matrix

The above tests are summarised in a test matrix, this explain the number of tests, and what each test will consist of in a concise table. The logic of the test numbering system is as follows:

- First digit: test definition. That means the number of impacts, locations and impact energy.
- Second digit: test specimen number. That is the number of the specimen which is tested.
- Third digit: the number of impacts.

Table A.6: Test 1: Test matrix.

Test No.	Impactor diameter [cm]	No. Impacts [-]	No. locations [-]	Impact energy [J]
1.1.1-5	2	5	1	0.36
1.2.1-5	2	5	1	0.36
2.1.1-4	3	4	1	1.83
2.2.1-4	3	4	1	1.83
3.1.1-3	4	3	1	5.80
3.2.1-3	4	3	1	5.80
4.1.1-2	5	2	1	14.15
4.2.1-2	5	2	1	14.15
5.1.1	6	1	1	29.34
5.2.1	6	1	1	29.34

A.2. Results

A C-scan was made at the end of each experiment. There are in total 10 C-scans, these are shown in fig. A.2.

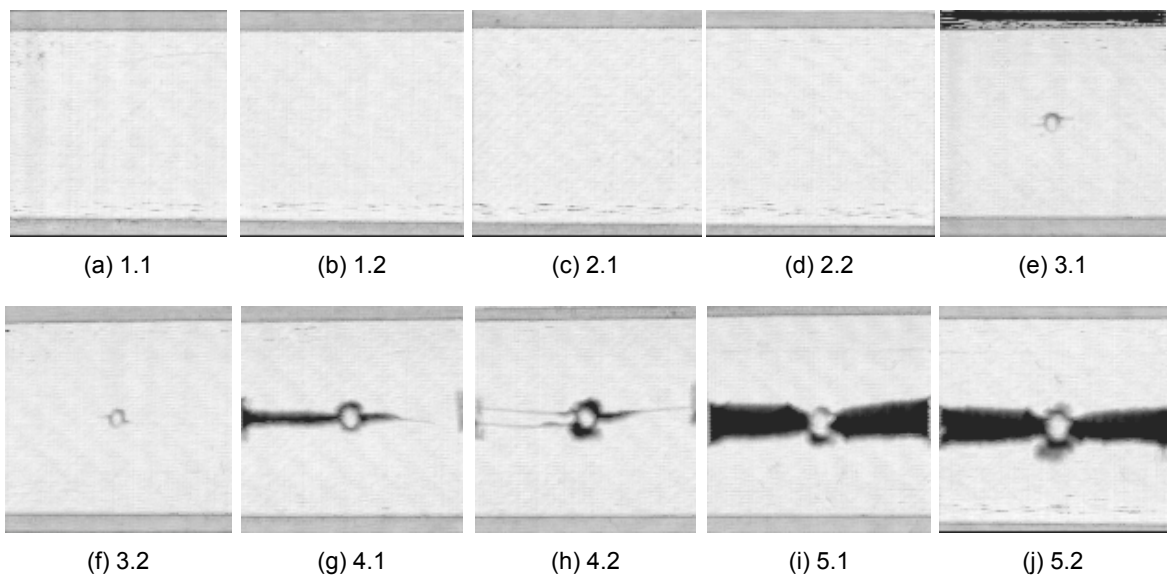
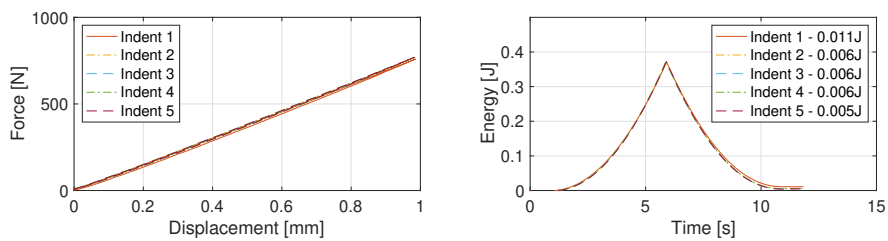


Figure A.2: Test 1 C-scans

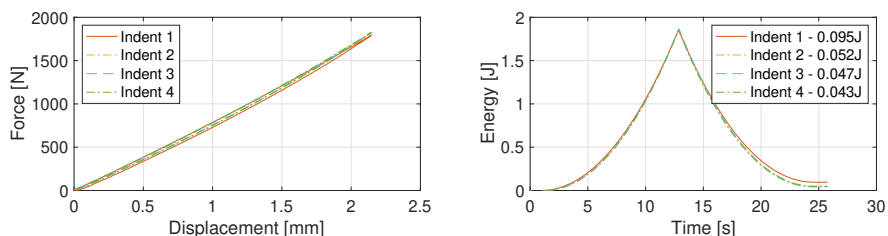
The force-displacement and energy-time curves are shown in figs. A.3 and A.4. The energy indicated in the legend of the energy-time graphs is the absorbed energy of each indentation.

A.3. Lessons Learned

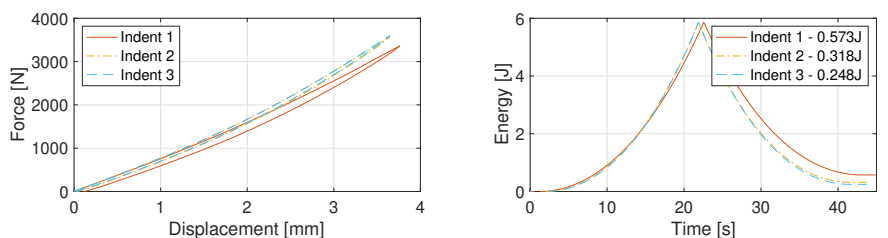
1. The most important lesson learned from this test is that the specimen boundary conditions are critical. In test 5.1.1 the absorbed energy is more than 0.5 J higher than in 5.2.1. A big difference can be seen in maximum force obtained between 5.1.1 and 5.2.1 as well. The lesson learned here is that the clamping conditions must be much better controlled.
2. Initially, the goal of this test was to see which level hailstorms would be hazardous. Even with the correct preparations, the realisation was made that this would not yield useful information for several reasons:
 - Even though it was claimed that the relation between the number of impacts and the impact energy could be claimed acceptable this would still be an inadequate method to



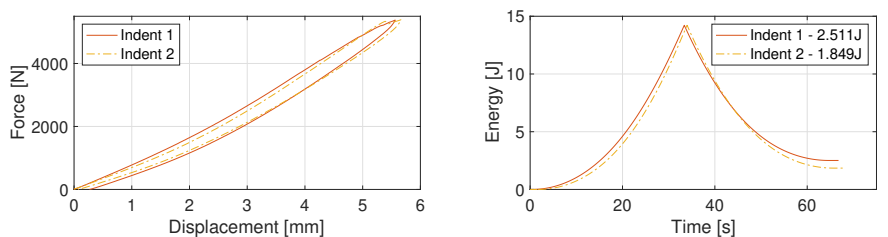
(a) Test 1.1.1-5. Impact Energy: 0.36J



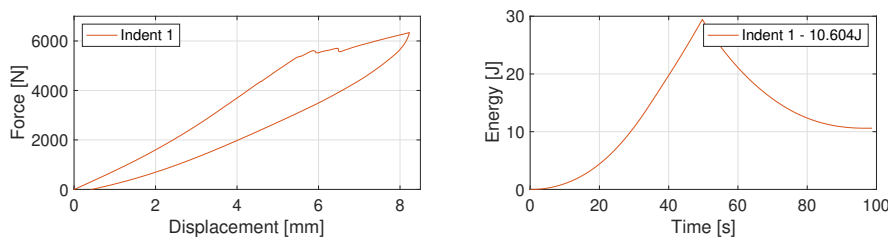
(b) Test 2.1.1-4. Impact Energy: 1.83J



(c) Test 3.1.1-3. Impact Energy: 5.80J



(d) Test 4.1.1-2. Impact Energy: 14.15J



(e) Test 5.1.1-1. Impact Energy: 29.34J

Figure A.3: X.1.1-N Results. Left: Force-displacement. Middle: Energy-time. Right: Absorbed energy.

apply to understand the problem of delaminations.

- This test mixes too many variables, that is: impactor diameter, number of impacts and impact energy. This to realise one relation: which hailstorms are hazardous. Having too many variables in this test disturbs concluding anything meaningful.

This test may not have served the purpose it was supposed to fulfil. However it is still a success

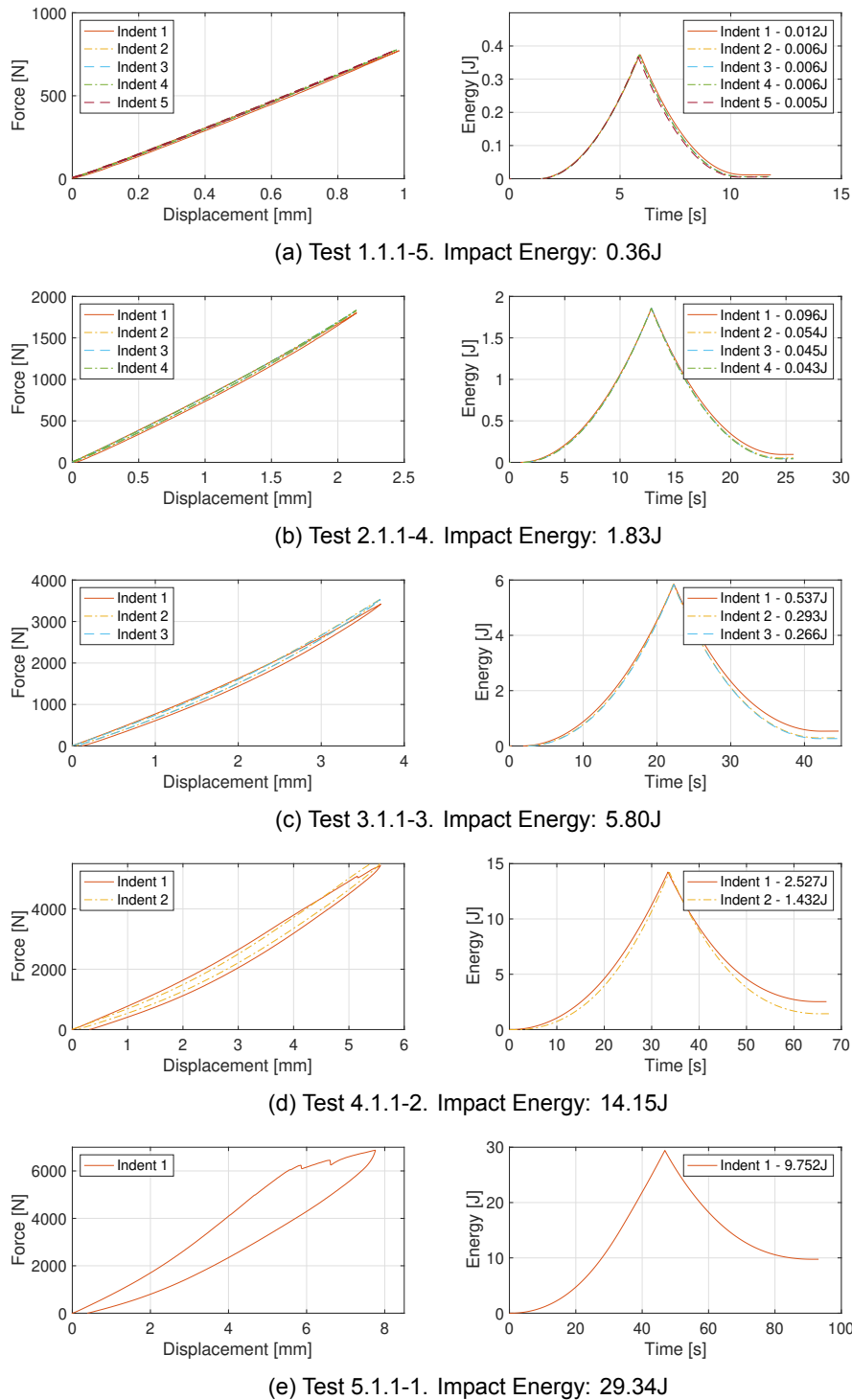


Figure A.4: Y.2.1-N Results. Left: Force-displacement. Middle: Energy-time. Right: Absorbed energy.

because it gathered a lot of insight into the problem and especially areas to pay closer attention to so that any following tests avoid making the same blind mistakes. In that way this test is a success and many improvements follow.

Chapter B

Laminate Manufacturing

B.1. General Concerns

There were a total of 30 specimens manufactured. Each specimen had final dimensions $\approx 297 \text{ mm} \times 146 \text{ mm}$. A large number of specimens were manufactured for reasons such as:

- All specimens came from the same batch. All specimens had equal properties.
- Enough to avoid running out of specimens.

The largest autoclave plate was $100 \text{ cm} \times 170 \text{ cm}$. Ideally, a laminate of $90 \text{ cm} \times 150 \text{ cm}$ would provide 30 specimens with the dimensions of $300 \text{ mm} \times 150 \text{ mm}$ if there were no material waste. Unfortunately waste was inevitable. Sources of waste were:

- Misalignment of layers while stacking caused by manual labour. A result was overlap edges. About 1 cm was required to be cut off from each side.
- The cutting saw was $\approx 2 \text{ mm}$ thick, this was also lost in material waste.

A solution to material waste was to account for it. That meant manufacturing a laminate of $92 \text{ cm} \times 152 \text{ cm}$ to solve this issue. However, the prepreg role was 60 cm wide. That makes an extra 2 cm very inconvenient considering the problem from a manufacturing perspective as 92 cm and 152 cm do not result in convenient ratios with 60 cm.

B.2. Laminate Manufacturing Process

Having identified the concerns, the manufacturing could start. The manufacturing was done in 4 steps: prepreg cutting, prepreg layup, laminate autoclave curing and cutting out the specimens.

1. Prepreg cutting. Before layup, the prepreg had to be cut to the correct dimensions. For the laminate with dimensions of $90 \text{ cm} \times 150 \text{ cm}$, the following pieces of prepreg were required to be cut:

Table B.1: The number of prepreg pieces needed per orientation for the entire laminate of 16 layers.

0° layer	90° layer	$\pm 45^\circ$ layer
$4 \times 60 \text{ cm} \times 150 \text{ cm}$	$8 \times 60 \text{ cm} \times 90 \text{ cm}$	$16 \times 54.8 \text{ cm} \times 110 \text{ cm}$
$4 \times 30 \text{ cm} \times 150 \text{ cm}$	$4 \times 30 \text{ cm} \times 90 \text{ cm}$	$8 \times 60 \text{ cm} \times 170 \text{ cm}$

A visual representation of the prepreg pieces is shown in fig. B.1.

2. The laminate stacking sequence was $[45, 0, -45, 90, 45, 0, -45, 90]_S$. The laminate was put into a vacuum table after every stacked layer. The vacuum table was used so often to minimise trapped air. It might have been problematic if this step was skipped due to the large size of the laminate.
3. The recommended autoclave cycle was used. The laminate cured at 120°C for 1.5 h at 6 bar [18]. The curing cycle can be seen in fig. B.2.
4. Cutting out specimens. Inherent to autoclave processes is that excess resin gets squeezed out of the laminate by the pressure. This requires the sides of the laminate after curing to be cut off. The final dimensions of the laminate were $88 \text{ cm} \times 148 \text{ cm}$. That results in specimen dimensions

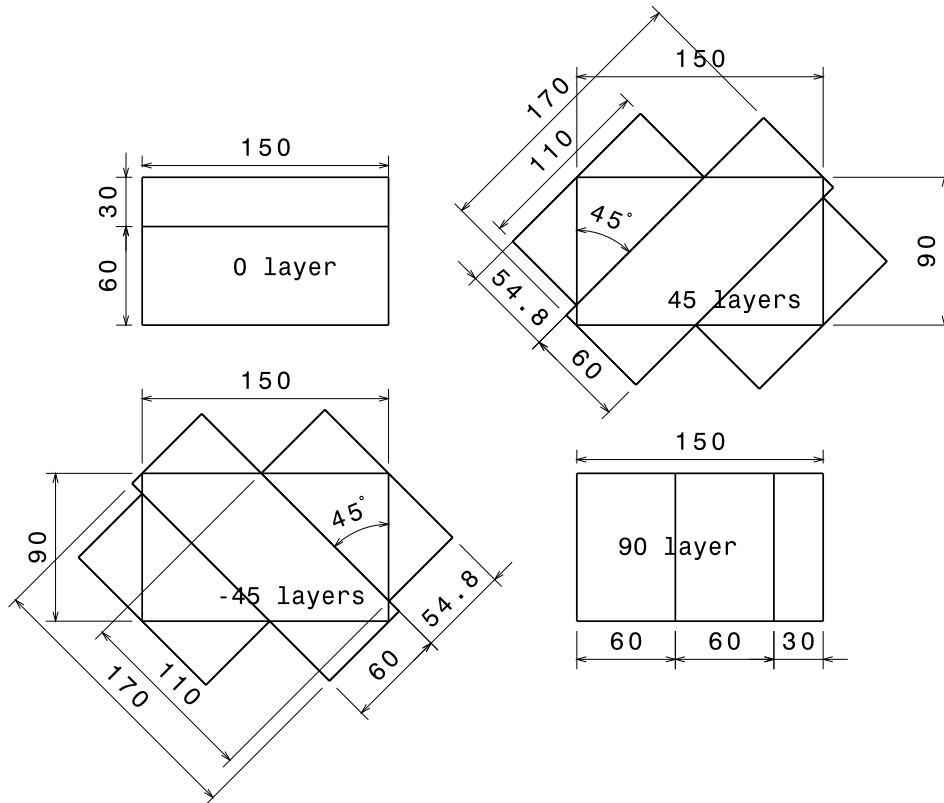


Figure B.1: Schematic drawings of the pieces of prepreg required for the layup of the laminate as described in section 4.3. The fibres are in all cases in the direction of the length of the prepreg. I.e. 0° fibres are oriented horizontally on the page.

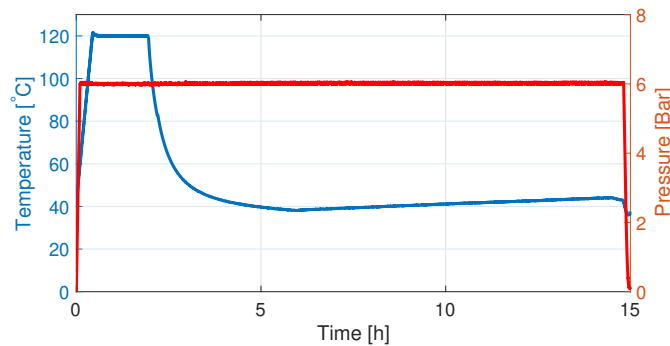


Figure B.2: Actual undergone autoclave cycle.

on average of $14.7 \text{ cm} \times 29.7 \text{ cm}$. See fig. B.3 for a visual representation of how the specimens were cut.

Cutting of the specimens was done manually. For that reason, the discussion talks about the average dimensions. The final dimensions were all $\pm 2 \text{ mm}$ of each other.

The fact that the final dimensions differ from each other does not affect the goal of this research. That is because a slightly smaller plate will not cause an entirely different damage response. Important is that the long edges of the specimens can still be clamped by friction, but differences of 2 mm should not affect the clamping condition drastically.

5. Making holes. There were multiple issues encountered during cutting of holes.

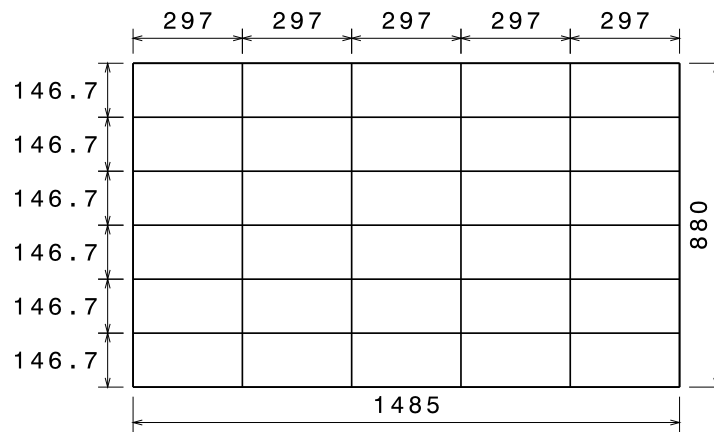


Figure B.3: Cutting lines drawn on the 88 cm × 148 cm for cutting the laminate into the required specimen dimensions.

Holes were initially cut out by water jet cutting. Water jet cutting was chosen as the cutting method due to its precise measurements and neat process. Unfortunately water jet cutting caused delaminations around the holes. This process was immediately stopped. Fortunately the damages areas were contained within the clamped areas of the specimen. These would likely have no effect on the results.

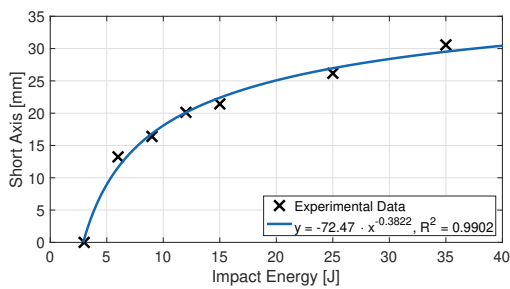
It was chosen to continue with a drilling process. The pitch in the length of the specimen was measured incorrectly. The holes were positioned at just little under 250 mm where it was planned to be. Rework of the drilled holes was required. Fortunately the damage done was limited. The holes became small ellipses instead of circles.

Chapter C

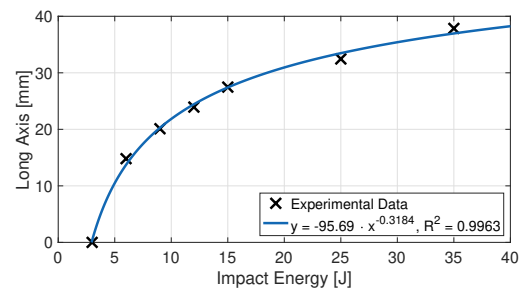
Additional Results

C.1. E-Series

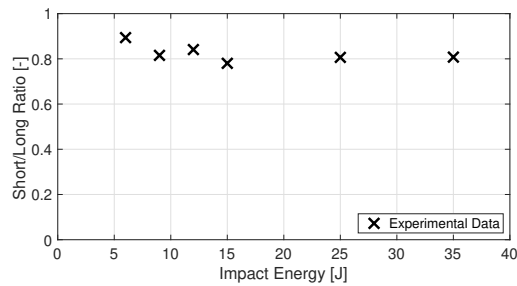
In addition to the delamination area versus impact energy trend, also the short and long axis trends in function of impact energy are illustrated in figs. C.1a and C.1b. Furthermore, the ratio of short to long axis is presented in fig. C.1c.



(a) Short axis trend.



(b) Long axis trend.



(c) Short axis/long axis ratio trend.

Figure C.1: E-series best-fit trends.

C.2. Optical Microscopy Specimen Cutting Plan

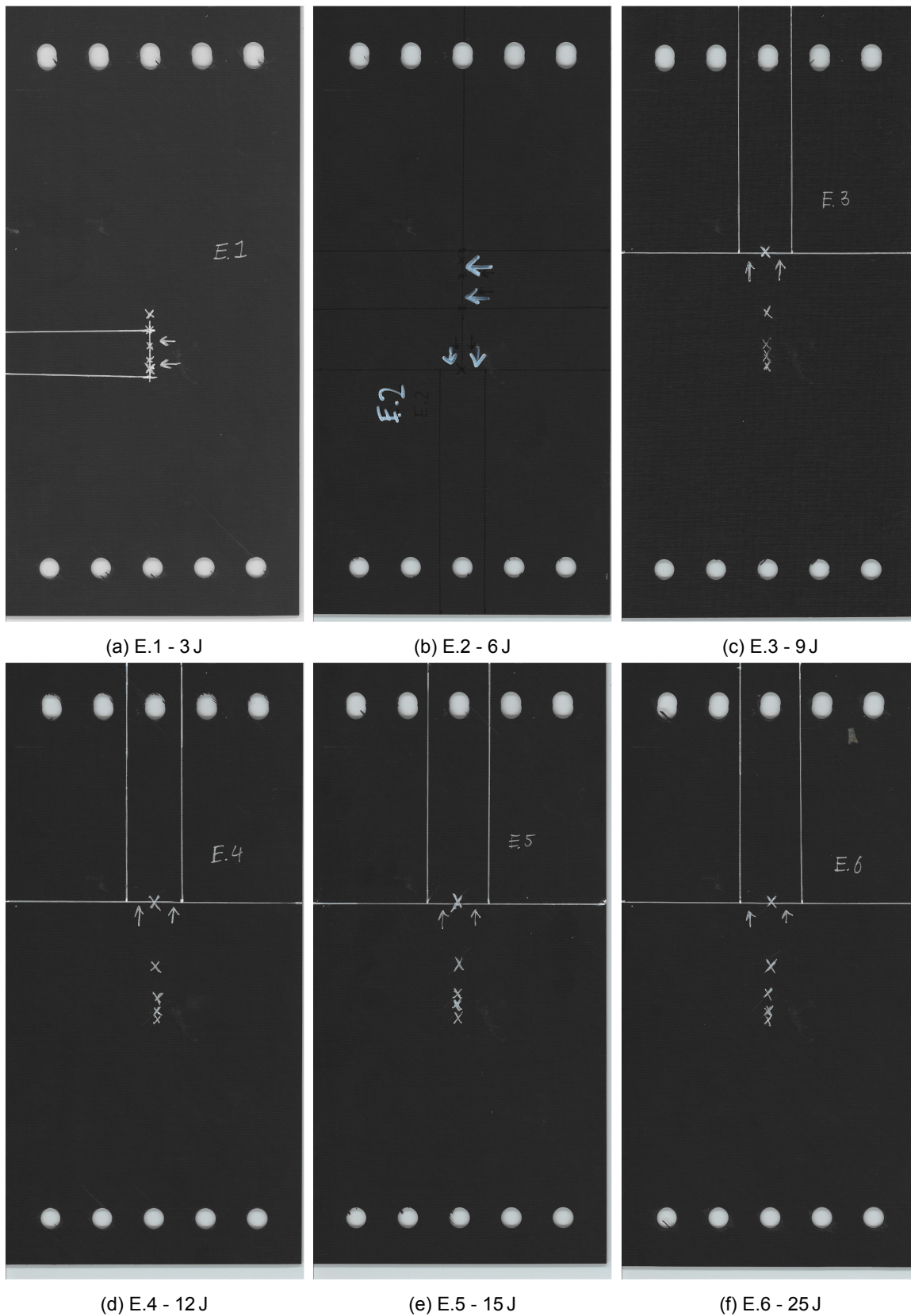


Figure C.2: E-series best-fit trends.

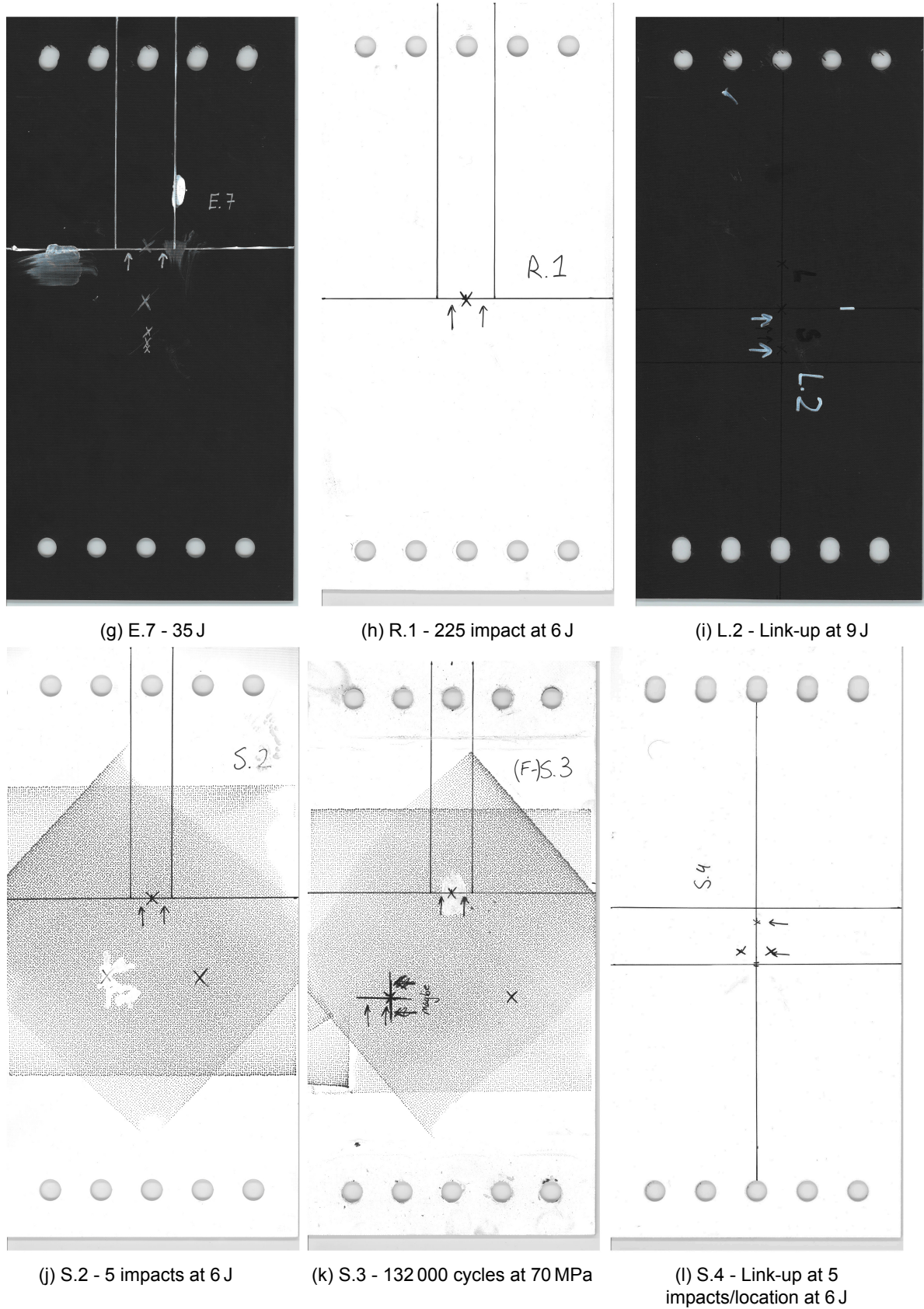


Figure C.2: E-series best-fit trends (cont'd).

C.3. Hemispherical Impactor

There was only one 3 cm impactor used for all experiments (with the exception of 'Test 1'). The drawing of the 3 cm hemispherical impactor is shown in fig. C.3. The material used for the impactor was Impax steel.

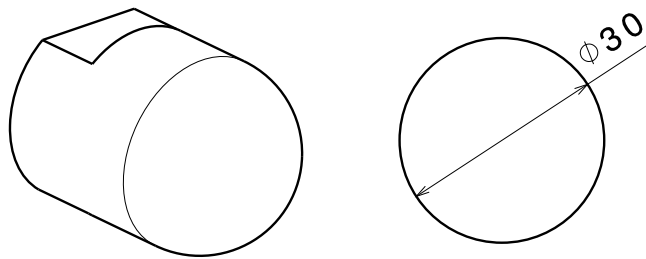


Figure C.3: 30 mm steel impactor used for all impact experiments.

C.4. MATLAB Method for Delaminations

A MATLAB code was used in this research to consistently determine delamination characteristics. To use this software, the delamination area of interest was cut out of the c-scan image and input into MATLAB. It can be seen that delaminations are darker on the c-scans, hence a threshold grayscale value was used to determine if the pixel was part of a delamination or not. The grayscale threshold value was 212, with 255 being pure white. Anything below 212 was considered to be part of the delamination. After all pixels were identified, these data point were able to be used for approximating an oval.

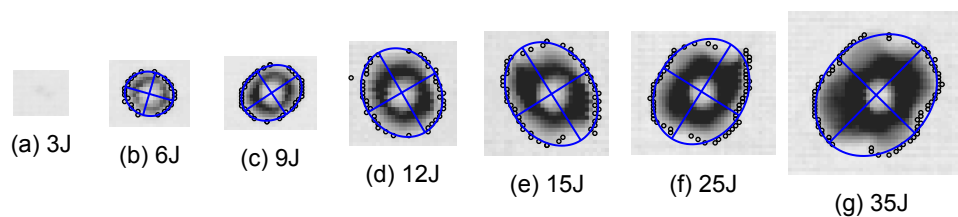
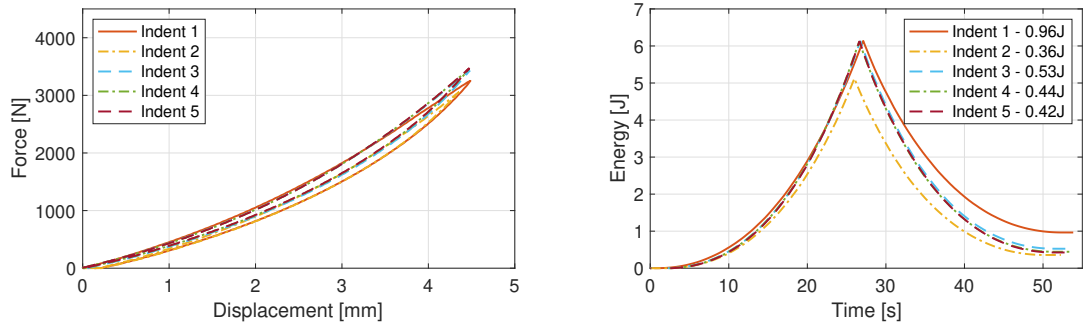


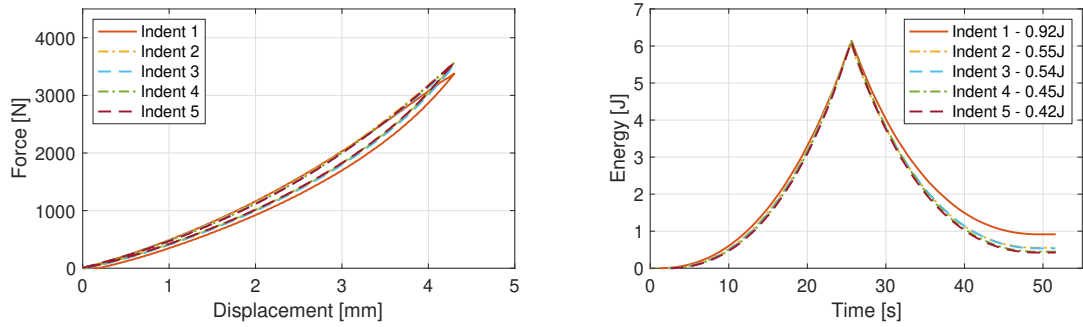
Figure C.4: E-series delamination size with ellipses of best fit.

It can be argued that this MATLAB method overestimates the delamination area, however this is not true. A comparison was made between the method presented here and simply counting the all the pixels ($1 \text{ pixel} = 1 \text{ mm}^2$) with grayscale values < 212 . The delamination area difference was close to nothing and fluctuating. For this reason, the oval-method was continued because of its ability to calculate a short and long axis for each delamination.

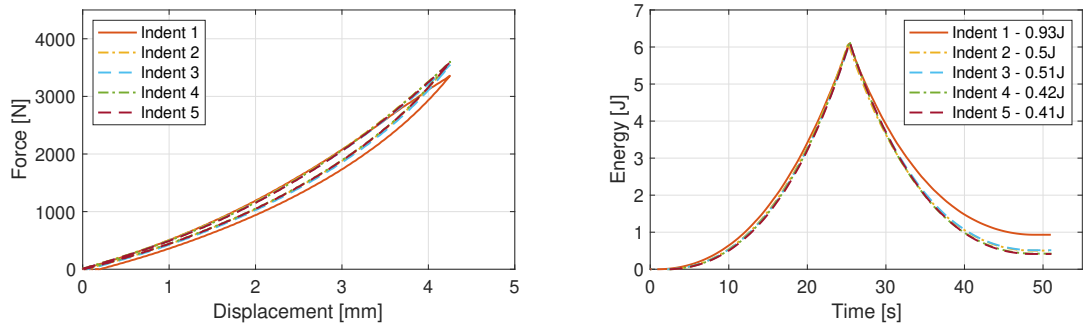
C.5. S-series



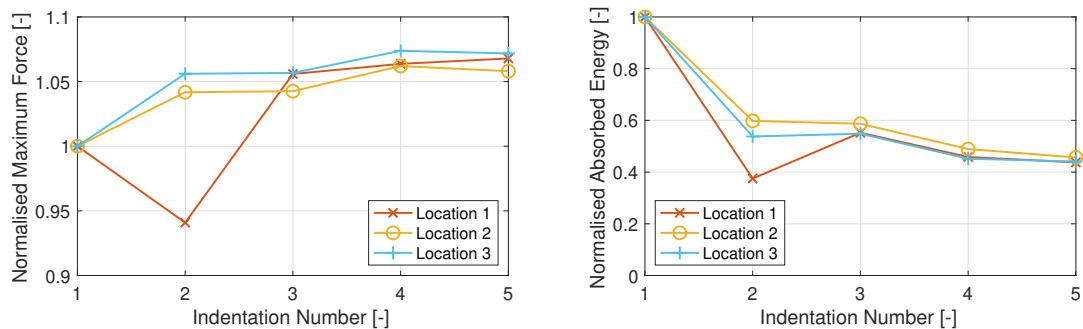
(a) S.1 Location 1



(b) S.1 Location 2



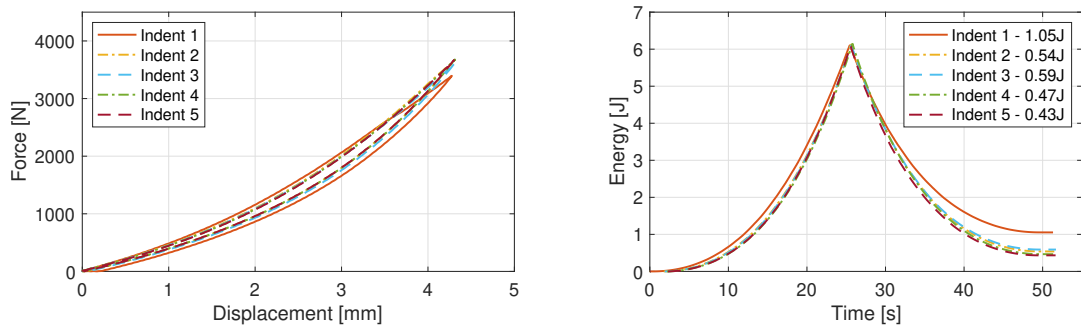
(c) S.1 Location 3



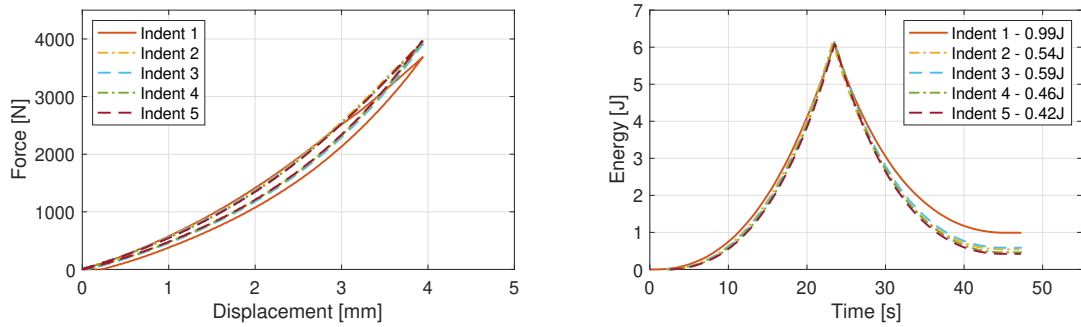
(d) S.1 Maximum force and Absorbed Energy.

Note: the second indent was wrongly programmed. A too low indentation energy was used.

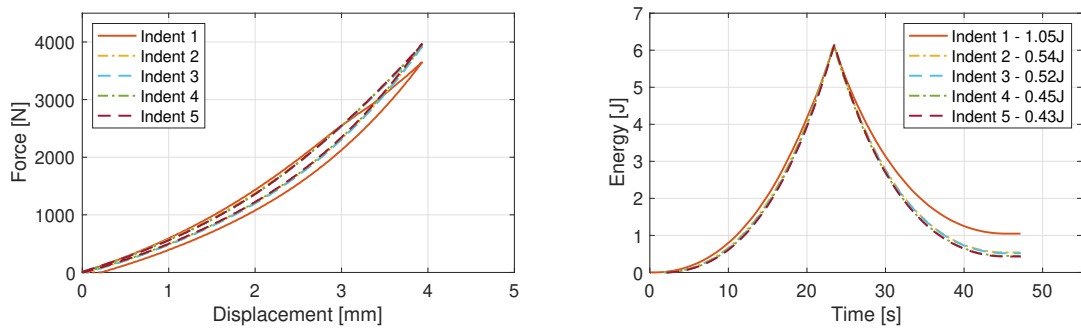
Figure C.5: Force-displacement and energy-time graphs for S.1.



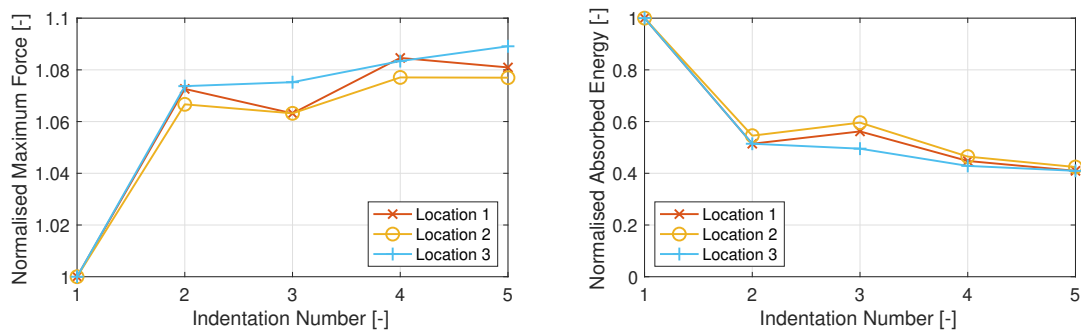
(a) S.2 Location 1



(b) S.2 Location 2

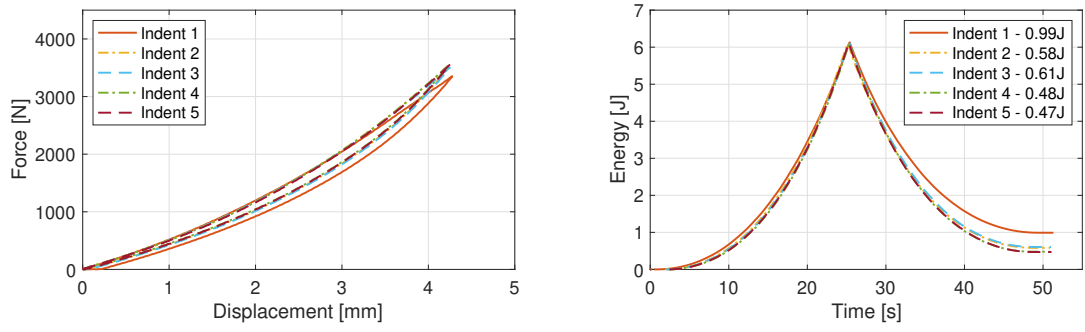


(c) S.2 Location 3

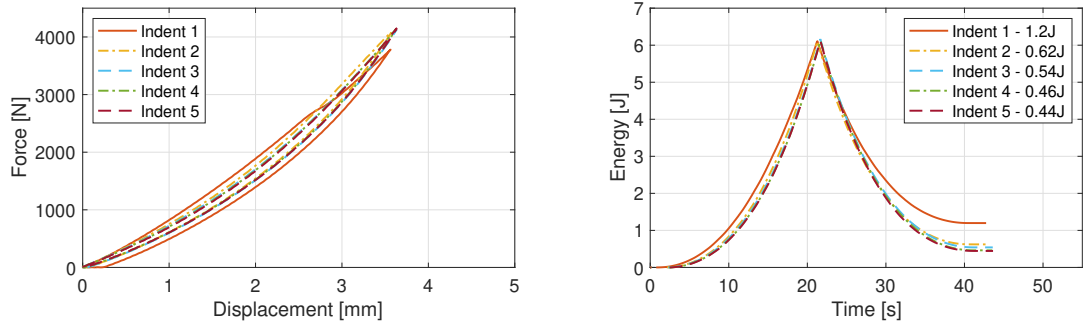


(d) S.2 Maximum force and Absorbed Energy.

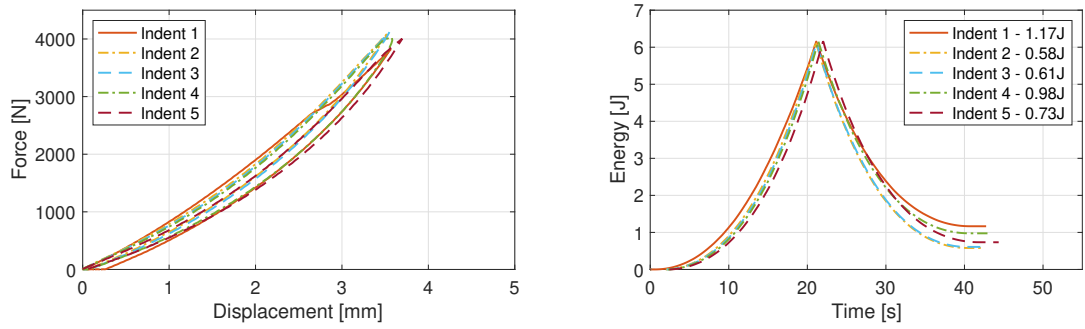
Figure C.6: Force-displacement and energy-time graphs for S.2.



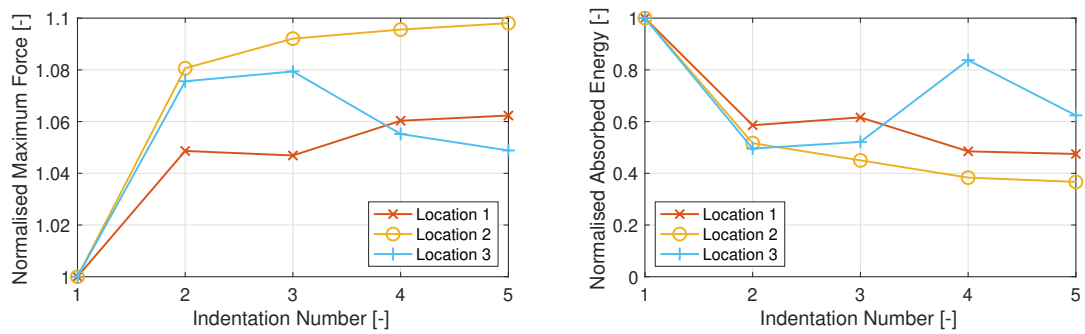
(a) S.3 Location 1



(b) S.3 Location 2

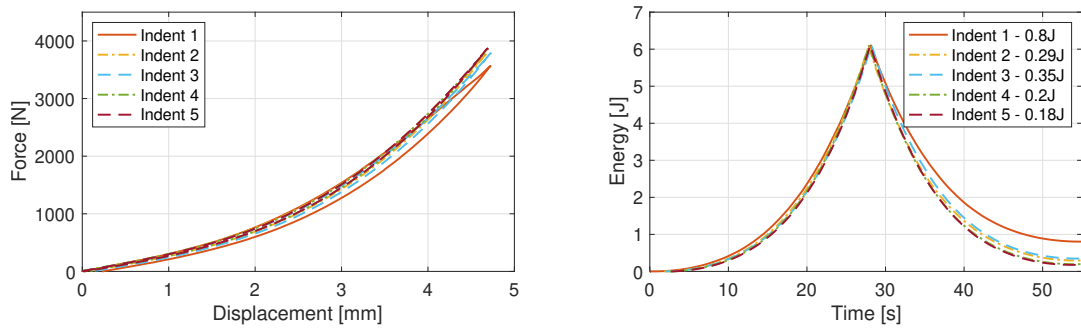


(c) S.3 Location 3

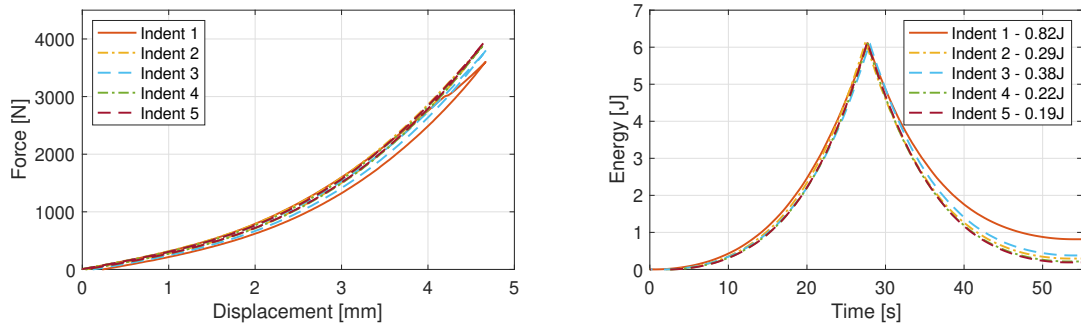


(d) S.3 Maximum force and Absorbed Energy.

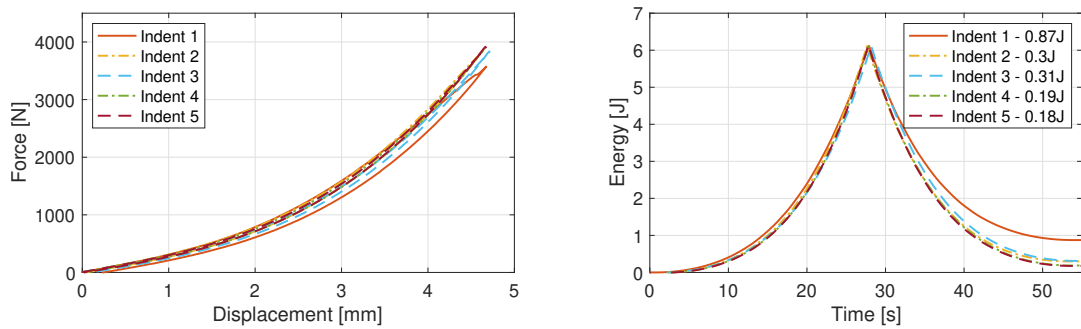
Figure C.7: Force-displacement and energy-time graphs for S.3.



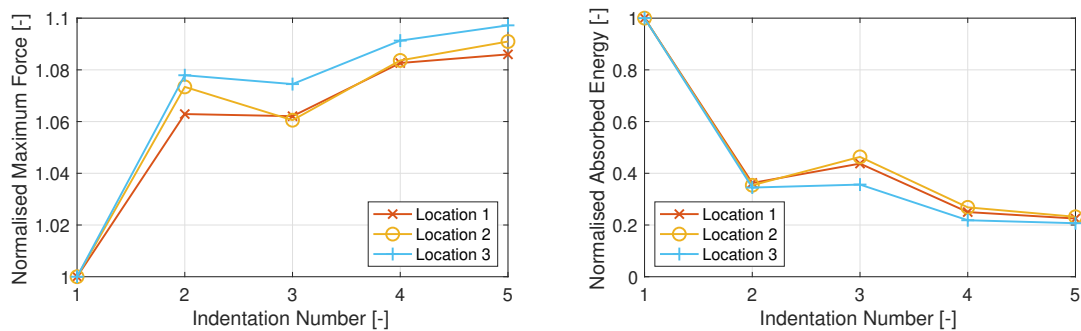
(a) S.4 Location 1



(b) S.4 Location 2



(c) S.4 Location 3



(d) S.4 Maximum force and Absorbed Energy.

Figure C.8: Force-displacement and energy-time graphs for S.4.

Bibliography

- [1] The dehavilland comet crash, jun 2012. URL <https://aerospaceengineeringblog.com/dehavilland-comet-crash/>.
- [2] 20 - fatigue of aerospace materials. In Adrian P. Mouritz, editor, *Introduction to Aerospace Materials*, pages 469 – 497. Woodhead Publishing, 2012. ISBN 978-1-85573-946-8. doi: <https://doi.org/10.1533/9780857095152.469>. URL <http://www.sciencedirect.com/science/article/pii/B9781855739468500200>.
- [3] 3 - materials and material requirements for aerospace structures and engines. In Adrian P. Mouritz, editor, *Introduction to Aerospace Materials*, pages 39 – 56. Woodhead Publishing, 2012. ISBN 978-1-85573-946-8. doi: <https://doi.org/10.1533/9780857095152.39>. URL <http://www.sciencedirect.com/science/article/pii/B9781855739468500030>.
- [4] 787 dreamliner by design, January 2019. URL <https://www.boeing.com/commercial/787/by-design/#/featured>.
- [5] F. J. Guild A. Malhotra. Impact damage to composite laminates: Effect of impact location. *Applied Composite Materials*, 21:165–177, February 2014.
- [6] G. Allegri. Failure in composites: Filling the knowledge gaps. ACCIS 2018 Conference, November 2018.
- [7] *ASTM D7136/D7136M-15 Standard Test Method for Measuring the Damage Resistance of a Fiber-Reinforced Polymer Matrix Composite to a Drop-Weight Impact Event*. ASTM International, 2015.
- [8] *ASTM D6264/D6264M-17 Standard Test Method for Measuring the Damage Resistance of a Fiber-Reinforced Polymer-Matrix Composite to a Concentrated Quasi-Static Indentation Force*. ASTM International, 2017.
- [9] *D6264/D6264M – 17 Standard Test Method for Measuring the Damage Resistance of a Fiber-Reinforced Polymer-Matrix Composite to a Concentrated Quasi-Static Indentation Force*. ASTM International, 2018.
- [10] C. Minot J. Aboissièrè B. Ostré, C. Bouvet. Experimental analysis of cfrp laminates subjected to compression after edge impact. *Composite Structures*, 152:767–778, September 2016.
- [11] J. Baaran. Easa_rep_resea_2007_3: Study on visual inspection of composite structures. Final report, Institute of Composite Structures and Adaptive Systems, jul 2009.
- [12] Boeing. Understanding the new widespread fatigue damage rule. *AERO*, 2012.
- [13] Ryan P. Emerson Bradley D. Lawrence. A comparison of low-velocity impact and quasi-static indentation. Technical report, U.S. Army Research Laboratory, 2012.
- [14] D.J. Bull. Damage assessment of particle-toughened carbon fibre composites subjected to impact and compression-after-impact using 3d x-ray tomography. Master's thesis, University of Southampton: Faculty of Engineering and the Environment, apr 2014.
- [15] N. Knight C. Knight. Hail and hailstorms. *National Center for Atmospheric Research*, 3:924–929, 2015.
- [16] D. Giaiotti F. Stel R. Fraile C. Palencia, A. Castro. Dent overlap in hailpads: Error estimation and measurement correction. *American Meteorological Society*, 50:1073–1087, Dec 2010.

- [17] National Research Council. *U.S. Supersonic Commercial Aircraft: Assessing NASA & O39;s High Speed Research Program*. The National Academies Press, Washington, DC, 1997. ISBN 978-0-309-05878-0. doi: 10.17226/5848. URL <https://www.nap.edu/catalog/5848/us-supersonic-commercial-aircraft-assessing-nasas-high-speed-research-program>.
- [18] *DT120 Versatile High Toughness Epoxy Matrix*. Delta Tech, 10 edition, February 2015.
- [19] P.R. Field, W. Hand, G. Cappelluti, A. McMillan, A. Foreman, D. Stubbs, and M. Willows. Hail threat standardisation. Technical report, EASA: European Aviation Safety Agency, nov 2010.
- [20] I. Giammanco, T. Brown-Giammanco, and H. Pogorzelski. Hailstorm characteristics: Leveraging the community collaborative rain hail and snow network hailpad & damage observations. apr 2016.
- [21] G. Huber. The influence of distance on interaction phenomena in impact fatigue. Internship report, Delft University of Technology, sep 2018.
- [22] P. Jakubczak J. Bieniaś, B. Surowska. Influence of repeated impact on damage growth in fibre reinforced polymer composites. *Maintenance and Reliability*, 17(2):194–198, mar 2015.
- [23] Anette Järneteg. Fibre composite residual strength after impact. Technical report, CSM Material-teknik AB.
- [24] M.K. Tippett J.L. Allen. The characteristics of united states hail reports: 1955–2014. Dec 2015.
- [25] C. Kassapoglou. *Modeling the Effect of Damage in Composite Structures : Simplified Approaches*. Aerospace Ser. John Wiley & Sons, Incorporated, 1 edition, March 2015.
- [26] D. Harris P. Bellamy P.E. Irving L. Cook, A. Boulic. Reliability of damage detection in advanced composite aircraft structures. Technical report, Safety Regulation Group, March 2013.
- [27] M. Mahinfalah and R.A. Skordahl. The effects of hail damage on the fatigue strength of a graphite/epoxy composite laminate. *Composite Structures*, pages 101–106, 1998.
- [28] L. Manon. Impact fatigue on composite panels. Internship report, Delft University of Technology, sep 2017.
- [29] M.J. Wisheart M.O.W. Richardson. Review of low-velocity impact properties of composite materials. *Composites Part A*, pages 1123–1131, apr 1993.
- [30] F. Mustapha N. Yidris M.R. Ishak N. Razali, M.T.H. Sultan. Impact damage on composite structures – a review. *The International Journal Of Engineering And Science*, 3(7):8–20, jul 2014.
- [31] Robin Olsson. A review of impact experiments at ffa during 1986 to 1998, 03 1999.
- [32] N. Blanco J.A. Mayugo P. Maimí, H. Rodríguez. *Numerical Modelling of Failure in Advanced Composite Materials*. Woodhead Publishing, 2015. Chapter 7.
- [33] H.J. Punge and M. Kunz. Hail observations and hailstorm characteristics in europe: A review. *Atmospheric Research*, pages 159–184, feb 2016.
- [34] R. Olsson R. Craven, P. Sztefek. Investigation of impact damage in multi-directional tape laminates and its effect on local tensile stiffness. *Composites Science and Technology*, 68:2518–2525, 2010.
- [35] R.L. Duvall T.M. Rice S.O. Neidigk, D.P. Roach. Detection and characterization of hail impact damage in carbon fiber aircraft structures. Technical Report DOT/FAA/TC-16/8, U.S. Department of Transportation, sep 2017.
- [36] L.S. Sutherland. A review of impact testing on marine composite materials: Part i – marine impacts on marine composites. *Composite Structures*, pages 197–208, dec 2017.
- [37] J.R.M. Almeida W.A. de Moraes, S.N. Monteiro. Thickness effect on repeated impact response of woven fabric composite plates. *Composites: Part B*, pages 80–85, dec 2012.
- [38] Swanee Yourkowski. *777 Tour Fun Facts & Data*, March 2003.